Electronic Supplementary Material (ESI) for Physical Chemistry Chemical Physics.

SUPPLEMENTARY INFORMATION

for

Phenyl Radical + Propene: A Prototypical Reaction Surface for Aromatic-Catalyzed 1,2-Hydrogen-Migration and Subsequent Resonance Stabilized Radical Formation

Zachary J. Buras,[1] Te-Chun Chu,[1] Adeel Jamal,[1] Nathan Yee,[1] Joshua E. Middaugh[1] and William H. Green[1*]

zjburas@mit.edu, jimchu@mit.edu, adeel.jamal@gmail.com, nyee@mit.edu, whgreen@mit.edu

[1]Department of Chemical Engineering
Massachusetts Institute of Technology
77 Massachusetts Ave
Cambridge, MA 02139
United States of America

*Corresponding Author:

Professor Dr. William H. Green; Email: whgreen@mit.edu; Phone: +1-617-258-8992

Table of Contents

S1. Modeling of Flash Photolysis with MBMS

S1.1 RMG Mechanism for Hydrocarbon Chemistry

RMG is an open-source tool for automatically generating detailed chemical mechanisms involving species that contain carbon, hydrogen, oxygen, nitrogen and sulfur (CHONS).[1] As mentioned in the Theoretical section of the main text, RMG relies on a kinetic database of training reactions, as well as rate rules, to estimate the kinetics of any CHONS reaction (provided the reaction falls under one of the ~50 reaction families). Therefore, the accuracy of the kinetic estimates made by RMG, and the corresponding quality of the final model, largely depend on what is in the database. Initially, there were few training reactions and rate rules related to the alkylaromatic chemistry encountered in the C_6H_5 + C_3H_6 system, and the subsequent predictions of RMG related to C_6H_5 + C_3H_6 were demonstrably poor. To remedy this situation, the 28 elementary reactions calculated on the "complete" C_9H_{11} PES (Kislov *et al.*'s full PES[2] + the aromatic-catalyzed 1,2-H-migration and subsequent RSR formation from this work) were added as training reactions to the RMG database. Besides simply importing the kinetic calculations into the database, the suitability of the matching reaction template, which is meant to convey only the critical features of the reaction (see Scheme 2), was checked and in many cases modified. For example, if either the reactant or product has a radical in a benzylic position that fact should be captured in some way by the reaction template because the added resonance stabilization will have a large impact on the overall kinetics. If each training reaction is matched by a suitable reaction template, then the training reaction data will be utilized as intended when RMG encounters an analogous reaction for a different system (e.g., 1-naphthyl radical + 2-butene compared to C_6H_5 + C_3H_6). Of the 28 training reactions added, 15 belonged to the reaction family for radical addition to an unsaturated bond (abbreviated as R_Addition_MultipleBond, the reverse reaction is a β-scission), 5 belonged to the *intramolecular* radical addition to an unsaturated bond family (Intra_R_Add_Exocyclic), 5 belonged to the intramolecular H-migration family (intra_H_migration), and 3 belonged the H-abstraction family (H_Abstraction).

After training RMG on the relevant alkylaromatic chemistry, a hydrocarbon (HC only) mechanism was automatically generated that contained 69 species and 191 reactions (RMG input file and mechanism in CHEMKIN format provided in separate ESI file). RMG was constrained to species with ≤ 18 carbon atoms in order to capture **i1** recombination with itself to make **i1**-dimer in the case that is important. Pressure-dependent kinetics were included up to PES's with 13 atoms total in order to capture the likely pressure dependence of CH_3 + C_3H_6. Pressure-dependence of the C_9H_{11} PES itself (20 atoms total) was neglected due to the predicted lack of P-dependence (Figure 2) and qualitatively confirmed by experiments (Figure 7).

In initial tests, the RMG HC mechanism captured most of the important C_6H_5 + C_3H_6 chemistry, but overestimated the extent of CH_3 recombination with **p10** (Scheme S 1). CH_3 + **p10** recombination was deemed too fast because the unaltered HC mechanism was predicting substantial concentrations of the corresponding products at m/z=106 amu, which as shown in Figure 8 was clearly not observed at all (at any condition). This was because the training reaction used by RMG to estimate CH_3 + **p10** recombination was for CH_3 + cyclopentadienyl radical (CPD'yl). While not a bad estimate considering that both **p10** and CPD'yl have resonance stabilization, it failed to capture the full extent of **p10**'s stabilization, therefore the rate coefficient was slightly too fast. The HC mechanism was manually amended by replacing the *k*(T)'s for the reactions in Scheme S 1 with a new estimate: 1/2× Troe *et al.*'s experimental measurement of CH_3 + **p1** → ethylbenzene,[3] by analogy to H + **p1** at various resonance sites.[4] The revised *k*(T)'s were slower than the previous estimates, and the overall model no longer predicted measurable MBMS signal at m/z=106 amu. More generally, the lack of kinetic data for the reactions in Scheme S 1 highlight them as candidates for future theoretical and/or experimental investigation.

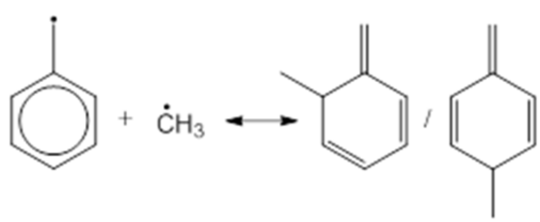

Scheme S 1: Methyl + benzyl radical recombination reactions with overestimated kinetics in RMG.

Estimates of k_{wall} for the two most important radicals in the system, C_6H_5 and **i1**, were also manually added to the HC mechanism. For C_6H_5, k_{wall} = 100 s^{-1}, which was fit to both 505.3

nm absorbance and 77 amu MBMS decays recorded simultaneously without C_3H_6 (Figure S 9, Figure S 18, Figure S 29 and Figure S 33). For **i1**, k_{wall} was estimated as half of the C_6H_5 value (50 s^{-1}), based on the lower expected reactivity of an alkyl radical compared to an aryl radical. Although other radicals in the system (e.g., H, CH_3, C_3H_5 and **p1**) should also have their own k_{wall} values, there was insufficient experimental information to obtain reliable estimates, and the main results presented in this work are insensitive to these parameters. For **i1**, although k_{wall} is a guess, at 700 K the model predictions are insensitive to it because unimolecular isomerization/decomposition occurs much faster. For C_6H_5, k_{wall} is important because it can alter the overall mass balance of the model, therefore it is reassuring that a relatively small value of 100 s^{-1} was sufficient to match experiments without C_3H_6. Note that this value of k_{wall} is much smaller than many of the values fit in the 505.3 nm absorbance experiments of section 4.2 (Table 2). As mentioned in that section, this was due to a small air leak during those experiments that was fixed prior to the current MBMS experiments. Also, the simple pseudo-first-order model used in section 4.2 does not account for self-reaction, whereas the current detailed model does, which would have the effect of decreasing k_{wall}. Finally, it is important to note that this fit value of k_{wall} is not meant to account for the fast wall catalysis of C_6H_5 to C_6H_6 observed in the absence of C_3H_6 (Figure S 9, Figure S 18, Figure S 29 and Figure S 33). Apparently this phenomenon is too complex to model as a first order rate and the current model does not attempt to describe it. Instead, as mentioned in section 4.3 of the main text, wall catalysis was determined to be negligible by control MBMS experiments conducted at increasing [C_3H_6], all of which the current gas-phase model was able to match sufficiently (including C_6H_6, most importantly). Similarly, wall catalysis of I to HI was not included in the model.

Other than the two modifications/additions mentioned above (and the barrier for C_6H_5 + C_3H_6 terminal addition being lowered by 0.75 kcal/mol to match the 505.3 nm absorbance experiments), RMG's HC mechanism was used as is. By minimizing the amount of manual intervention in the HC mechanism construction the real accuracy of RMG can be gauged when comparing to experiments. If the comparison is satisfactory, then RMG can be confidently applied to analogous systems (e.g., 1-naphthyl radical + 2-butene). If the comparison is not satisfactory, sources of discrepancies can be easily identified and rectified (e.g., the overestimated CH_3 + **p1** reaction mentioned above).

S1.2 Iodine Sub-Mechanism

As demonstrated by the various side and secondary products observed with MBMS in Figure 8, I atom is not merely an inert photolysis co-product of C_6H_5, but an active participant in much of the observed chemistry. In particular, I atom recombination with various radicals, R, to form iodide-containing species RI is prevalent. As such, any attempts at quantitatively modelling the MBMS experiments must include the contribution of I atom. Because RMG does not currently have the capability (or, more importantly, the data) to model halogen-containing species, the sub-mechanism of iodine chemistry had to be constructed manually. Fortunately, two recent mechanisms for shock tube pyrolysis of iodobenze under both neat[5] and acetylene-diluted conditions[6] provided a starting point for the current sub-mechanism.

Table S 1 lists the eight iodide-containing species involved in the sub-mechanism and their thermochemical parameters. Four of the species were in the mechanism of Comandini *et al*. (I, HI, I_2 and C_6H_5I),[6] wherein the thermochemistry was obtained from the Active Thermochemical Tables (ATcT).[7] The thermochemistry of the remaining four species (CH_3I, C_3H_5I, p10-I and i1-I) was estimated by using Benson Group-Additivity Values (GAV).[8] Table S 2 lists the 16 reactions in the sub-mechanism, seven of which are recombination reactions with I atom (reactions #1 and 8-13). Of these $R + I \rightarrow RI$ reactions, only two of them include pressure-dependence: R = H and I. Even then, as noted in the footnotes, only for R = I has a pressure-dependent rate coefficient been measured for the same bath gas used in this work (helium). Nonetheless, the literature recombination kinetics listed in Table S 2 (with experimental conditions given in the footnotes) provide some reasonable estimate of the real kinetics at the conditions of this work, particularly for larger R's (such as **p10**), that are more likely to be in the high-P limit.

Table S 1: Thermochemistry and structures of iodide-containing species included in sub-mechanism

Species	Structure	ΔH_f°(298 K) (kcal mol^{-1})	S_{int}°(298 K) (cal mol^{-1} K^{-1})	C_P° (cal mol^{-1} K^{-1}) 300 K	400 K	500 K	600 K	800 K	1000 K	Reference
I	-	25.5	43.2	5.0						6
HI	-	6.4	49.4	7.0	7.0	7.1	7.3	7.6	7.9	6
C_6H_5I	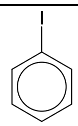	38.7	80.1	24.0	30.6	36.3	41.1	47.7	52.3	6
I_2	-	14.9	62.3	8.8	8.9	9.0	9.0	9.0	9.1	6
CH_3I	-	3.3	60.5	10.6	12.5	14.0	15.3	17.5	19.2	8
C_3H_5I	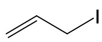	22.9	78.6	18.5	22.4	26.2	28.9	33.5	36.9	8
p10-I	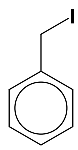	30.0	93.0	28.1	36.3	43.9	49.6	58.5	64.7	8
i1-I	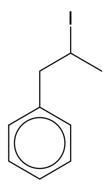	17.5	111.0	40.1	51.7	61.6	69.5	81.4	89.6	8

Table S 2: Kinetics of reactions involving iodide-containing species included in sub-mechanism

Reaction #	Reaction	Arrhenius Parameters[a] A	n	E_A	Reference
1	I + **i1** ↔ **i1**-I	5.8×10^{-11}	0	0	9, b
2	I + **i1**↔ HI + **p2**	2.0×10^{-11}	0	0	10, c
3	I + **i1** ↔ HI + **p3**	1.3×10^{-11}	0	0	10, c
4	I + **i2** ↔ HI + **p4**	0.7×10^{-12}	0	0	10, c
5	H + C_6H_5I ↔HI + C_6H_5	1.4×10^{-18}	2.5	-0.14	11
6	C_6H_5 + C_6H_5I ↔ $_2H_{10}$ + I	3.3×10^{-12}	0	11.0	6
7	C_6H_5I → C_6H_5 + I	3.3×10^{-13}	0	45.9	12
8	C_6H_5 + I → C_6H_5I	1.7×10^{-11}	0	0	6, d
9	H + I + M ↔ HI + M	1.3×10^{-31}	-1.87	0	13, e
10	CH_3 + I ↔ CH_3I	1.0×10^{-11}	0	0	14, f
11	C_3H_5 + I ↔ C_3H_5I	1.6×10^{-10}	0	0	15, g
12	**p10** + I ↔ **p10**-I	8.3×10^{-11}	0	0	16, h
13	I +I + M ↔ I_2 + M	5.5×10^{-34}	0	-1.14	17, i
14	I + C_3H_6 ↔ HI + C_3H_5	3.0×10^{-11}	0	18.0	18
15	H + HI ↔ H_2 + I	6.6×10^{-11}	0	0	6
16	C_6H_5 + HI ↔ C_6H_6 + I	5.0×10^{-12}	0	0	6, d

[a]Modified Arrhenius expression used: $k(T) = AT^n e^{-\frac{E_A}{RT}}$. Units are kcal, molecule, s, cm. [b]Estimated by analogy to I + C2H5 → C2H5I measured at 298 K, 100 Torr Kr bath gas and increased by 5 × to match MBMS experiments. [c]Estimated as 0.3 × recombination rate (reaction #1) by analogy to I + C_2H_5 → HI + C_2H_4 and adjusted for number of hydrogens. [d]Estimate. [e]Ar bath gas. [f]Measured at 400 K, 82 Torr CH_3I bath gas. [g]Measured at 296 K, 750 Torr N2 bath gas. [h]Measured at 750-950 K, 190-1900 Torr Ar bath gas. [i]He bath gas.

The most important reactions of the sub-mechanism are those involving **i1** (#1-4) because by diverting **i1** from unimolecular reaction, they affect the major product distribution of C_6H_5 + C_3H_6. Unfortunately, **i1** is far too specific of a radical for any previously published work to have studied the kinetics of its reaction with I atom. The closest analogue in the literature is ethyl radical, C_2H_5, + I, the recombination kinetics for which were measured at 300 K and 100 Torr Krypton,[9] and the corresponding disproportionation reactions which were measured as ~1/3× recombination.[10] In this work, it was found that a better match with the MBMS experiments could be obtained by increasing the recombination rate by 5×. The disproportionation rate was also increased accordingly, accounting for the different types and numbers of H-atoms on **i1** (and **i2**) compared to C_2H_5. Perhaps the ~5× difference between **i1** + I and C_2H_5 + I recombination is due to the latter, as a much smaller system, being further down the fall-off curve. Reassuringly, the fit **i1** + I → **i1**-I rate is actually slightly smaller than the literature rate for the similarly sized **p10** + I → **p10**-I rate (reaction #12). Other than for reactions #1-4, all of the rate coefficients in the sub-mechanism were taken directly from literature (usually an experiment) for the specific reaction of interest and used without further adjustment.

The remaining six reactions merit some discussion as well. Reaction #5 is fast, and could become problematic in the presence of a high H concentration where a cycle might be established between C_6H_5 and H. Fortunately at the conditions of the MBMS experiments in this work H concentration is low, and what little H that is formed preferentially reacts with C_3H_6 rather than C_6H_5I due to ~2 orders of magnitude difference in concentration. The possibility of other radicals besides H initiating the halogen-atom transfer reaction of #5 (i.e., R + C_6H_5I →RI + C_6H_5) was also considered, but due to the relatively high C-I bond energy in C_6H_5I (~67 kcal/mol[19]) such a reaction would be ≥ 10 kcal/mol endothermic for any R other than H in this system (e.g., CH_3, which is present in high concentration).[20]

Although S_N2 reactions such as #6 are highly favorable thermodynamically, kinetically they are slow. For C_6H_5 substituting for I in C_6H_5I the barrier is ~11.0 kcal/mol, and even if H is the nucleophile the barrier is still ~10 kcal/mol.[11] Therefore these types of reactions will not be important at the conditions of this work (≤700 K).

Thermal decomposition of C_6H_5I (#7) was already mentioned in the main text as the reason for imposing a 900 K upper bound on flash photolysis experiments with that precursor. H-abstraction from C_3H_6 by I atom (#14) will not be important due to a high barrier (18 kcal/mol), and reactions #15 and 16 are unimportant due to a low concentration of both H and HI. As mentioned in the previous section, catalytic hydrogenation of I to HI is not included in the sub-mechanism, although it is observed experimentally in the absence of C_3H_6 (Figure S 9, Figure S 18, Figure S 29 and Figure S 33). Therefore, this model is not expected to match experimental HI profiles well.

As a final note, although I atom chemistry is important to take into account when quantitatively analyzing product distributions, it has no effect on pseudo-first-order measurements of the total C_6H_5 consumption rate measured by direct absorption (section 4.2), which happen too quickly for I atom secondary reactions to play a role.

S1.3 Photoionization Cross Sections (PICS)

The concentration of each species *i* in the combined HC and iodine chemical mechanism, C_i, is solved for using the design equations for an isothermal, isobaric, homogeneous batch reactor. C_i can then be related to the *instantaneous* MS signal, $S_{i,instantaneous}$, through a simple proportionality:

$$S_{i,instantaneous} = \mathrm{R(m/z)}\sigma_{\mathrm{PI,i}}C_i \qquad \text{(S1)}$$

Where R(m/z) is the mass discrimination factor discussed in section S1.4 and $\sigma_{\mathrm{PI,I}}$ is the photoionization cross section (PICS) for species *i* discussed in this section. The subscript *instantaneous* indicates that transport delays during MB sampling are not taken into account yet (section S1.5). Although Eq. S1 is a drastic simplification of the complex relationship between concentration and MBMS signal,[21] it will suffice for the purposes here and is hopefully transparent.

Any attempt to extract quantitative information from MS using PI must contend with the need for PICS. Although PICS have been measured for many common organic molecules[22-25] and for a handful of common radicals,[26-28] these measurements are a pittance compared to the number of possible organic molecules/radicals, even for a fixed molecular formula of reasonable size. Therefore, estimates of PICS are almost always needed. Fortunately, the ionization energy used for PI in this work (10.5 eV) is slightly above (~1 eV) the threshold ionization energy of many organic molecules in a region where PICS are often ~10 Megabarns (Mb).[22, 25, 29] Furthermore, from the sizable (but obviously finite) database of measured PICS in the literature, smart estimates can be made for analogous molecules with unknown PICS. As a last resort, experimental measurements of PICS can also be made for particularly important molecules/radicals. All three approaches to obtaining PICS were taken here (literature, smart estimates and measurements).

Table S 3 shows all of the important species (both molecules and radicals) in the C_6H_5 + C_3H_6 MBMS model for which PICS were needed. For most of the smaller species (parent m/z < 130 amu) literature PICS were available, but for almost all of the larger species there were no previously published measurements. The four internal standards (1,3-butadiene, furan, cyclohexane and heptane) are also included and noted in Table S 3. Even for species with measured PICS (including the internal standards), there is $\pm$15% uncertainty, which translates into at least $\pm$15% uncertainty in all MBMS model versus data comparisons.

Table S 3: Structures and photoionization cross sections, $\boldsymbol{\sigma_{PI}}$, at 10.5 eV of all important species in model of MBMS experiments.

Species	Structure	Cation	m/z (amu)	σ_{PI} at 10.5 eV (Mb)[a]	Reference
CH_3	-	CH_3^+	15	$6.7^{+2.4}_{-1.8}$	26
C_3H_5	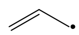	$C_3H_5^+$	41	6.1 ± 1.2	27
1,3-Butadiene[b]	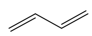	$C_4H_6^+$	54	16.3 ± 3.3	25
Furan[b]	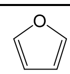	$C_4H_4O^+$	68	14.4 ± 3.0	25
C_6H_5	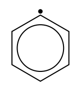	$C_6H_5^+$	77	17.0 ± 2.5	28
C_6H_6	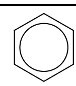	$C_6H_6^+$	78	31.8 ± 6.4	22
Cyclohexane[b]	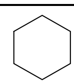	$C_6H_{12}^+$	84	21.3 ± 4.3	22
p10	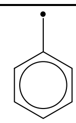	$C_7H_7^+$	91	25.5 ± 4.0	30, c
Heptane[b]	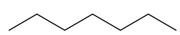	$C_7H_{16}^+$	100	9.9 ± 1.5	24
p1	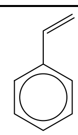	$C_8H_8^+$	104	42.9 ± 4.3	23
p2/p3/p4	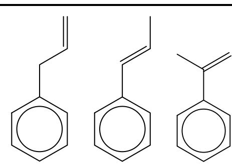	$C_9H_{10}^+$	118	38.8 ± 7.0	This work, see text
i1	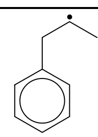	$C_7H_7^+$	91	5	Estimate, see text
		$C_9H_{11}^+$	119	5	
I2	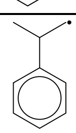	$C_9H_{11}^+$	119	10	Estimate, see text
Propylbenzene	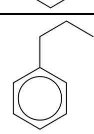	$C_9H_{12}^+$	120	30.0 ± 4.5	23
I	-	I^+	127	74^{+33}_{-23}	26, d
HI	-	HI^+	128	44 ± 7	26 31

i1-CH_3	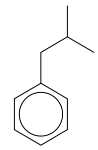	$_0H_{14}^+$	134	30	Estimate[e]
CH_3I	-	CH_3I^+	142	48.2 ± 7.9	[26]
Biphenyl	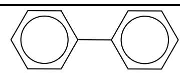	$_2H_{10}^+$	154	64	Estimate[f]
i1-C_3H_5	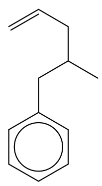	$_2H_{16}^+$	160	40	Estimate[g]
C_3H_5I	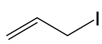	$C_3H_5^+$	41	27.5	Estimate, see text
		$C_3H_5I^+$	168	22.5	
p10-I	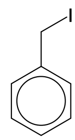	$C_7H_7^+$	91	45.5	Estimate, see text
		$C_7H_7I^+$	218	4.5	
i1-dimer	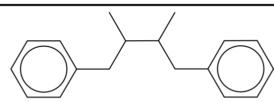	$_8H_{22}^+$	238	60	Estimate[h]
i1-I	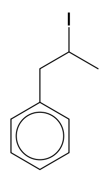	$C_9H_{10}^+$	118	24	Estimate, see text
		$C_9H_{11}^+$	119	48	
		$C_9H_{11}I^+$	246	8	
I_2	-	I_2^+	254	50	Estimate[i]

[a]Uncertainty represents two standard deviations when applicable. Values without stated uncertainties are estimates. [b]Internal standard. [c]Inferred as $1.5 \times$ C_6H_5 σ_{PI}. [d]PICS is for ground state ($^2P_{3/2}$) I atom. In this work, excited ($^2P_{1/2}$) I atom is assumed to be quenched to the ground state by C_3H_6 faster than the ~1 ms resolution of the MBMS experiment. [e]Estimated by analogy to σ_{PI} at 10.5 eV for the following series of alkylbenzene molecules: toluene (31.4 Mb), ethylbenzene (28.7 Mb) and propylbenzene (30.0 Mb). [f]Estimated as $2 \times$ C_6H_6 $\sigma_{PI}$by applying bond-additive approach of Bobeldijk et al.[32] [g]Estimated as the sum of σ_{PI} for propylbenzene (30 Mb) and propene (10 Mb) by applying bond-additive approach of Bobeldijk et al.[32] [h]Estimated as $2 \times$ propylbenzene $\sigma_{PI}$by applying bond-additive approach of Bobeldijk et al.[32] [i]Estimated as at least 50 Mb by analogy to iodide-containing compounds with known σ_{PI}: HI and CH_3I.

Going down Table S 3, the first species worth commenting on specifically are the phenylpropene isomers, **p2-p4**. None of these four isomers (trans-1-, cis-1-, 2- and 3-phenylpropene) have had their PICS quantified at any IE, although Zhang *et al*. measured the relative PIE curve for all of them.[33] Given that **p2** and **p3** are expected to be measurable primary products of C_6H_5 + C_3H_6 (Figure 2) it was deemed worthwhile to experimentally measure the PICS of at least one of the isomers. **p2** was chosen because it was predicted to be the most important of the H-loss products. The procedure for measuring the PICS of **p2** is provided in section S2. The value measured and reported in Table S 3 (38.8±7.0 Mb) is consistent with other alkenylaromatic molecules, like styrene (42.9±4.3 Mb). The same PICS was used for all phenylpropene isomers.

The overall PICS for **i1**, obtained by roughly fitting the 600 K MBMS experiments, is 10 Mb, which seems anomalously low when compared to the closed-shell aromatic compounds with PICS ~30-40 Mb. However, as discussed by Xu and Pratt it is not uncommon for radicals to have PICS 2-4× lower than their closed-shell analogues (propylbenzene in the case of **i1** with a PICS of 30±4.5 Mb) due to a correspondingly lower occupancy of the HOMO from which the electron is ejected.[34] The fragmentation pattern of **i1** was also roughly fit to the 600 K MBMS experiments. Specifically, a fast rise (~1 ms, at the time-resolution limit of the MBMS experiment as discussed in section S1.5) at m/z=91 amu could only be explained by a fragment of **i1** that is 1:1 with the parent cation (5 Mb each). Although surprising initially, it is possible that the **i1** parent cation undergoes a fast 1,2-H-migration to form the **i4** parent cation, which can then easily fragment to $C_7H_7^+$ + ethene + e^-, where $C_7H_7^+$ could be either a benzyl or tropylium cation.[35] Such cation rearrangements have been observed before, particularly if the resulting fragments are thermodynamically favorable as in this case.[36] The same small total PICS (10 Mb, no fragmentation) was also used for **i2**, which is present in low concentration in the model anyway.

Of the six closed-shell iodide-containing species, only two have PICS measured in literature (HI and CH_3I), and both are ~50 Mb. Therefore, for the remaining four closed-shell iodide-containing species (C_3H_5I, **p10**-I, **i1**-I and I_2) it was assumed that each of their overall PICS are ≥50 Mb. In the case of all but **i1**-I, the overall PICS was simply set at 50 Mb and not adjusted any further.

Given the relatively low C-I bond energy compared to C-C and C-H bonds,[20] fragmentation of RI compounds to R^+ is facile, even at 10.5 eV, and must be taken into account. This is especially true for C_3H_5I and **p10**-I, for which the C-I bond in question is at a particularly vulnerable allylic and benzylic site, respectively. The R^+:RI^+ fragmentation pattern for C_3H_5I was measured by us as 55:45 (Figure S 6) and for C_7H_7I it was previously measured as ~10:1 close to 10.5 eV.[35] Both fragmentation patterns were applied to the 50 Mb total PICS estimate for C_3H_5I and **p10**-I.

Understanding the fragmentation pattern of **i1**-I was most crucial to interpreting the 600 K MBMS experiments. Although **i1**-I cannot be purchased commercially, the bromide, **i1**-Br, can and the measured fragmentation pattern of **i1**-Br (Figure S 7) exhibited significant cations not only at the parent and **i1**$^+$ (119 amu) m/z, but also at 118 amu. This suggests a fragment channel to **p3**$^+$ + HBr + e$^-$, which seems reasonable given the weak benzylic C-H bond. **i1**-I is expected to form the same fragments as **i1**-Br, but to a greater extent due to the weaker C-I bond relative to C-Br. Attempts to synthesize **i1**-I *via* the Finkelstein reaction were mostly unsuccessful due to low conversion of **i1**-Br and thermal production of phenylpropene isomers.[37] Therefore, the only current recourse to quantifying **i1**-I and its fragments was to fit their PICS to the 600 K experiments while maintaining the constraint that the overall PICS $\geq$ 50 Mb. An overall PICS of 80 Mb and a 3:6:1 fragmentation pattern between $C_9H_{10}^+$:$C_9H_{11}^+$:$C_9H_{11}I$ was fit. Finally, as noted in Table S 3, several of the closed-shell hydrocarbons had their PICS estimated by applying the bond-additivity concept of Bobeldijk *et al.*[32] For example, the unknown PICS of biphenyl was estimated as 2× the PICS of C_6H_6 ($2 \times 32 = 64$ Mb), and **i1**-C_3H_5 was estimated as the sum of C_3H_6 and propylbenzene ($10 + 30 = 40$ Mb).

S1.4 Mass Discrimination Factors, R(m/z)

As expressed in Eq. S1, R(m/z) is essentially a conversion factor between PICS-weighted concentration in the reactor and MBMS signal. Generally, R(m/z) increases monotonically as a function of m/z, and accounts for the greater radial spread of lighter species in the gas expansion (resulting in lower centerline concentrations and lower MBMS signals).[21]

Individual values of R(m/z) are calculated for each of the four internal standards using their known concentrations (~1e-11 cm^{-3}) and PICS by rearranging Eq. S1:

$$\mathrm{R(int\text{-}std\ m/z)} = S_{int\text{-}std}/(\sigma_{\mathrm{PI,int\text{-}std}} C_{int\text{-}std}) \quad \text{(S2)}$$

The four resulting R(m/z)'s are then fit to a power law:

$$\mathrm{R(m/z)} = b(\mathrm{m/z})^c \quad \text{(S3)}$$

A representative R(m/z) fit *with* C_3H_6 is shown in Figure S 1. All 15 MBMS experiments were conducted with the internal standards present, therefore individual R(m/z)'s were fit to each experiment. Table 3 summarizes the fit values of the exponent, *c*, for each experiment, which is typically ~0.5.[21] Without C_3H_6, however, R(m/z) was essentially flat and a constant value was used. It should also be mentioned here that brief control experiments were conducted at each T,P condition without the internal standards, to ensure that their presence was not altering the product distribution.

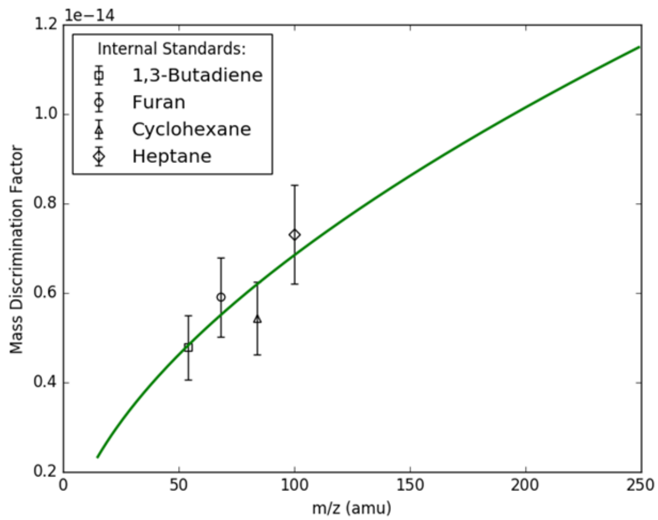

Figure S 1: Representative mass discrimination factors (markers) and fit (line) at 707 K, 10 Torr (Experiment 7). Error bars are from $\pm 15\%$ uncertainty in internal standard PICS.

Once R(m/z) had been fit, all of the PICS-weighted concentration profiles in the model, $\sigma_{PI,i}C_i$, were multiplied by their corresponding R(m/z) according to Eq. S1, in order to obtain the simulated, instantaneous signal profiles, $S_{i,instantaneous}$, which are not yet comparable to experiments because transport delays still need to be accounted for (next section).

S1.5 Molecular Beam Sampling

The effect of effusive or molecular beam sampling on measured species profiles in kinetic studies has previously been described and quantified from a theoretical level.[38, 39] Although it is feasible to apply such a rigorous sampling model to a simple chemistry mechanism, for a complex chemistry mechanism, such as the one used in this work consisting of almost 100 species, a simpler model for sampling (and transport more generally) is desired. Moreover, theoretical models for sampling do not take into account transport within the reactor, i.e., if radicals are not initially distributed uniformly in the radial dimension following photolysis (usually due to a non-uniform photolysis beam profile) it will take some finite time for the non-uniformities to “smooth out” by diffusion. For the MBMS experiment reported here, diffusion within the reactor due to inhomogeneities does seem to be the rate-limiting transport step, as evidenced by the much slower appearance of products at 50 Torr compared to 10 Torr (Figure 7).

For these reasons, a simple model for transport that implicitly includes diffusion in the reactor was adapted from Baeza-Romero *et al.*[40] In their model, all of the steps involved in transporting a species i from somewhere inside the reactor to the ionization region of the MS (diffusion to the pinhole, flow through the pinhole and transport to the ionization region *via* an effusive or supersonic expansion, as well as transport out of the ionization region for neutral molecules) are lumped into a single first-order rate, $k_{sampling}$:

$$i \xrightarrow{k_{sampling}} i, sampled \xrightarrow{k_{sampling}} i, exit$$

Therefore, for any arbitrarily complex chemical mechanism a set of ODE's can be set up and numerically solved for the observed MBMS signal, $S_{i,sampled}$, after accounting for transport effects:

$$dS_{i,sampled}/dt = k_{sampling}\,(S_{i,instantaneous} - S_{i,sampled}) \qquad \text{(S4)}$$

The set of ODE's represented by Eq. S4 are only solved for dilute, time-dependent species. A new reactor type called "mbsampledReactor" was created in RMG to solve this set of ODE's and is freely available upon request to the authors. $S_{i,sampled}$ is directly comparable to experiments.

An advantage of this simple transport model is that $k_{sampling}$ is the only parameter that needs to be fit, which is done by comparison to the rise time of the I atom MBMS signal at 127 amu (Figure S 2). I atom is used for fitting $k_{sampling}$ because it is formed in the reactor nearly instantaneously after photolysis and unlike C_6H_5 it has a long lifetime. In the limit of instantaneous sampling ($k_{sampling} \rightarrow \infty$) the model prediction is clearly not accurate, but after tuning $k_{sampling}$ to 750 s^{-1} the agreement is good in this case (especially for the rise time, which is chemistry-independent). The modelled I atom signal decreases at longer times due to the reactions in Table S 2. Values of $k_{sampling}$ were fit to the I atom rise time in this manner for all 15 MBMS experiments, and are typically ~1000 s^{-1} (Table 3) although there is a trend toward slower sampling for higher P and with added C_3H_6, consistent with diffusion in the reactor being the rate-limiting transport step.

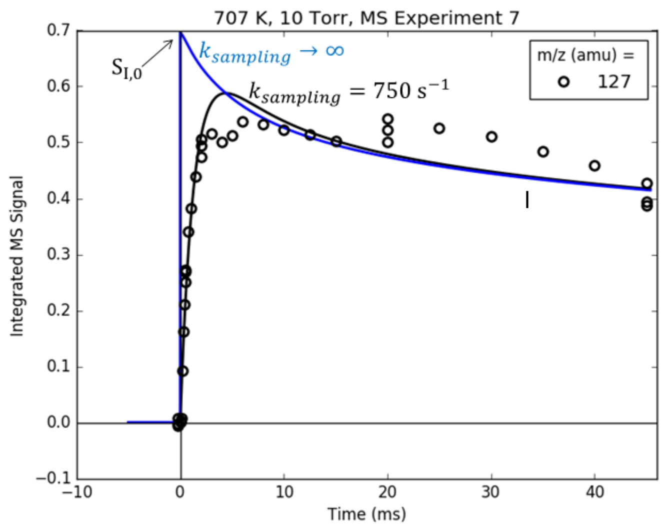

Figure S 2: Representative measured iodine atom MS time-profile (markers) and comparison to two different models of MBMS sampling: $\boldsymbol{k_{sampling}} \to \infty$ (blue) and $\boldsymbol{k_{sampling} = 750\ \mathrm{s}^{-1}}$.

As shown for the 50 Torr MBMS experiments in Figure 7, this simple, one-parameter transport model is not sufficient to completely describe sampling at higher P's. In particular, the same $k_{sampling}$ that was fit to the MBMS rise time of I atom was used for all other species in the solution of Eq. S4, regardless of mass or size. If diffusion within the reactor is rate-limiting, then $k_{sampling}$ should decrease (get slower) with increasing species mass and collision diameter, σ. According to the Chapman-Enskog equation,[41] for a relatively heavy species in a He bath gas the mass of the heavy species will have little effect on the diffusion coefficient, *D*, whereas $D \propto \sigma^{-2}$. Therefore, although I atom has a similar mass as the major products of C_6H_5 + C_3H_6 (127 versus 78-119 amu), because its collision diameter is likely at least 2× smaller it will have a *D* ~4× faster. This would explain why the C_6H_5 + C_3H_6 products at 50 Torr (and 25 Torr) appear in the MS even slower than predicted by the model. Nonetheless, the higher-P experiments still quantitatively determine the product distributions after diffusion has homogenized the composition (or if instantaneous product ratios are used instead, Figure S 32 and Figure S 36).
Although faster time-resolution for the MBMS measurements is desirable and achievable down to 10-100's of microseconds,[21, 40] with the current time-resolution of ~1 ms it is still possible to discern differences in chemical timescales. For example, as shown in section 4.4 it is possible to distinguish the faster growth time scale of C_6H_6 (direct H-abstraction) compared to **p1** (CH_3-loss through an intermediate, **i1**). Furthermore, high time resolution is achieved using the laser absorbance portion of the apparatus, which can easily measure processes as fast as 10's of

microseconds.[42] For the purposes of this work (quantifying the primary products of C_6H_5 + C_3H_6), a 1 ms MBMS time resolution was deemed sufficient.

Finally, as discussed in more detail in the next section, the I Atom MBMS profile is also used to quantify the initial radical concentration by back-extrapolating the $k_{sampling} \rightarrow \infty$ simulation to t=0. The value obtained, $S_{I,0}$, indicated in Figure S 2 is proportional to $C_{I,0}$ (and $C_{C6H5,0}$) according to Eq. S1.

S1.6 Initial Radical Concentration

As mentioned briefly in the previous section, $C_{I,0}$ (which is assumed $=C_{C6H5,0}$) is obtained from the following rearranged version of Eq. S1:

$$C_{I,0} = S_{I,0}/(\sigma_{PI,I}R(m/z=127\ \text{amu})) \tag{S5}$$

where $S_{I,0}$ is obtained by fitting and back-extrapolating the I atom MBMS profile (Figure S 2). Values of $C_{I,0}$ obtained in this manner (labelled MS $C_{I,0}$) are summarized in Table 3. Compared to the $C_{I,0}$ values measured simultaneously by IR absorbance (labelled IR $C_{I,0}$), MS $C_{I,0}$ is typically ~2× lower, but still within their combined (large) uncertainties for most experiments. The systematic difference is likely due to an inhomogeneous photolysis beam profile, or a beam diameter that is slightly smaller than the reactor inner diameter where MBMS sampling occurs. In either case, MS $C_{I,0}$ should be (and was) used as the initial radical concentration in the model, because it is more representative of the local environment relevant to the MBMS experiments.

Another possible explanation for the systematic ~2× difference in IR and MS $C_{I,0}$ is the presence of excited ($^2P_{1/2}$) I atom, I^*, which has been measured as ~30% of the total I atom yield immediately following 266 nm photodissociation of C_6H_5I.[19] Because the PICS of I^* has been measured to be up to 7× lower than the PICS of I (ground state, $^2P_{3/2}$),[43] even a small amount of I^* in the overall I atom mixture could substantially lower the 127 amu MBMS signal. However, it was assumed that I^* was quenched to I by collision with C_3H_6 at a faster rate than the resolution of the MBMS experiment (~1 ms).[44, 45] This assumption is supported by the independence of MS CI,0 on [C3H6] shown in Table 3. Interestingly, even without C3H6 (no quenching gas) MS $C_{I,0}$ is still the same, perhaps suggesting quenching on the walls during sampling.

S2. Experimental Procedure for Quantifying PICS

10.5 eV photoionization cross sections (PICS) were quantified by flowing both a controlled but imprecisely known concentration of species *i*, and a known concentration of the calibration gas mixture (calmix, consisting of 100 ppm propene, 1,3-butadiene, furan, benzene, cyclohexane, toluene and heptane) through the quartz flow reactor while recording PI TOF-MS signal, *S*. A portion of the gas mixture was trapped at the inlet of the reactor by a pneumatically controlled sample loop, and the relative concentration, *C*, of *i* to calmix in the mixture was quantified using Gas Chromatography (GC)/MS. PICS for species i, σ_{i}, could then be quantified using one of the calmix species as an internal standard:

$$\sigma_{\mathrm{i}} = \sigma_{\mathrm{calmix}} \times \left(\frac{S_i}{S_{calmix}}\right) \times \left(\frac{C_{calmix}}{C_i}\right)$$

PICS were quantified in this manner for different concentration ratios and for *i* = hexane, styrene and 3-phenylpropene. At each concentration ratio three replicate measurements were taken (both GC/MS and PI TOF-MS measurements were repeated). Average PICS with 95% confidence intervals are reported in Figure S 3, Figure S 4 and Figure S 5 below, using either toluene or heptane as the internal standard. The measured PICS for both hexane[24] and styrene[23] are in good agreement with literature, which is encouraging, especially considering that the absolute PICS of hexane and styrene differ by about an order of magnitude. Most importantly, the measured PICS for 3-phenylpropene is 38.8$\pm$7.0 MB (no literature value available for comparison), which seems reasonable given that many of the other closed-shell aromatic-containing compounds in Table S 3 have PICS ~30-40 MB.

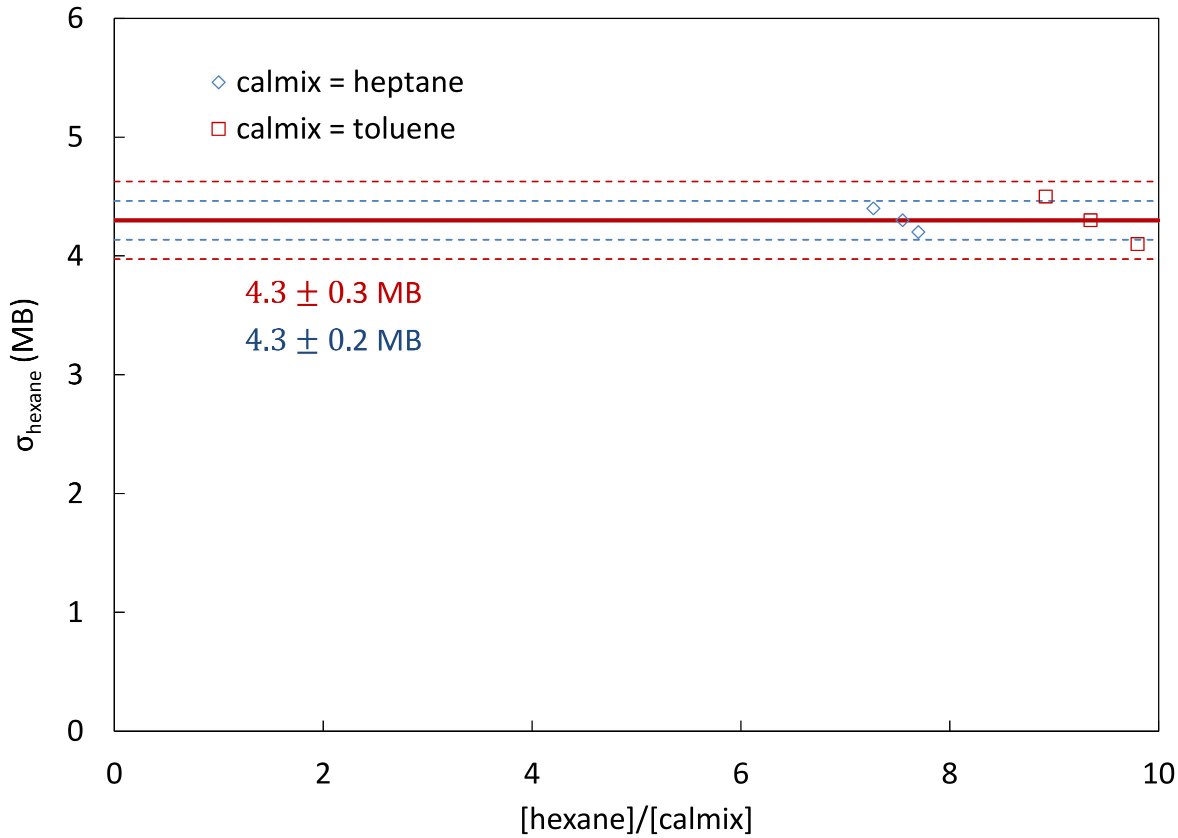

Figure S 3: Quantification of hexane 10.5 eV PICS. Literature value is 4.5±0.7.[24]

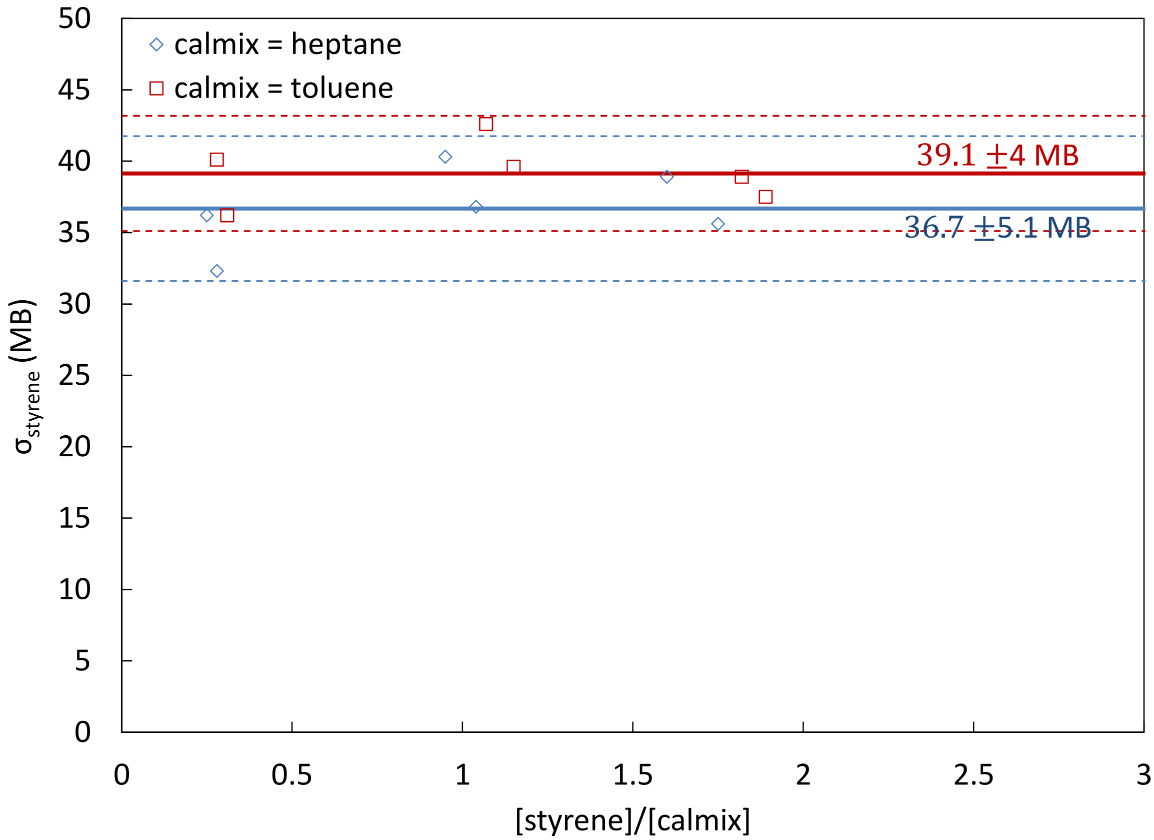

Figure S 4: Quantification of styrene 10.5 eV PICS. Literature value is 42.9±4.3.[23]

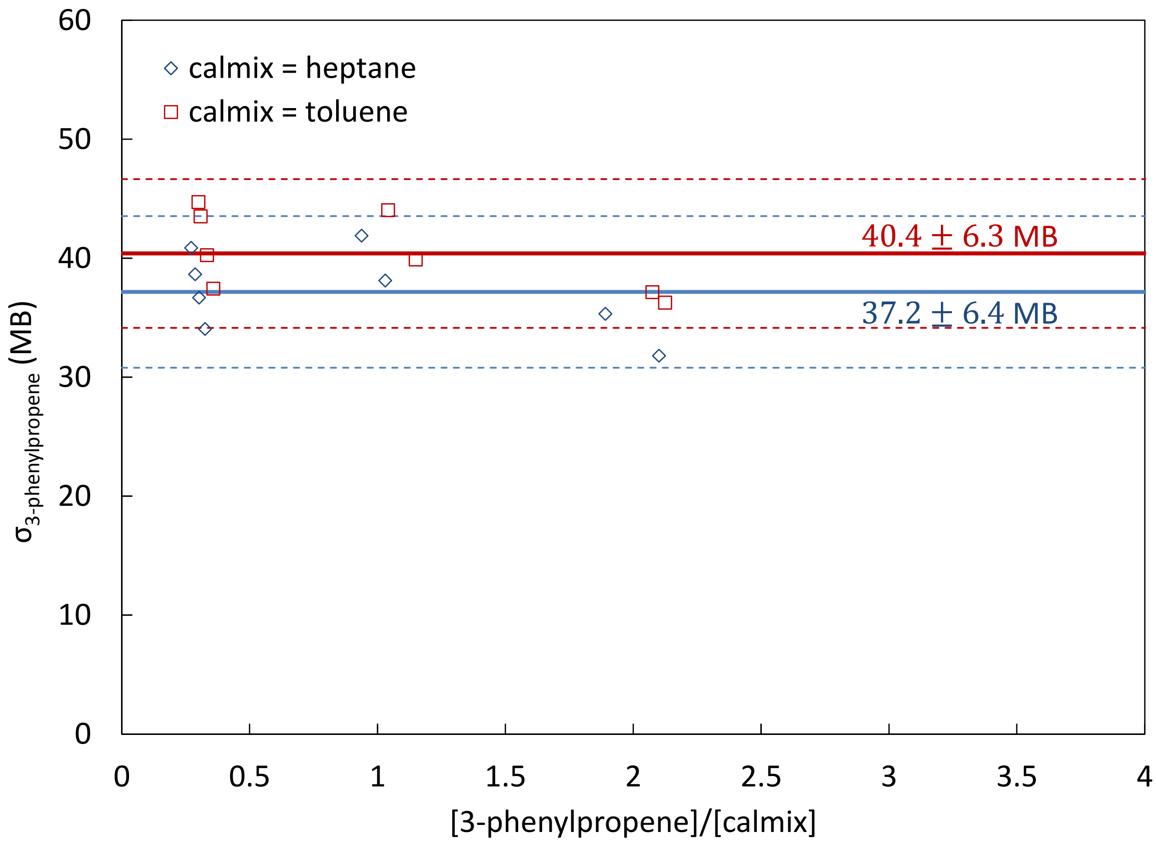

Figure S 5: Quantification of 3-phenylpropene 10.5 eV PICS.

While this experimental procedure for quantifying PICS seems to work well for stable molecules with relatively strong CC and CH bonds, for heavier molecules with weaker bonds it is expected that wall-effects and thermal decomposition will make precise concentration measurements more difficult. For example, attempts to quantify PICS for nitrosobenzene, C_6H_5NO, were less successful, likely because of both adsorption of C_6H_5NO on the walls of the sampling loop, and thermolysis of the weak C-N bond upon heating of the loop to encourage desorption.

S3. Measured Fragmentation Patterns

S3.1 C_3H_5I

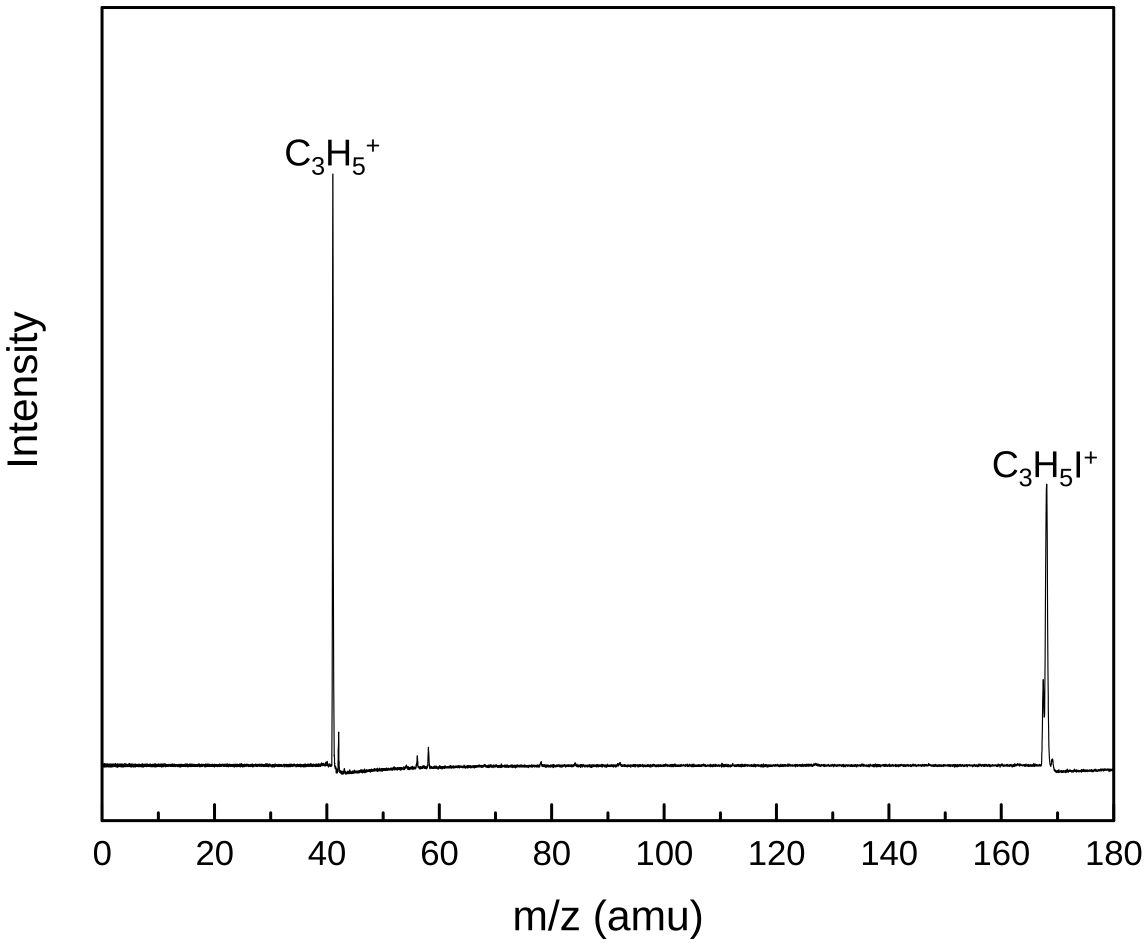

Figure S 6: Measured fragmentation pattern of C_3H_5I at 10.5 eV displaying signals at m/z = 168 ($C_3H_5I^+$ parent ion) and 41 amu ($C_3H_5^+$ daughter ion). Signal at 58 amu is from acetone impurity.

S3.2 ***i1**-Br*

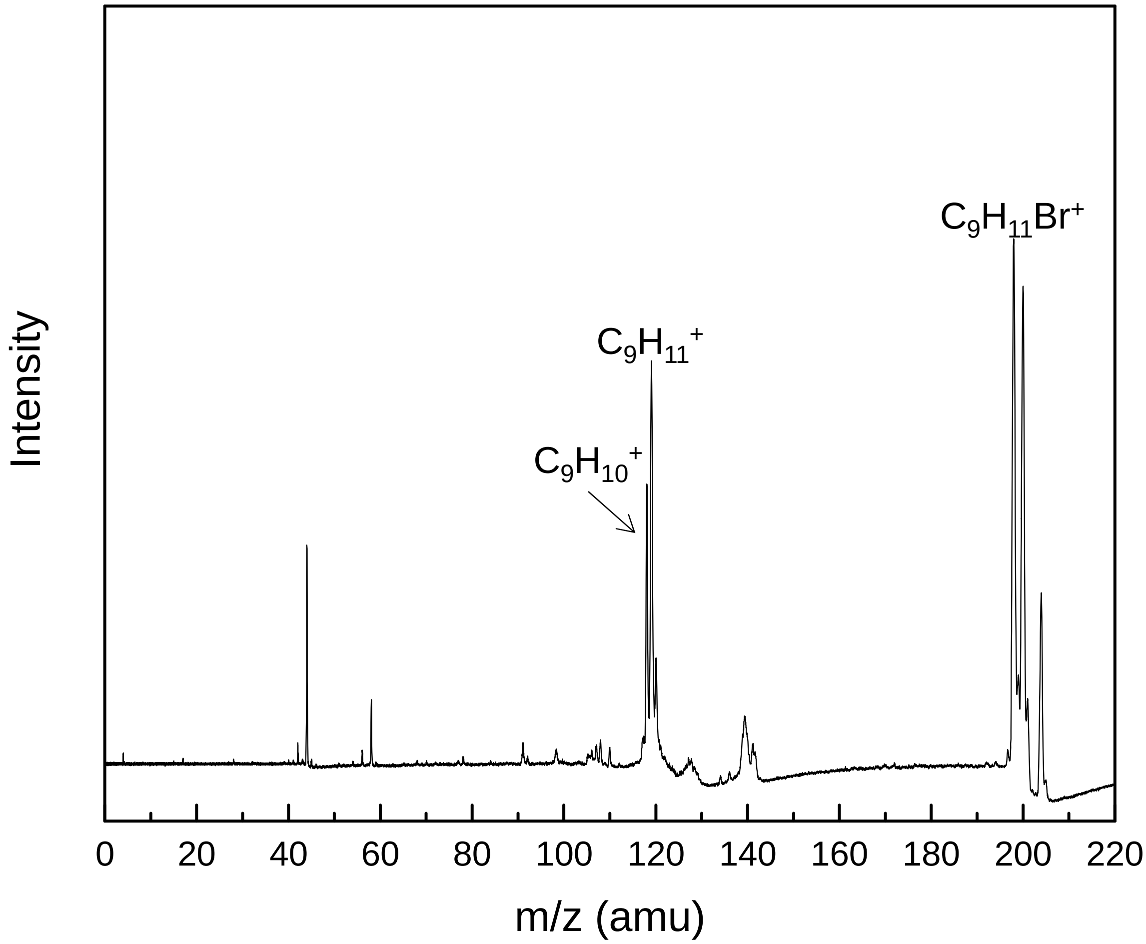

Figure S 7: Measured fragmentation pattern of **i1**-Br at 10.5 eV displaying signals at m/z = 198/200 ($^{79}Br/^{81}Br$ isotopologues of $C_9H_{11}Br^+$ parent ion), 119 ($C_9H_{11}^+$ daughter ion) and 118 amu ($C_9H_{10}^+$ daughter ion). Signals at 58 and 204 amu are from acetone and iodobenzene impurities, respectively. Source of 44 amu signal is unkown.

S4. Predicted Methyl Radical MBMS Profiles

Figure S 8 shows predicted methyl radical, CH_3, time profiles in the MBMS at 600 and 700 K. CH_3 is a coproduct of styrene from C_6H_5 + C_3H_6, which is the major product channel at 700 K. However, even though the concentration of CH_3 in the reactor should be relatively high we were unable to detect it with MBMS for the three reasons mentioned in section 4.4 of the main text: low MBMS signal due to mass discrimination factor and small PICS, overlap with a C_3H_6 fragment and lack of a CH_3 wall reaction in the model. At 600 K, the maximum predicted MS signal is ~0.003 (units of flight-time integrated signal area), whereas the smallest signals detected were ~0.001. At 700 K, the predicted CH_3 signal has increased ~3× due to more styrene production, and should be distinguishable from the noise. However, at both temperatures the model predicts CH_3 to persist over the full 45 ms measurement time, which is not reasonable given that phenyl radical decays within ~10 ms largely due to wall reactions. Therefore, if CH_3 wall reaction were included in the model, the maximum predicted CH_3 MBMS signal in Figure S 8 would drop significantly, likely below the MBMS detection limit. However, in the absence of any measurable CH_3 signal on which to base k_{wall} for CH_3, no value was fit.

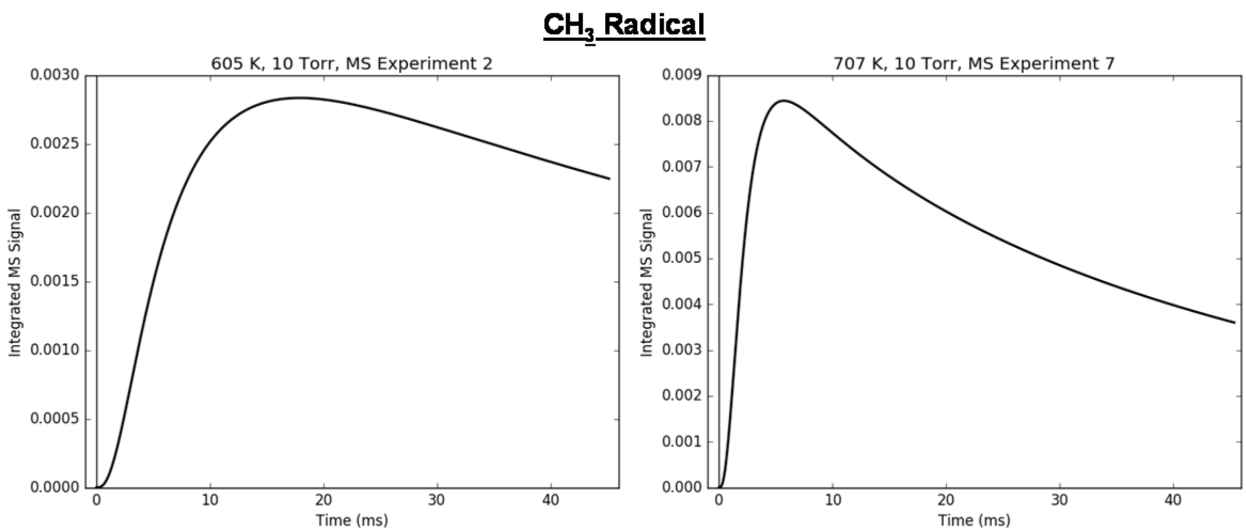

Figure S 8: Predicted time profile for methyl radical, CH_3, in MBMS at 600 (left) and 700 K (right).

S5. Measured MBMS Profiles

Measured and modelled time-dependent MBMS profiles are shown below for all 15 experiments in Table 3 at all m/z's where transient behavior was observed. Interpretive commentary is also provided for each Experiment #.

Experiments without any propene, C_3H_6, (# 1, 6, 12 and 14) merit special attention, as they exhibit evidence of wall catalysis. However, as mentioned in the main text and shown below, the primary product distribution was found to be insensitive to [C_3H_6] ("low", "medium" and "high" concentrations) suggesting that wall catalysis is not impacting the main results of this work.

Experiments #5 and 13 are also important, as they exhibit the largest disagreement between the primary product measurements and the model at 600 and 700 K, respectively. Nonetheless, the disagreements are all within a factor of two, which is acceptable given that the model relies on many uncertain parameters (e.g., calculated barrier heights, initial radical concentration and PICS). Additionally, when compared in aggregate across all 15 MBMS experiments, the model and measurements are in sufficient agreement to give confidence to extrapolations of the model.

S5.1 Experiment 1: 600 K, 10 Torr, No Propene

Figure S 9 summarizes the results of Experiment #1, which was conducted without C_3H_6. There are several noteworthy observations. Most obviously, the model does not match most of the MBMS measurements. In fact, of the six m/z's where transient behavior was observed, only 154 amu, biphenyl, has good agreement between the model and measurements. The other five m/z signals are all influenced by the walls in some way that is not described by our gas-phase model. Specifically, phenyl radical, C_6H_5, at m/z=77 amu is being rapidly converted to benzene, C_6H_6, at 78 amu, much faster than can be explained by gas-phase chemistry. Although the model does predict some C_6H_6 formation through self-disproportionation between two C_6H_5 radicals, it is not nearly enough to explain the large and rapidly-appearing 78 amu signal. Hydrogen (H)-abstraction from the iodobenzene precursor, C_6H_5I, is not included in the model but is expected to be slow at our experimental conditions owing to the strength of a phenylic C-H bond.[20] If C_6H_6 was being formed purely in the gas phase, then the time constant of its growth should match the time constant of both C_6H_5 decay and biphenyl growth, which it clear does not.

Similarly, I atom at 127 amu somehow gains a hydrogen atom, H, to form HI at 128 amu, although the time-scale is longer than C_6H_6 formation. I atom also recombines with itself to form molecular iodine, I_2, at 254 amu in much higher concentration than predicted by the model, which uses a recommended P-dependent rate for 2I (+ M) → I_2 (+M) in a helium bath gas that is very slow at our conditions.[17]

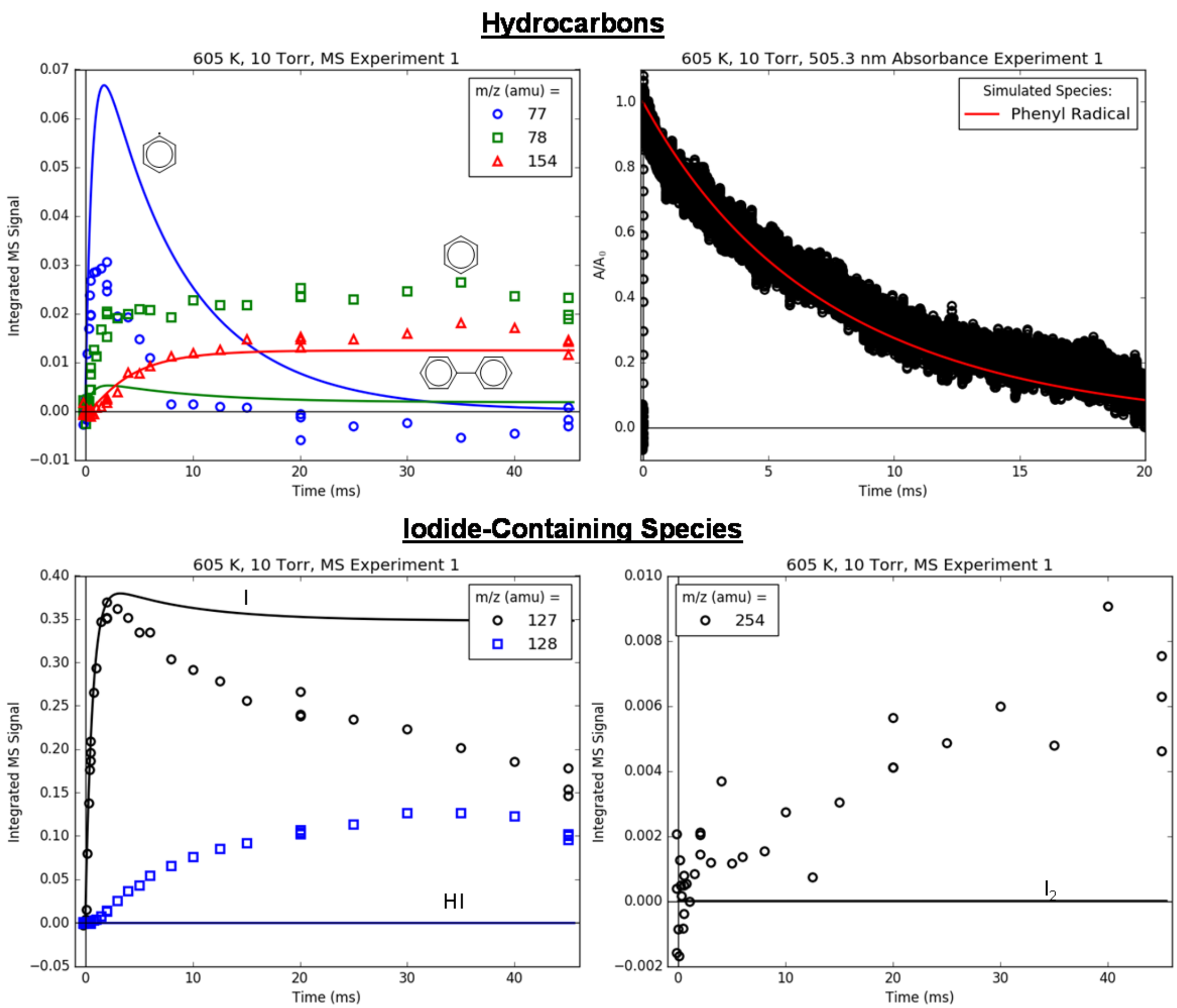

Figure S 9: Summary of all time profiles measured (markers) with MBMS in Experiment 1 (600 K, 10 Torr, no propene). Lines are model results. Simultaneously recorded 505.3 nm absorbance is also shown with model comparison.

The proposed mechanism for most of these unexpected observations involves an Eley-Rideal type of heterogeneous reaction on the quartz reactor walls between a gas-phase radical and an adsorbed H atom (denoted H-wall):

$$C_6H_5/I\,(g) + H - \mathrm{wall} \rightarrow C_6H_6/HI(g)$$

H atom might have adsorbed on and saturated the walls from previous experiments. The reaction above is essentially an H-abstraction between the wall and gas-phase C_6H_5/I, similar to what has been observed between gas-phase fluorine atoms and deuterium adsorbed on various surfaces (including quartz).[46] The mechanism for I_2 formation is probably different, but also likely involves the walls. For example, ro-vibrationally excited I_2 formed immediately after I atom recombination might be stabilized by the walls much more than by the helium bath gas, which is an inefficient collision partner.

If the proposed mechanism for $C_6H_6/HI/I_2$ formation above is correct, then by adding a sufficient amount of an excess reagent (e.g., C_3H_6) wall catalysis might be suppressed in favor of fast gas-phase chemistry (e.g., C_6H_5 + C_3H_6 and subsequent product formation). This was the approach taken here, where primary product branching was measured at three different propene concentrations ("low", "medium" and "high") that vary by 4× in order to verify insensitivity to [C_3H_6], and therefore insensitivity to wall catalysis as well. Comparing Experiments #2-5 (600 K) and #7-9 (700 K), the primary product branching does appear to be largely insensitive to [C_3H_6], confirming that wall catalysis is not influencing the main results of this work.

Although we have found a way to sidestep the effects of wall catalysis in the current work, efforts should continue to be made to reduce the effects further. Specifically, we found the geometry of the sampling pinhole to be quite critical to preventing wall catalysis, as quantified by the ratio of maximum 78 to 77 amu signal without C_3H_6. As shown in Figure S 9, the 78:77 ratio is currently ~1 using the "funnel-shaped" pinhole geometry of Wyatt *et al.*[47] Similar experiments with a straight pinhole (essentially a 300 micron diameter tube through the 2.5 mm thick reactor walls) resulted in ratios ~10:1, likely due to enhanced contact between radicals and the walls during sampling. Efforts to reduce wall catalysis even further should first focus on the pinhole. The reactor was also treated with boric acid following the procedure of Krasnoperov *et al.*,[48] but the resulting boron oxide (B_2O_3) coating was found to have negligible effect on the wall catalysis shown in Figure S 9. A better coating would have only strong C-F bonds exposed, such as in Teflon or Halocarbon wax, but neither of these coatings are suitable at the temperatures of interest to us (>600 K).

Returning to the results shown in Figure S 9, although the maximum C_6H_5 concentration is overpredicted by the model by ~2×, the sum of measured C_6H_5 and C_6H_6 signals is much closer to the model, effectively closing the mass balance. A k_{wall} of 100 s^{-1} for C_6H_5 was found to fit both the time scale of the 77 amu decay from MBMS (~10 ms) and the 505.3 nm absorbance decay adequately. No k_{wall} was fit for I atom, because it was not found to be necessary to match the experiments with C_3H_6 (see next experiment, for example).

S5.2 Experiment 2: 600 K, 10 Torr, Low Propene

All of the results from Experiment #2 are shown and discussed in the main text, but they are reproduced here for convenience. Figure S 10 summarizes the main results of Experiment #2 by comparing only the primary product MBMS profiles, whereas Figure S 11 shows the measured and modeled results for all of the m/z's with time-dependence.

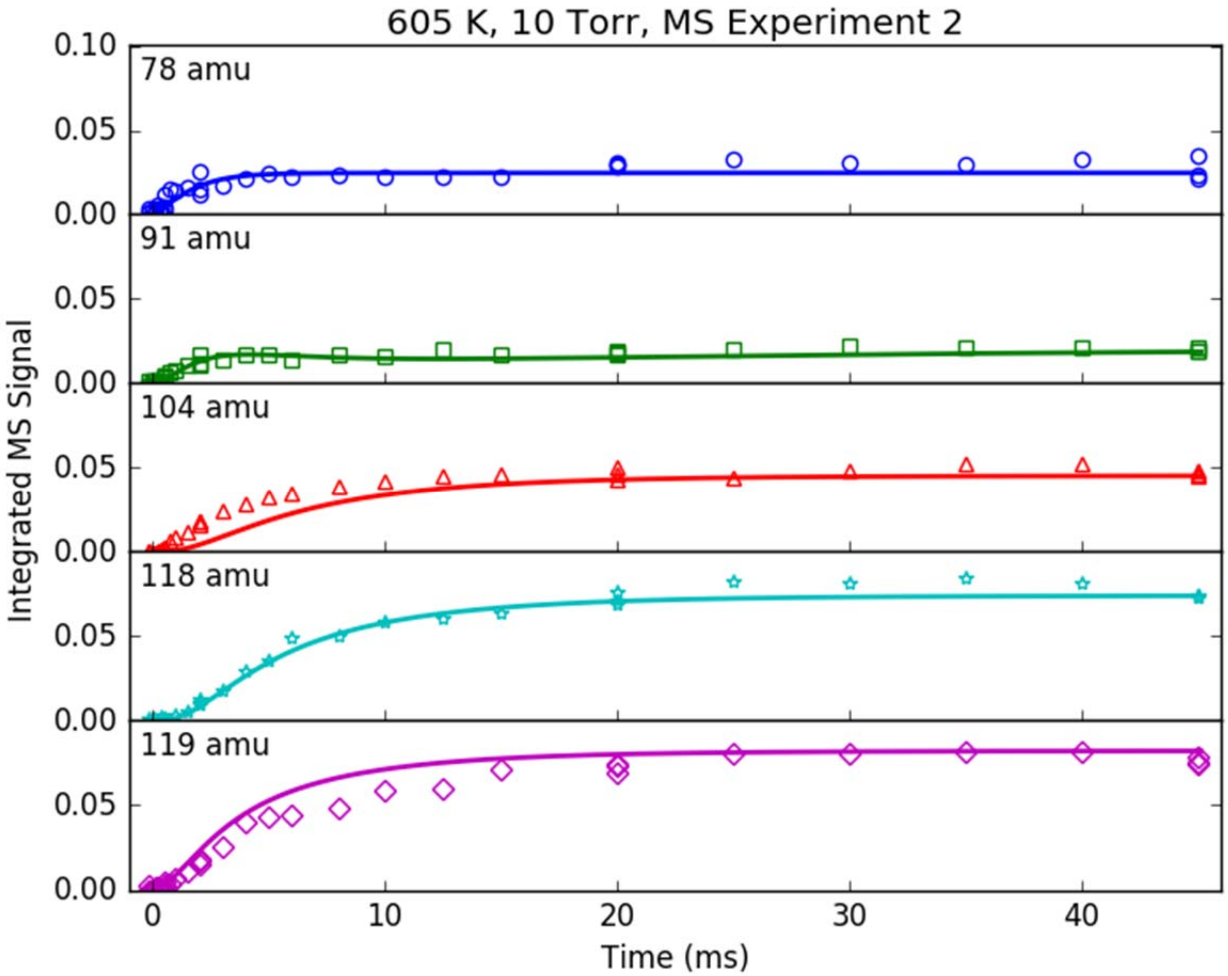

Figure S 10: Time profiles of primary phenyl radical + propene products measured (markers) with MBMS in Experiment 2 (600 K, 10 Torr, “Low” propene). Lines are model results.

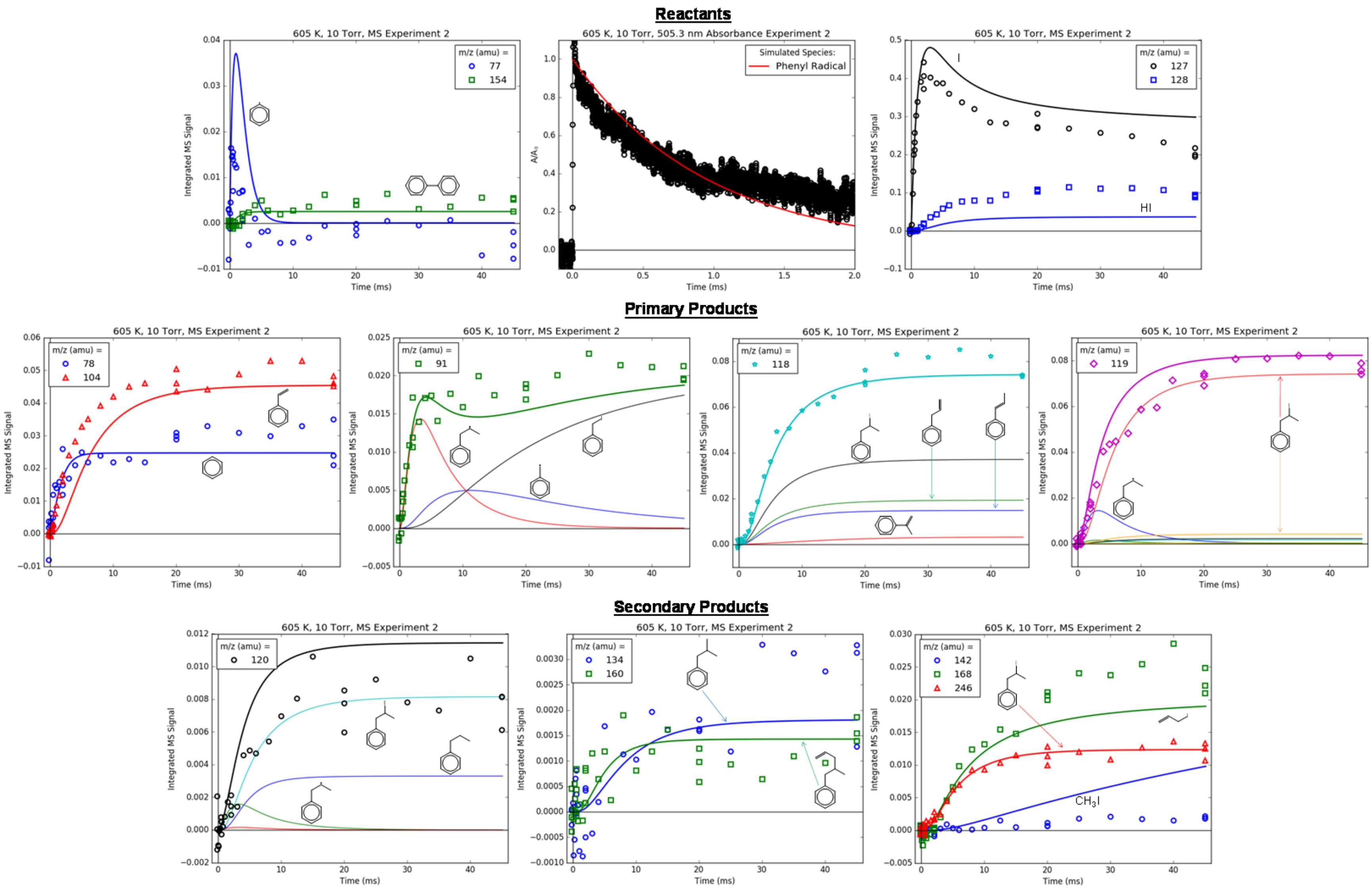

Figure S 11: Summary of all time profiles measured (markers) with MBMS in Experiment 2 (600 K, 10 Torr, "Low" propene). Lines are model results. Simultaneously recorded 505.3 nm absorbance is also shown with model comparison.

S5.3 *Experiment 3: 600 K, 10 Torr, Medium Propene*

Experiment #3 is identical to #2, except [C_3H_6] has been doubled (Table 3). As expected, the measurements for Experiment #3, summarized in Figure S 12 and Figure S 13, are similar to #2. In particular, the relative 78 amu (C_6H_6) signal did not decrease significantly upon doubling [C_3H_6], suggesting that the C_6H_6 observed is from gas phase H-abstraction between C_6H_5 and C_3H_6 rather than from heterogeneous H-abstraction from the wall (see commentary for Experiment #1). Although all of the primary products are noticeably underpredicted by the model, the disagreement is generally within the 15% uncertainty of the PICS alone, and in the case of 118 and 119 amu, which are mostly attributable to fragments of **i1**-I, the PICS (and fragmentation pattern) are just estimates. Regarding secondary products, both 134 (**i1**-CH_3) and 168 amu (C_3H_5I) are underpredicted, but are still within a factor of 2 of the model.

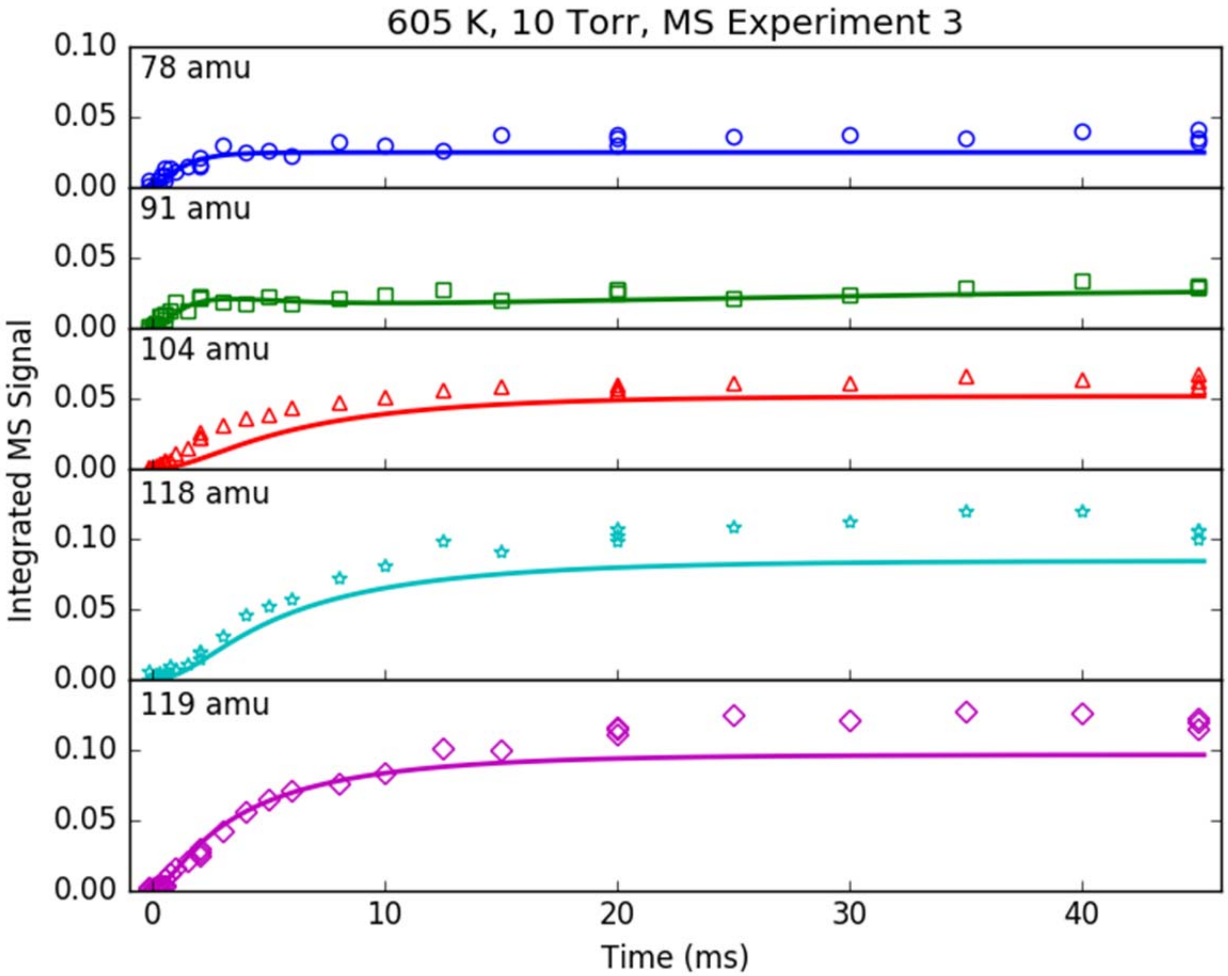

Figure S 12: Time profiles of primary phenyl radical + propene products measured (markers) with MBMS in Experiment 3 (600 K, 10 Torr, "Medium" propene). Lines are model results.

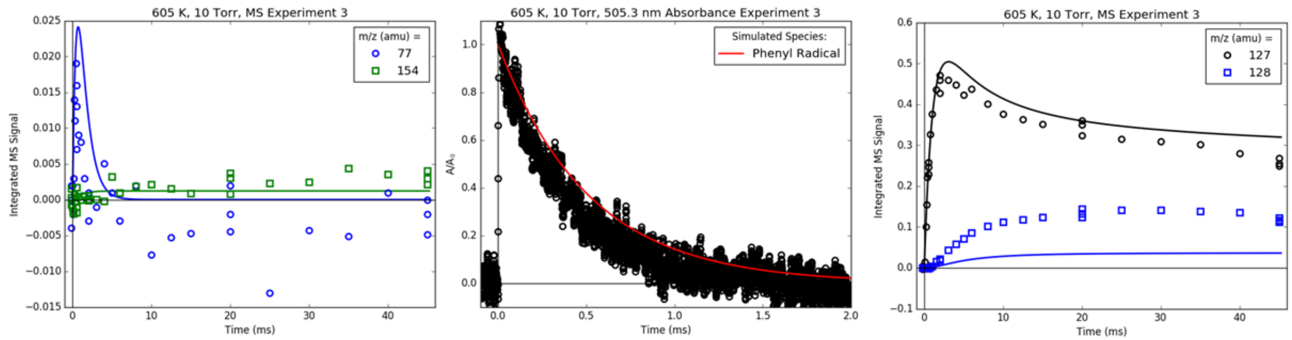

Primary Products

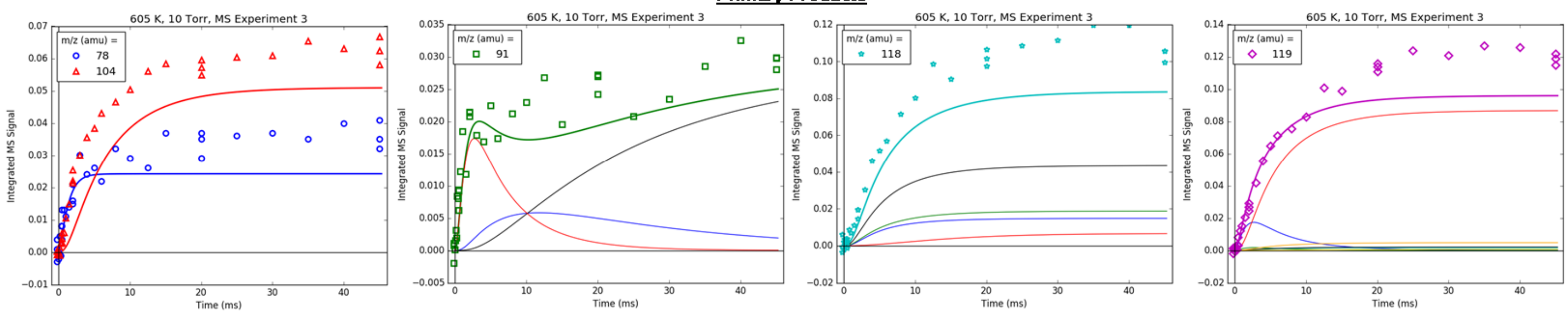

Secondary Products

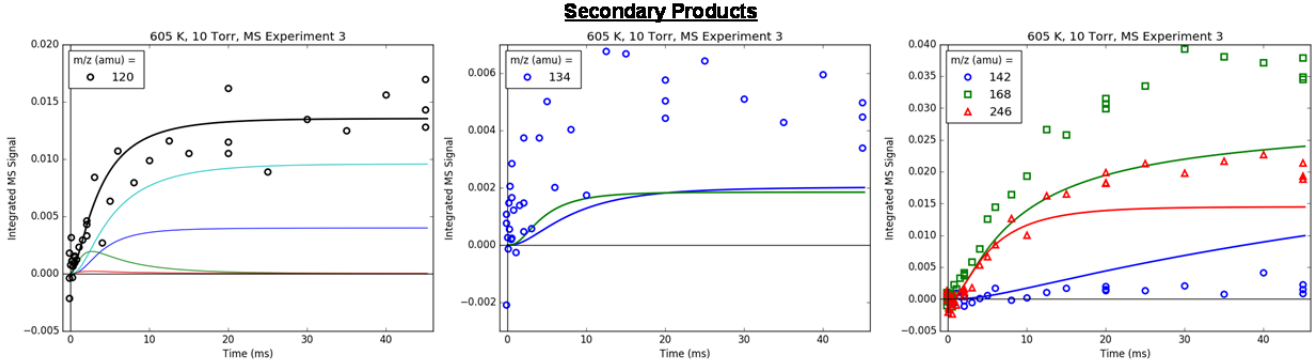

Figure S 13: Summary of all time profiles measured (markers) with MBMS in Experiment 3 (600 K, 10 Torr, "Medium" propene). Lines are model results. Simultaneously recorded 505.3 nm absorbance is also shown with model comparison.

S5.4 Experiment 4: 600 K, 10 Torr, High Propene

Experiment #4 was conducted at the highest [C_3H_6] and as expected the model and measurements are still in satisfactory agreement. As already mentioned for Experiment #3, the agreement of the gas-phase model with the measured 78 amu MBMS signal at three different [C_3H_6] (varied over a factor of 4 from Experiment #2-4) is especially important, as it demonstrates that wall catalysis is not perturbing the primary C_6H_5 + C_3H_6 product distribution.

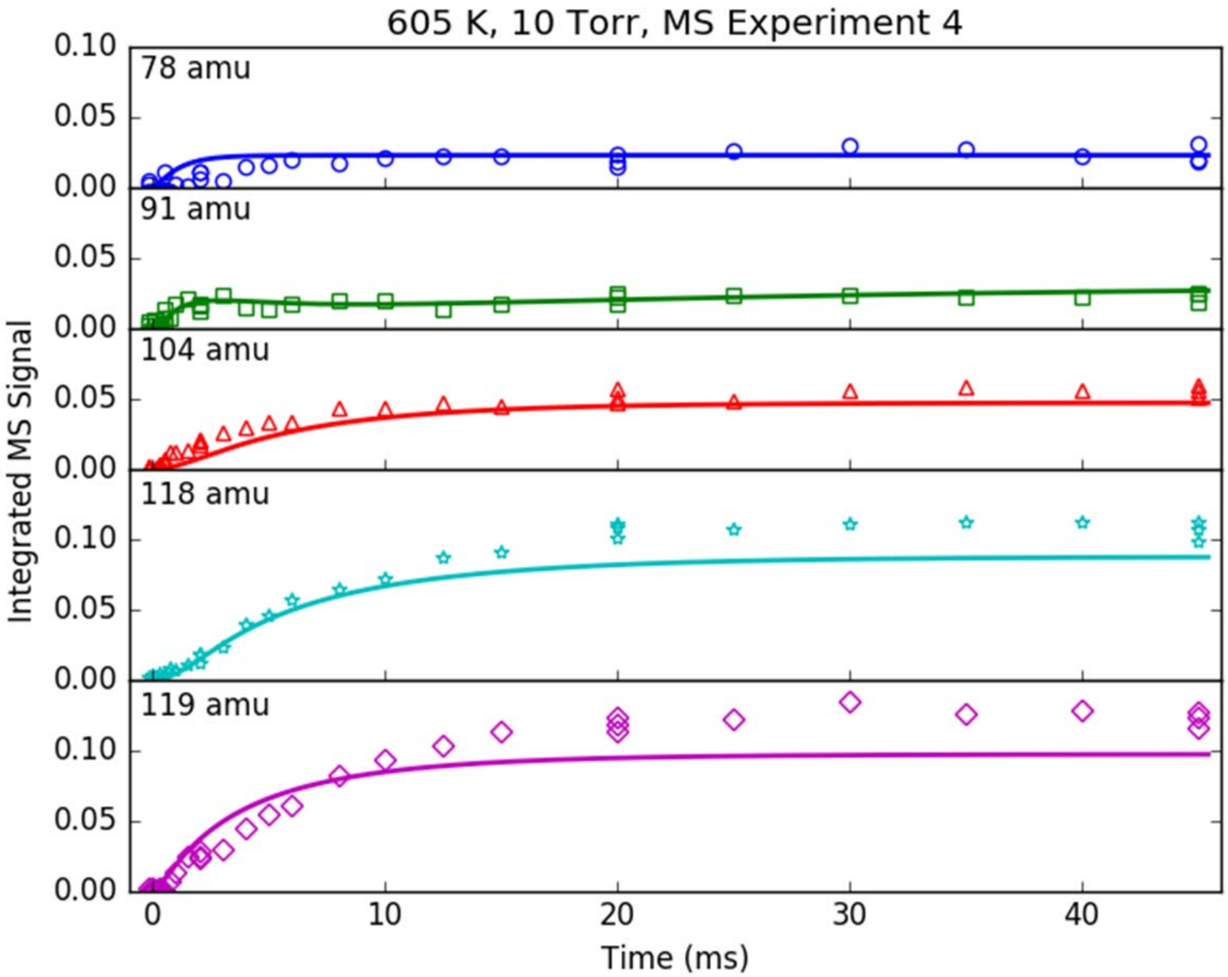

Figure S 14: Time profiles of primary phenyl radical + propene products measured (markers) with MBMS in Experiment 4 (600 K, 10 Torr, “High” propene). Lines are model results.

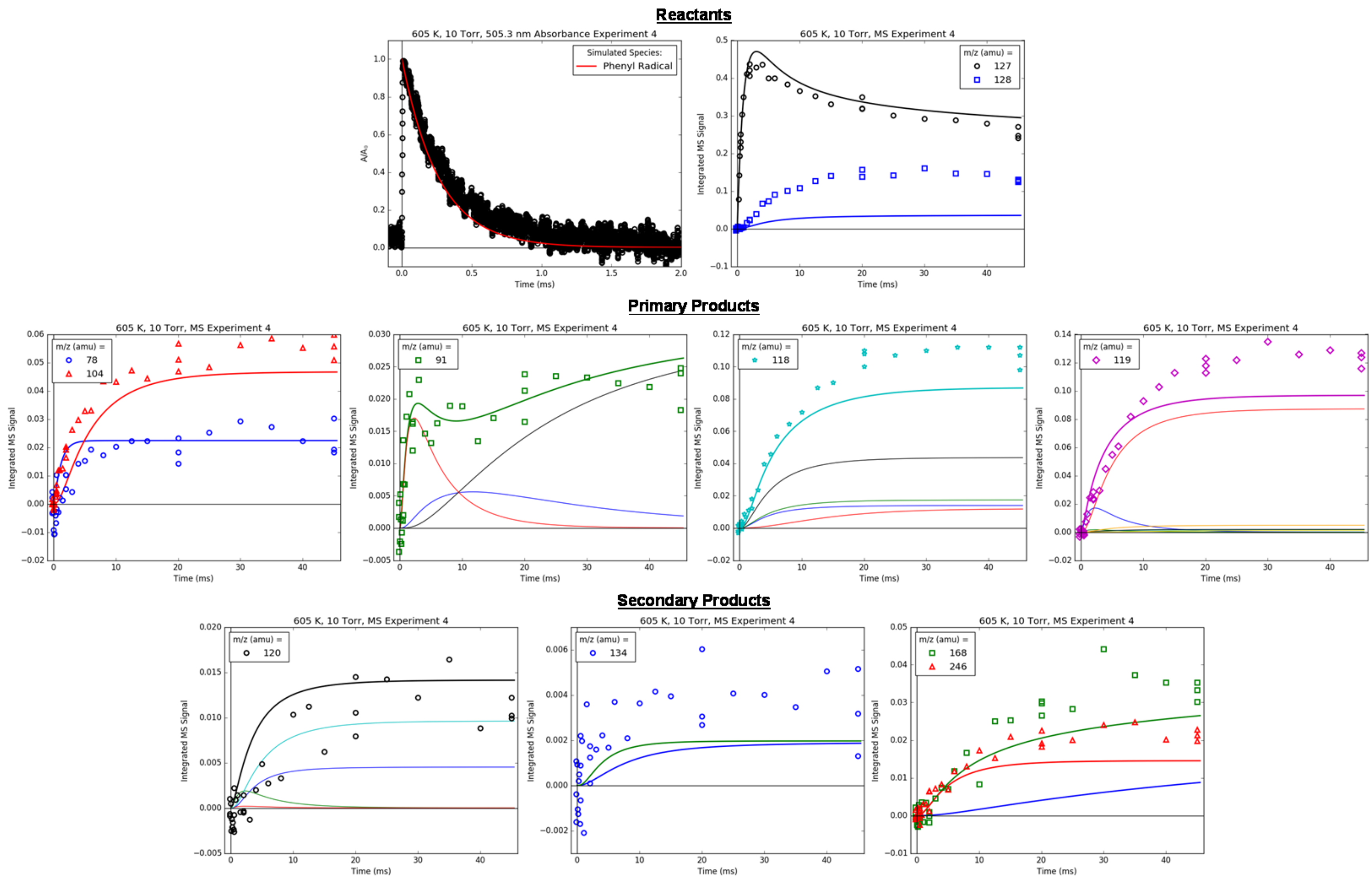

Figure S 15: Summary of all time profiles measured (markers) with MBMS in Experiment 4 (600 K, 10 Torr, "High" propene). Lines are model results. Simultaneously recorded 505.3 nm absorbance is also shown with model comparison.

S5.5 Experiment 5: 600 K, 10 Torr, Medium Propene, 2xC_6H_5I/C_6H_5 Control

Experiment #5 was conducted at identical conditions as #3, but with ~2× the radical and precursor concentration ([C_6H_5] and [C_6H_5I]). Because of the higher initial concentration, the signal to noise is better for Experiment #5 than any of the other 600 K experiments (#2-4). The agreement with the model is still satisfactory for all of the m/z's with time-dependence, except for 78 amu, which is underpredicted by almost 2×. The reason for this discrepancy is unclear. Perhaps the C_6H_5 self-disproportionation rate estimated by RMG is too slow (although the co-product, o-benzyne was not observed) or maybe wall catalysis is exacerbated at higher radical concentrations. In either case, it is preferable to operate at the lowest possible radical (and precursor) concentration to minimize such effects, which was the case for all of the other 600 K experiments.

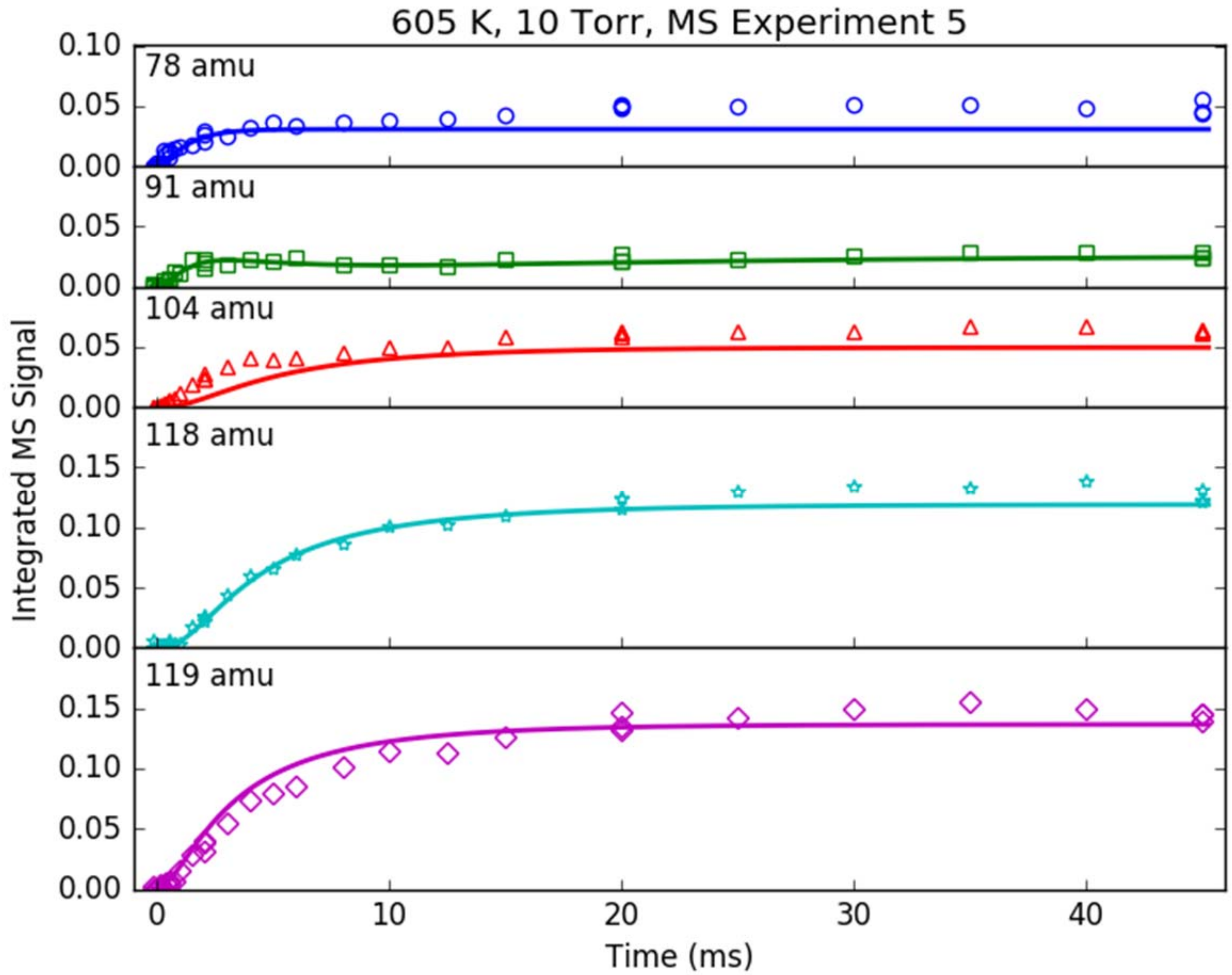

Figure S 16: Time profiles of primary phenyl radical + propene products measured (markers) with MBMS in Experiment 5 (600 K, 10 Torr, "Medium" propene, **2** ×C_6H_5I/C_6H_5 control experiment). Lines are model results.

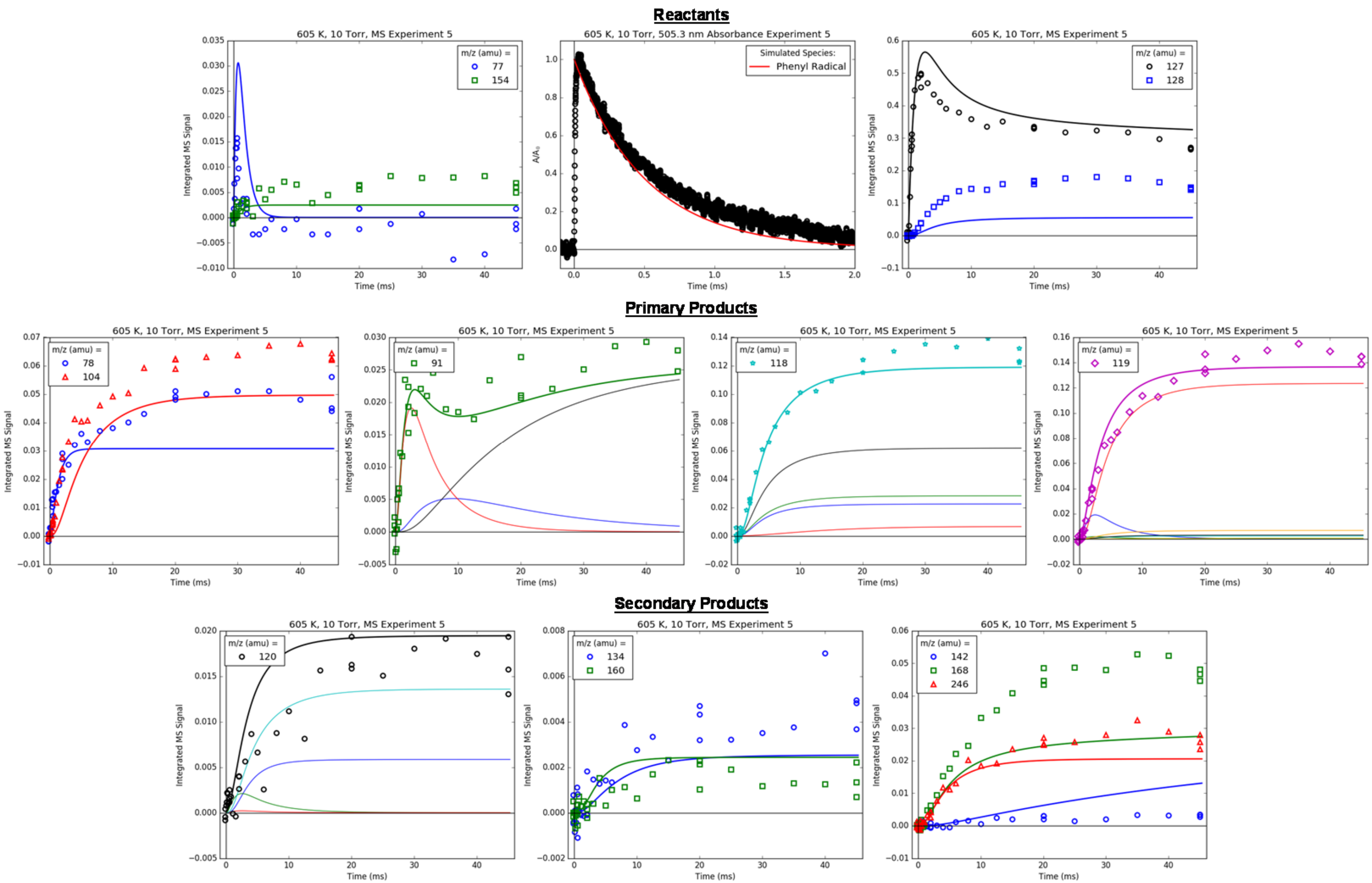

Figure S 17: Summary of all time profiles measured (markers) with MBMS in Experiment 5 (600 K, 10 Torr, "Medium" propene, **2** $\times C_6H_5I/C_6H_5$ control experiment). Lines are model results. Simultaneously recorded 505.3 nm absorbance is also shown with model comparison.

S5.6 *Experiment 6: 700 K, 10 Torr, No Propene*

Experiment #6 was conducted without C_3H_6, and all of the commentary regarding Experiment #1 (also without C_3H_6, but at 600 K) still applies. The only feature of Experiment #6 worth additional comment is that compared to #1 there appears to be less HI formation. This could be due to the higher temperature driving desorption of H atoms from the walls,[49] or it might simply be due to the fact that chronologically #6 was actually run before #1 when the reactor was freshly-cleaned and B_2O_3 coated. Also unlike Experiment #1, no I_2 was measured.

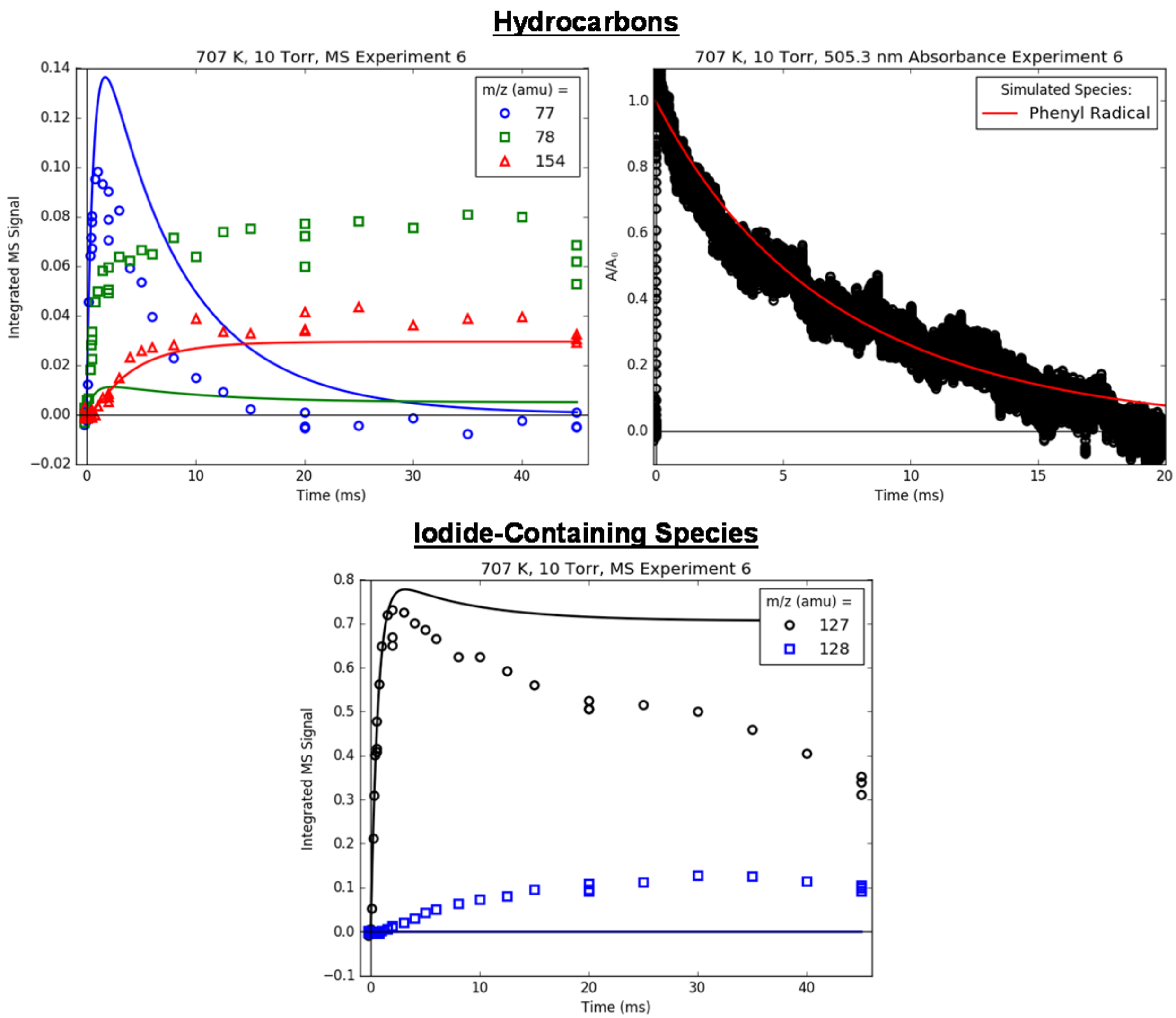

Figure S 18: Summary of all time profiles measured (markers) with MBMS in Experiment 6 (700 K, 10 Torr, no propene). Lines are model results. Simultaneously recorded 505.3 nm absorbance is also shown with model comparison.

S5.7 Experiment 7: 700 K, 10 Torr, Low Propene

All of the results from Experiment #7 are shown and discussed in the main text, but they are reproduced here for convenience.

As noted in the main text, CH_3I at 142 amu is dramatically overpredicted by the model (no transient signal was even observed in Experiment #8-10) likely due to the lack of P-dependence in the $CH_3 + I \rightarrow CH_3I$ rate taken from literature and used in the model.[14] This explanation for the lack of observed CH_3I is supported by higher-P experiments (#13 and 15) where MBMS signal at 142 amu was observed, and increased with P. Interestingly, C_3H_5I at 168 amu exhibited the opposite trend: at lower P it matches the model (Figure S 20), but with increasing P (#13 and 15) the signal disappears, in disagreement with the model. This suggest that like I_2 (see Experiment #1), C_3H_5I might be partially formed by heterogeneous recombination on the walls, which will get slower at higher P due to slower diffusion to the walls. This is consistent with the 408.4 nm absorbance results shown in section S6, where removing $C_3H_5 + I \rightarrow C_3H_5I$ from the gas-phase model resulted in much better agreement with the measured baseline-shift.

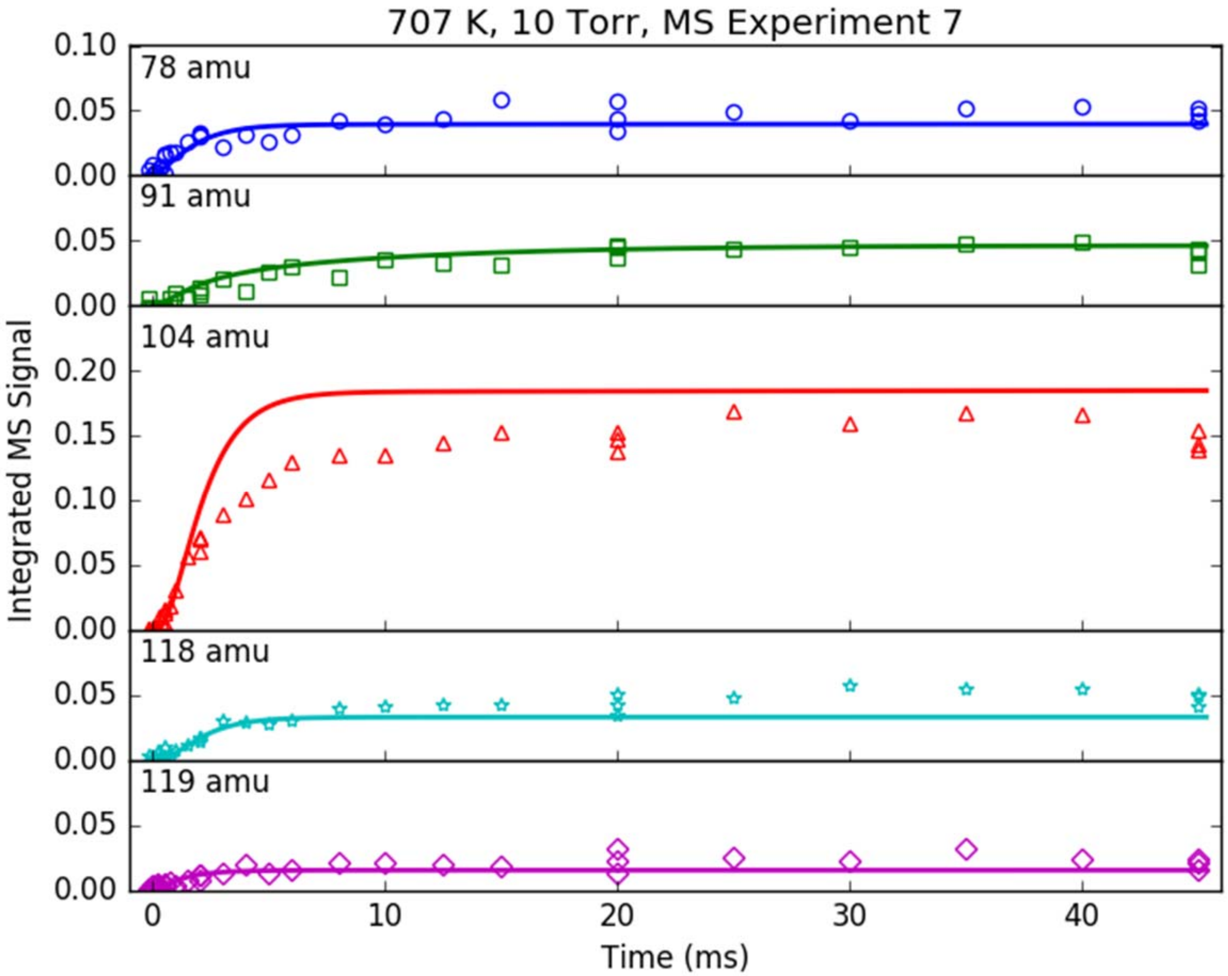

Figure S 19: Time profiles of primary phenyl radical + propene products measured (markers) with MBMS in Experiment 7 (700 K, 10 Torr, "Low" propene). Lines are model results.

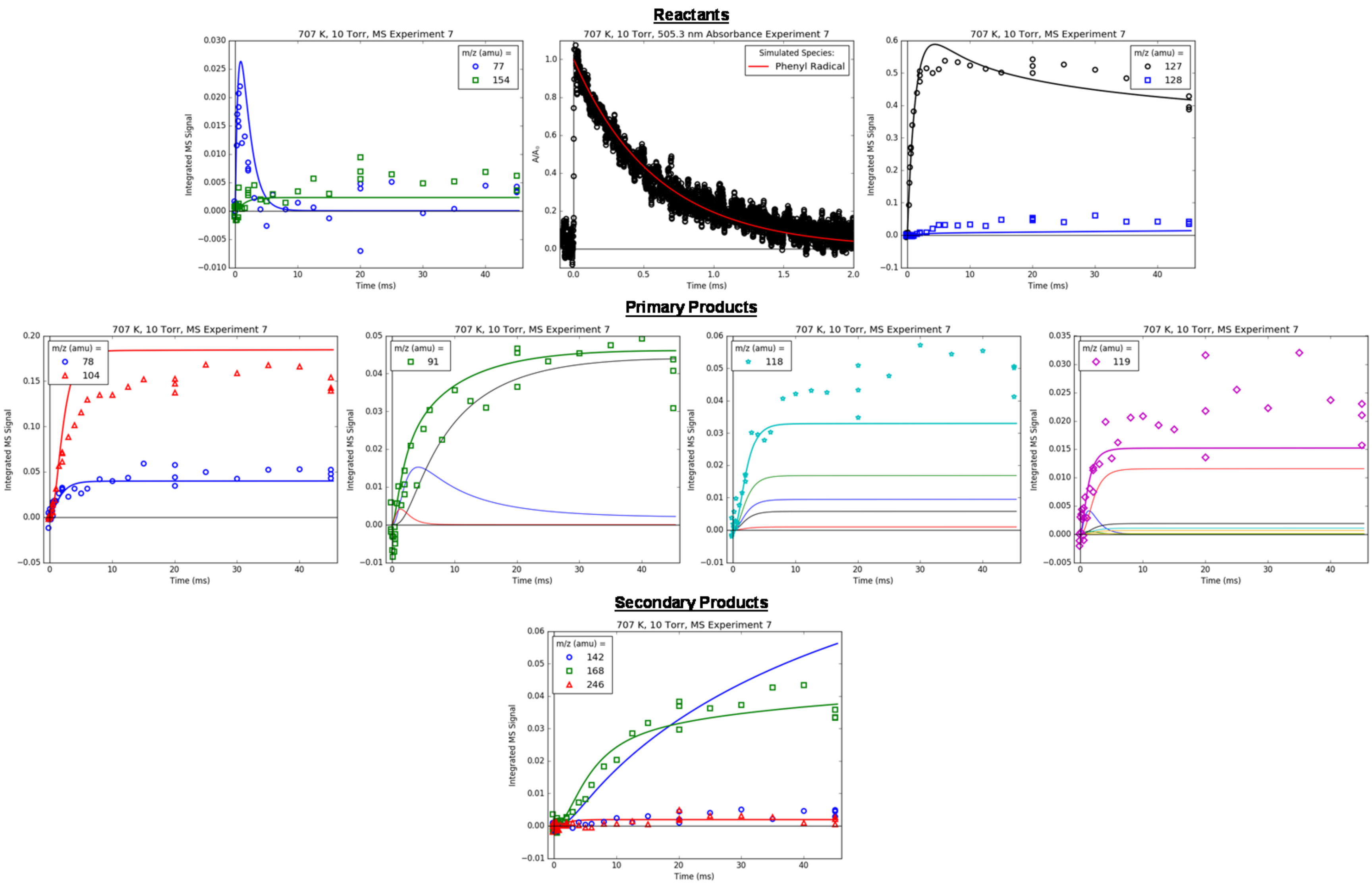

Figure S 20: Summary of all time profiles measured (markers) with MBMS in Experiment 7 (700 K, 10 Torr, "Low" propene). Lines are model results. Simultaneously recorded 505.3 nm absorbance is also shown with model comparison.

S5.8 Experiment 8: 700 K, 10 Torr, Medium Propene

Experiment #8 is identical to #7, except [C_3H_6] has been doubled (Table 3). As expected, the measurements for Experiment #8, are similar to #7. In particular, the relative 78 amu (C_6H_6) signal did not decrease significantly upon doubling [C_3H_6], suggesting that the C_6H_6 observed is from gas phase H-abstraction between C_6H_5 and C_3H_6 rather than from heterogeneous H-abstraction from the wall (see commentary for Experiment #1).

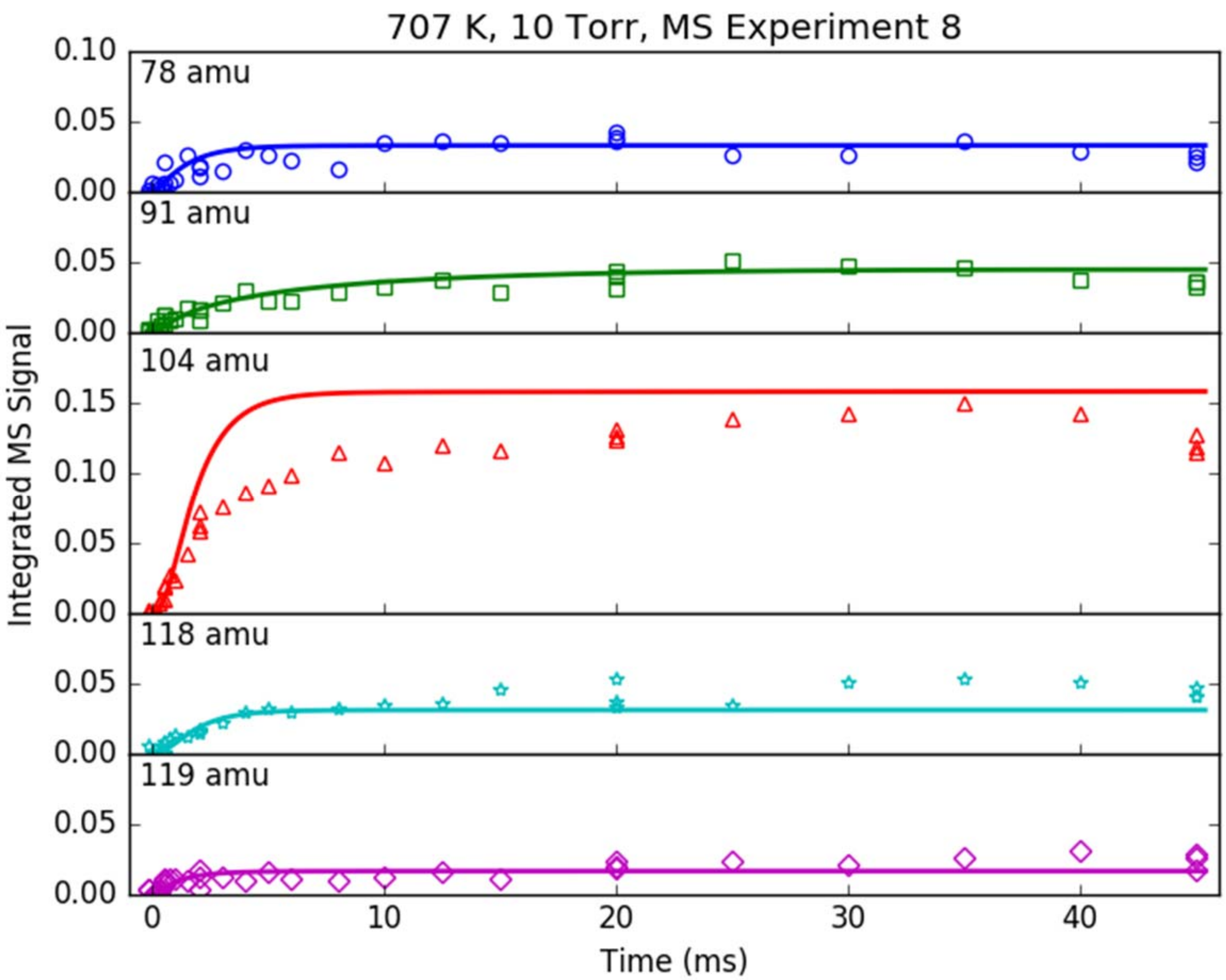

Figure S 21: Time profiles of primary phenyl radical + propene products measured (markers) with MBMS in Experiment 8 (700 K, 10 Torr, "Medium" propene). Lines are model results.

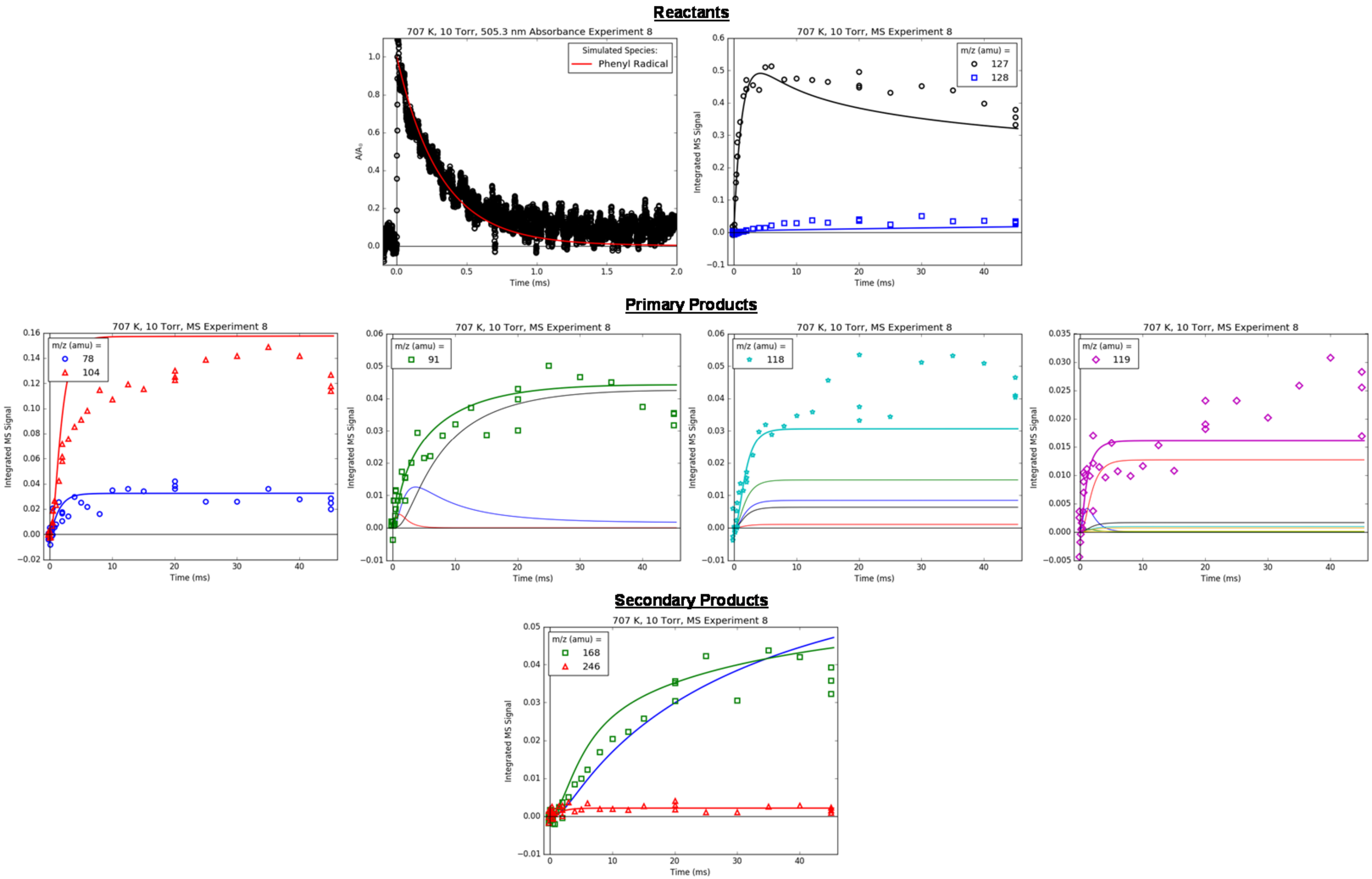

Figure S 22: Summary of all time profiles measured (markers) with MBMS in Experiment 8 (700 K, 10 Torr, “Medium” propene). Lines are model results. Simultaneously recorded 505.3 nm absorbance is also shown with model comparison.

S5.9 Experiment 9: 700 K, 10 Torr, High Propene

Experiment #9 was conducted at the highest [C_3H_6] and as expected the model and measurements are still in satisfactory agreement. As already mentioned for Experiment #8, the agreement of the gas-phase model with the measured 78 amu MBMS signal at three different [C_3H_6] (varied over a factor of 4 from Experiment #7-9) is especially important, as it demonstrates that wall catalysis is not perturbing the primary C_6H_5 + C_3H_6 product distribution. Also note that the signal to noise is generally worse compared to #7 and 8 due to the higher [C_3H_6] attenuating both VUV intensity and molecular beam density. Finally, this was one of the few experiments where the 505.3 nm absorbance did not match the model well. Most likely this is due to an imperfect background subtraction causing an apparent (non-reproducible) baseline shift, but it might also indicate the presence of a small leak that causes phenylperoxy radical, C_6H_5OO, formation (and subsequent visible absorbance[50]).

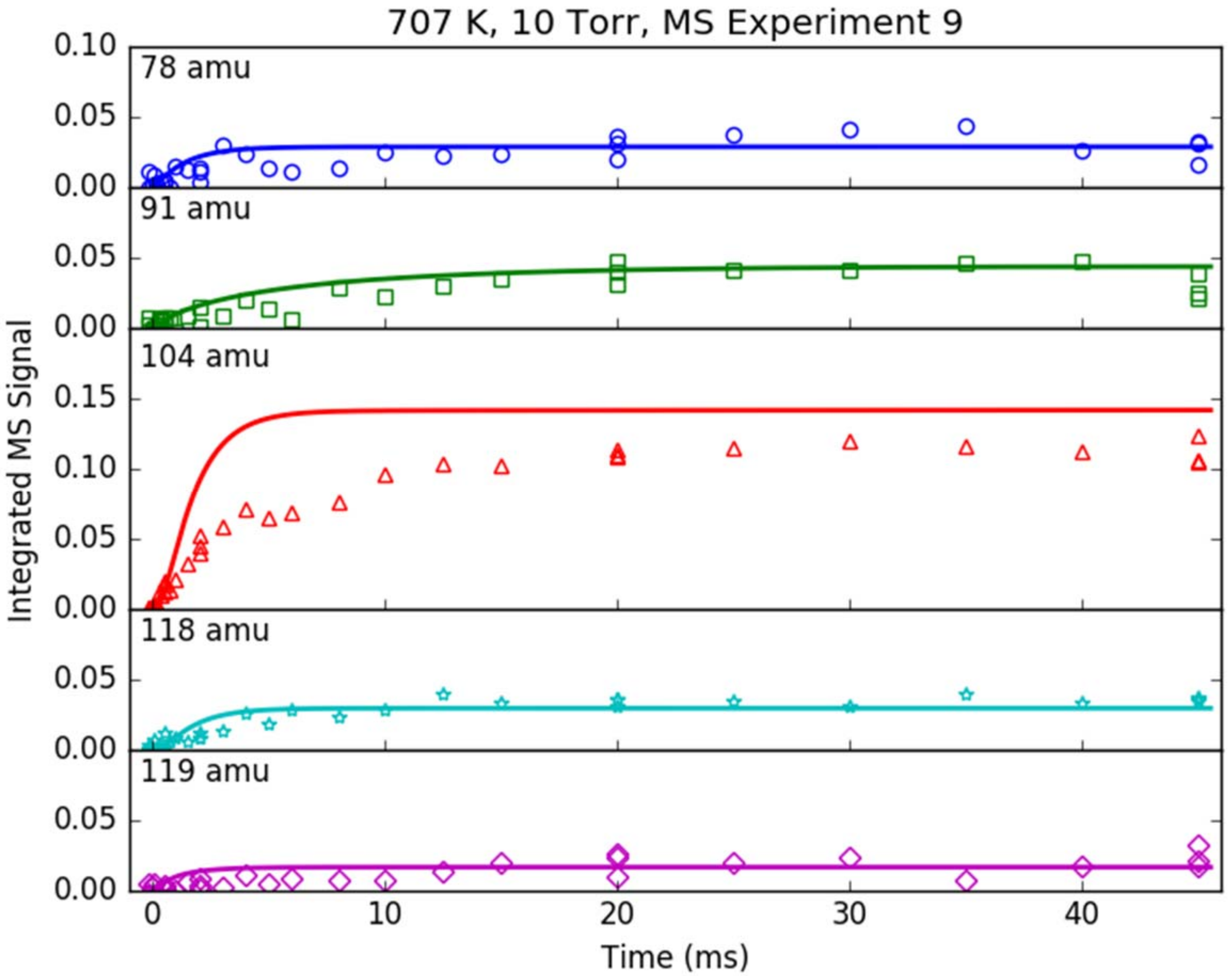

Figure S 23: Time profiles of primary phenyl radical + propene products measured (markers) with MBMS in Experiment 9 (700 K, 10 Torr, "High" propene). Lines are model results.

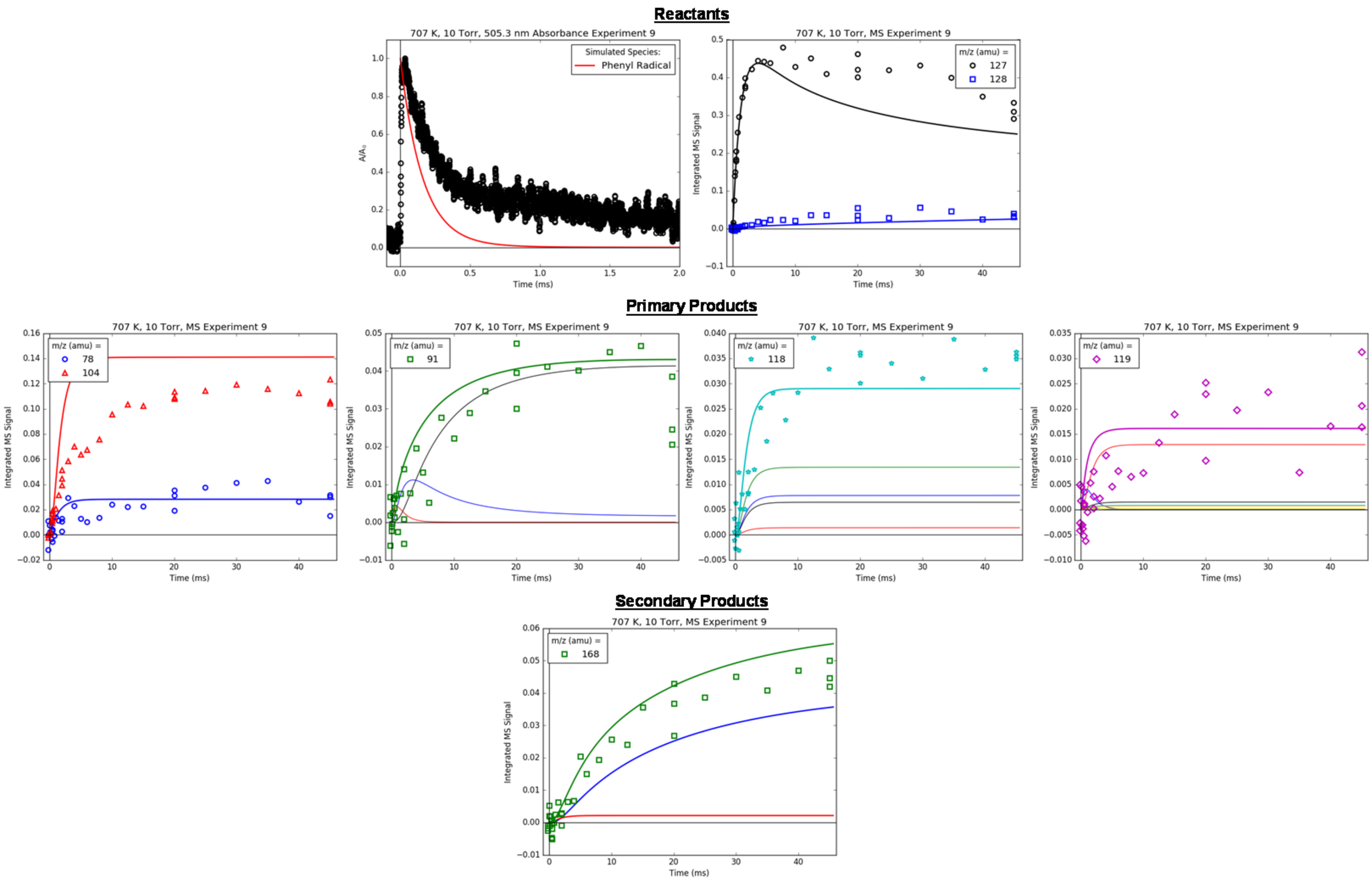

Figure S 24: Summary of all time profiles measured (markers) with MBMS in Experiment 9 (700 K, 10 Torr, "High" propene). Lines are model results. Simultaneously recorded 505.3 nm absorbance is also shown with model comparison.

S5.10 *Experiment 10: 700 K, 10 Torr, Medium Propene, 2xC_6H_5I Control*

Experiment #10 was conducted at identical conditions as #8, but with 2×[C_6H_5I]. C_6H_5 was maintained around the same concentration in both experiments by adjusting the photolysis laser fluence (Table 3). The agreement between model and experiment is still satisfactory.

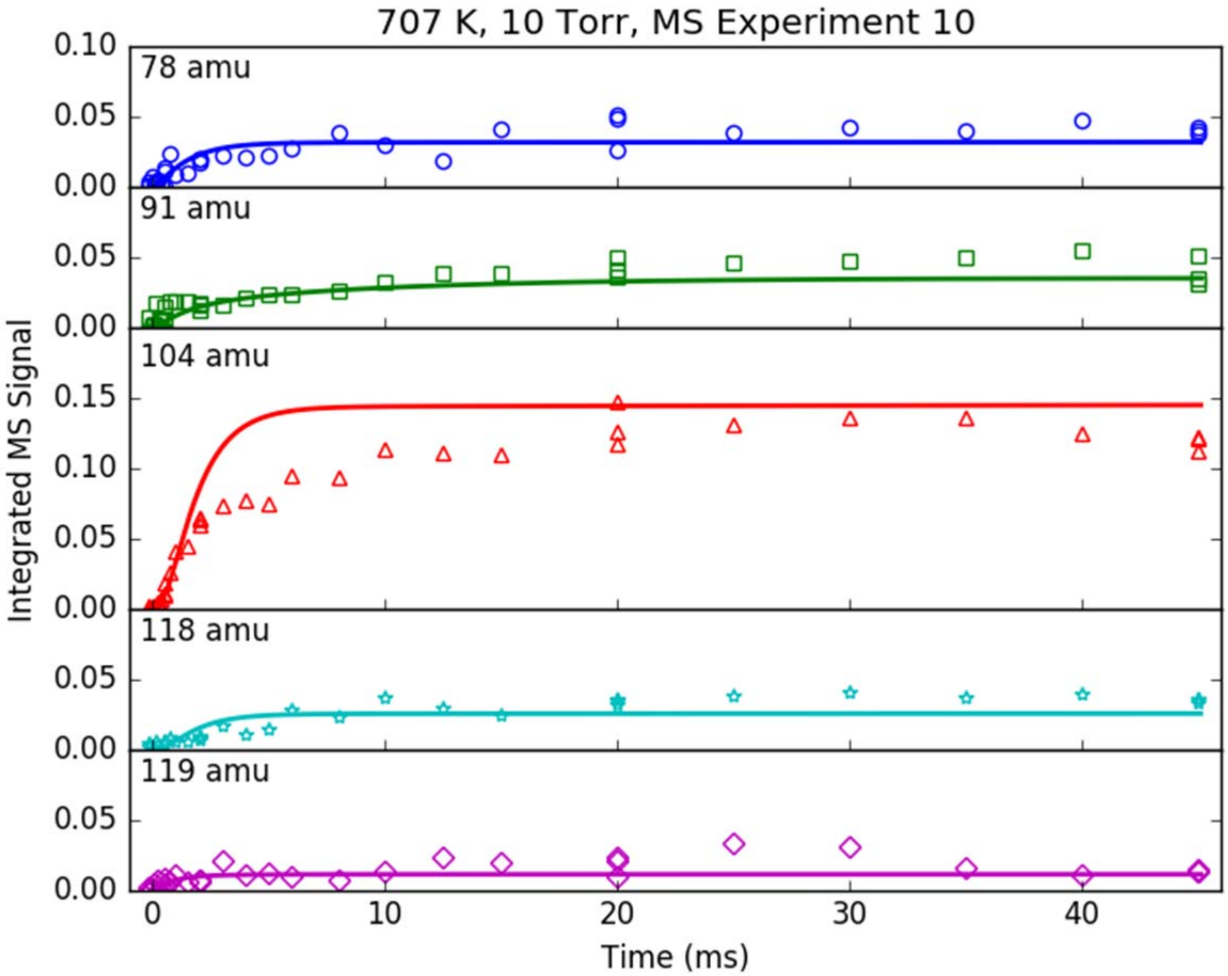

Figure S 25: Time profiles of primary phenyl radical + propene products measured (markers) with MBMS in Experiment 10 (700 K, 10 Torr, "Medium" propene, **2** ×C_6H_5I control experiment). Lines are model results.

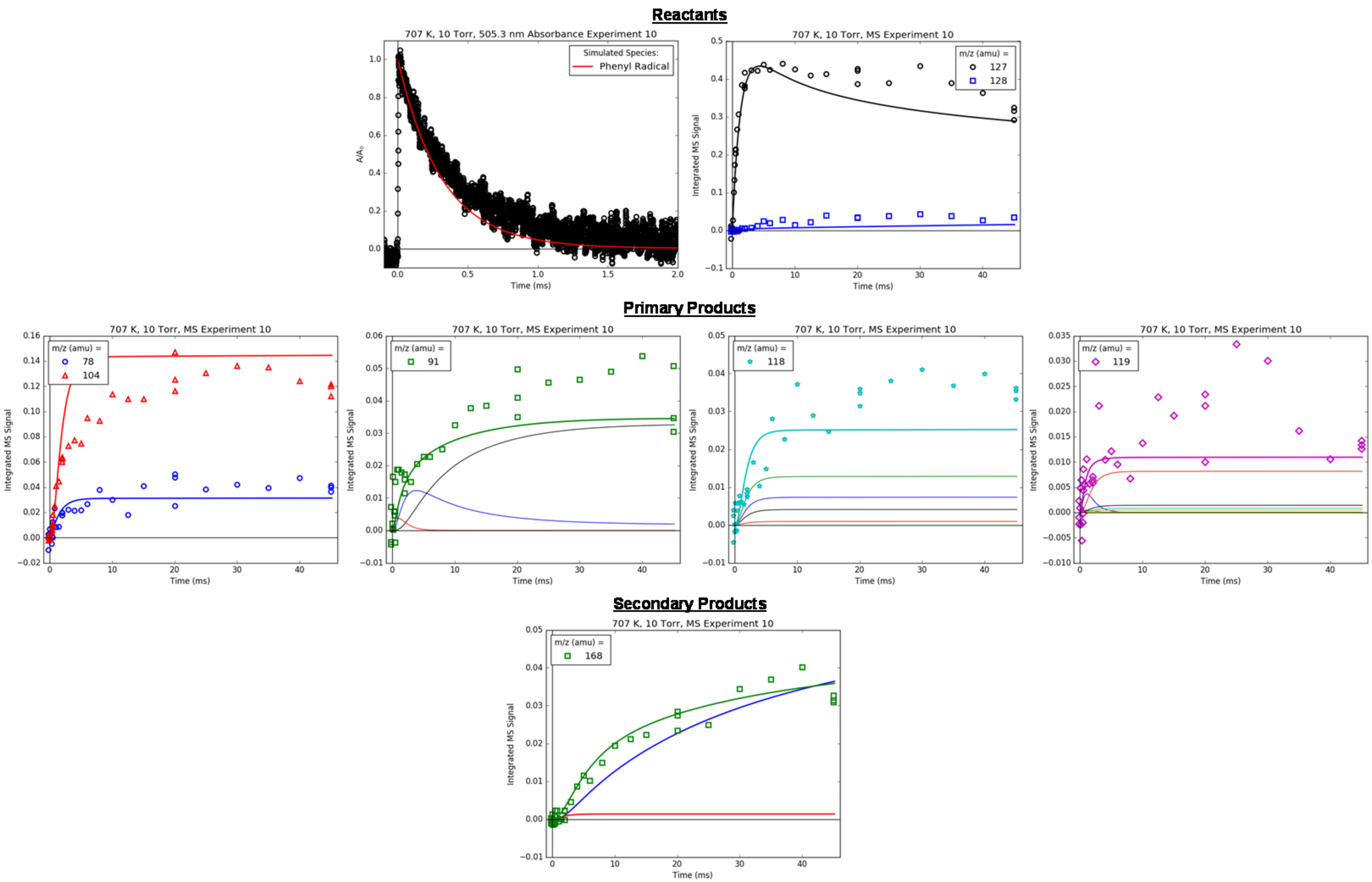

Figure S 26: Summary of all time profiles measured (markers) with MBMS in Experiment 10 (700 K, 10 Torr, "Medium" propene, **2** ×C_6H_5I control experiment). Lines are model results. Simultaneously recorded 505.3 nm absorbance is also shown with model comparison.

S5.11 Experiment 11: 700 K, 10 Torr, Medium Propene, 2xC_6H_5I/C_6H_5 Control

Experiment #11 was conducted at identical conditions as #8, but with ~2× [C_6H_5] and [C_6H_5I]. Because of the higher initial concentration, the signal to noise is better for Experiment #11 than any of the other 700 K experiments (#7-9). The agreement with the model is still satisfactory for all of the m/z's with time-dependence (except for CH_3I, for the reasons discussed in the Experiment #7 commentary).

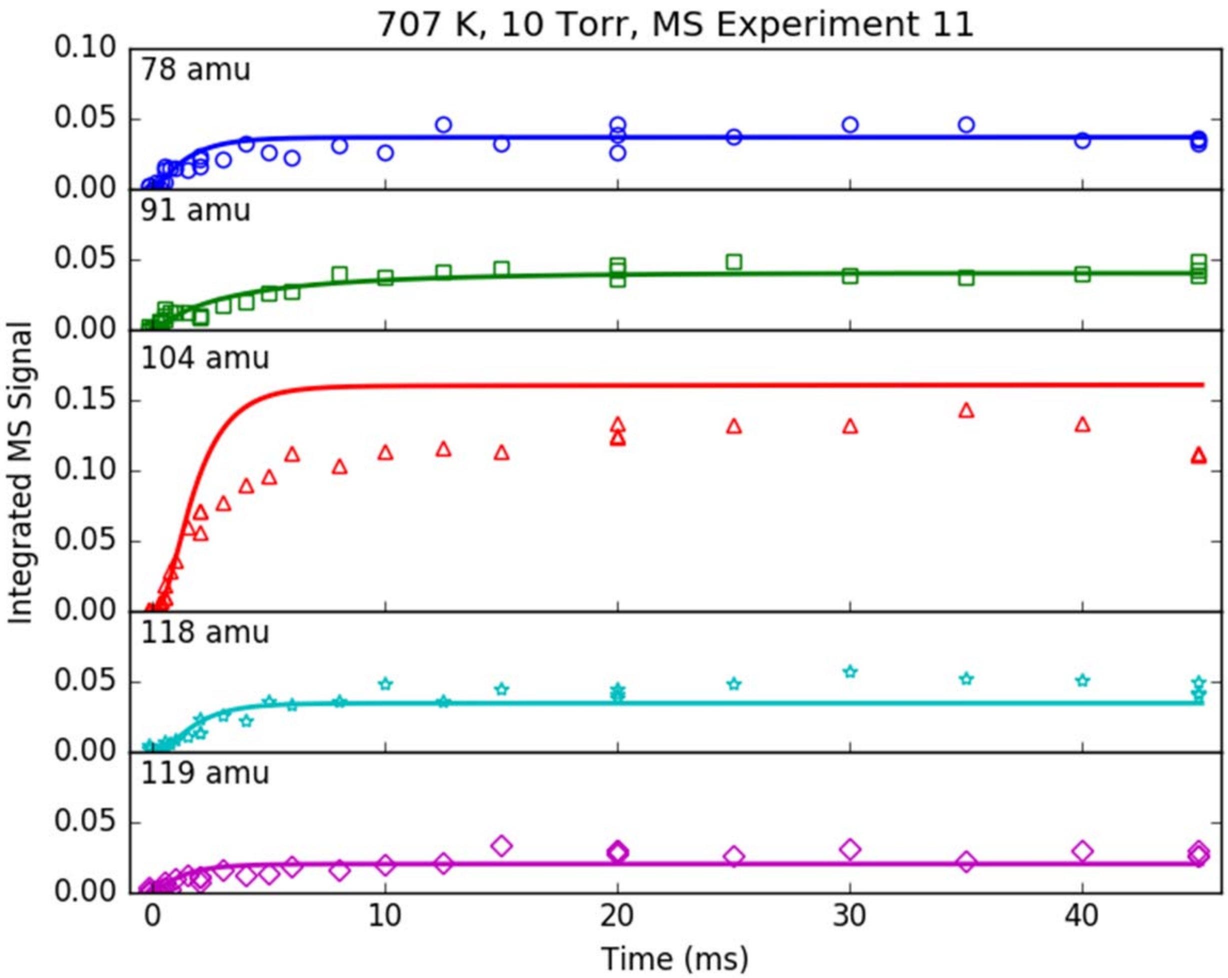

Figure S 27: Time profiles of primary phenyl radical + propene products measured (markers) with MBMS in Experiment 11 (700 K, 10 Torr, "Medium" propene, **2** ×C_6H_5I/C_6H_5 control experiment). Lines are model results.

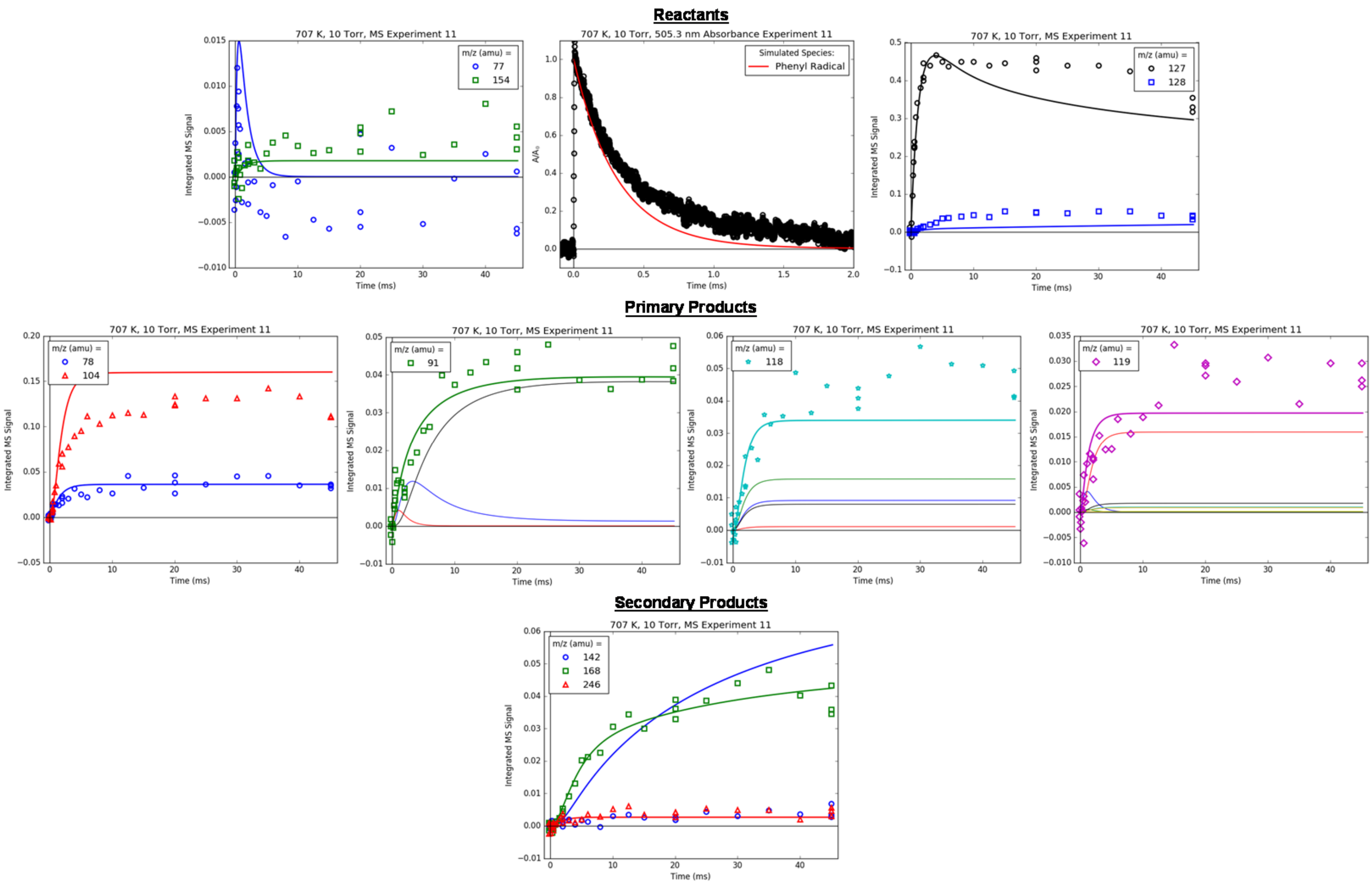

Figure S 28: Summary of all time profiles measured (markers) with MBMS in Experiment 11 (700 K, 10 Torr, "Medium" propene, **2** $\times C_6H_5I/C_6H_5$ control experiment). Lines are model results. Simultaneously recorded 505.3 nm absorbance is also shown with model comparison.

S5.12 Experiment 12: 700 K, 25 Torr, No Propene

Experiment #6 was conducted without C_3H_6, and all of the commentary regarding Experiment #1 (also without C_3H_6, but at 600 K and 10 Torr) still applies. Unlike the other experiments without C_3H_6 (#1, 6 and 14) biphenyl is noticeably underpredicted by ~2×. As discussed in the main text, the PICS for biphenyl is an estimate based on the bond-additivity approach of Bobeldijk,[32] so it is expected that the modeled biphenyl signal will have large uncertainty.

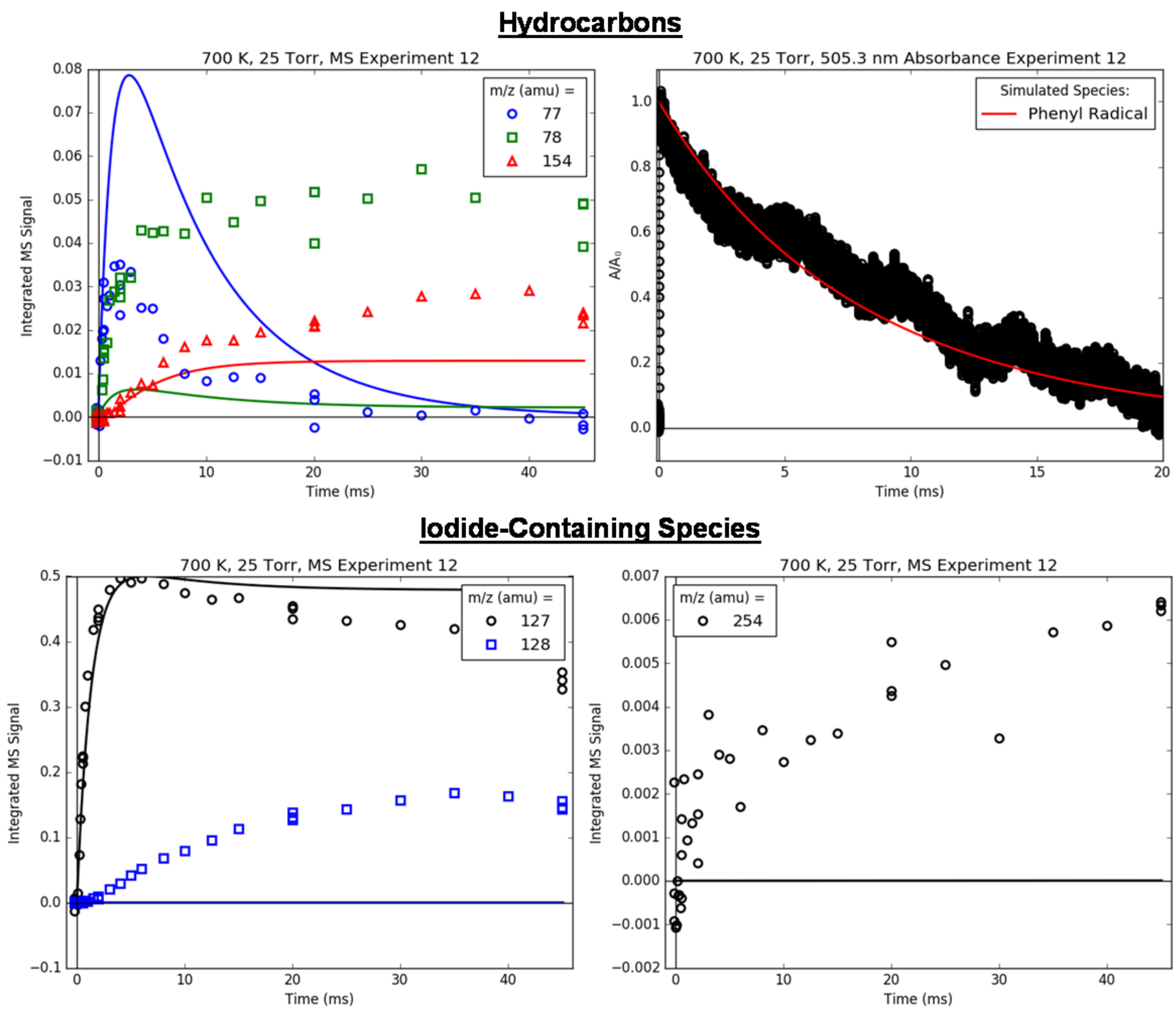

Figure S 29: Summary of all time profiles measured (markers) with MBMS in Experiment 12 (700 K, 25 Torr, no propene). Lines are model results. Simultaneously recorded 505.3 nm absorbance is also shown with model comparison.

S5.13 Experiment 13: 700 K, 25 Torr, Low Propene

Experiment #13 is identical to #7 (and #15) except that the pressure is higher: 25 instead of 10 (or 50) Torr. As mentioned at the beginning of this section, Experiment #13 exhibits the worst agreement between the measured and predicted primary product branching at 700 K. Specifically, 91, 118 and 119 amu are all underpredicted by ~2×. However, all of these products have relatively low concentrations compared to the major product, styrene, at 104 amu, which is described well by the model.

There are several other concerning features of Experiment #13. First, there is a clear baseline shift in the 505.3 nm absorbance that might indicate C_6H_5OO formation, which could explain some of the other discrepancies with the model. Second, although the steady-state 104 amu signal matches the model well, the measured time-dependence is slower than the model. As discussed in section S1.5 this is due to slower diffusion at higher-P inhibiting MBMS sampling. The delayed growth at 104 amu (and other time-dependent m/z's) becomes even more pronounced at higher-P (#15), consistent with this explanation. Figure S 32 shows all of the primary product profiles normalized by the instantaneous styrene/104 amu signal, such that transport delays should largely cancel out. As shown, the ratio of styrene to any of the other primary products is essentially flat as a function of reaction time after the first few milliseconds, confirming that although the absolute signals are distorted by transport effect, the ratios between products at any given time are still reliable. Finally, as discussed for Experiment #7, the iodide containing species exhibit contradictory behavior as a function of P. The large signal at 168 amu from C_3H_5I has disappeared when increasing P from 10 to 25 Torr, while the signals at the parent m/z of the other two iodide-containing species, CH_3I and **i1**-I at 142 and 248 amu, respectively, have increased. The latter behavior is consistent with P-dependent kinetics, while the former is contradictory. As already discussed, this might indicate that C_3H_5I is actually formed on the walls instead of in the gas-phase.

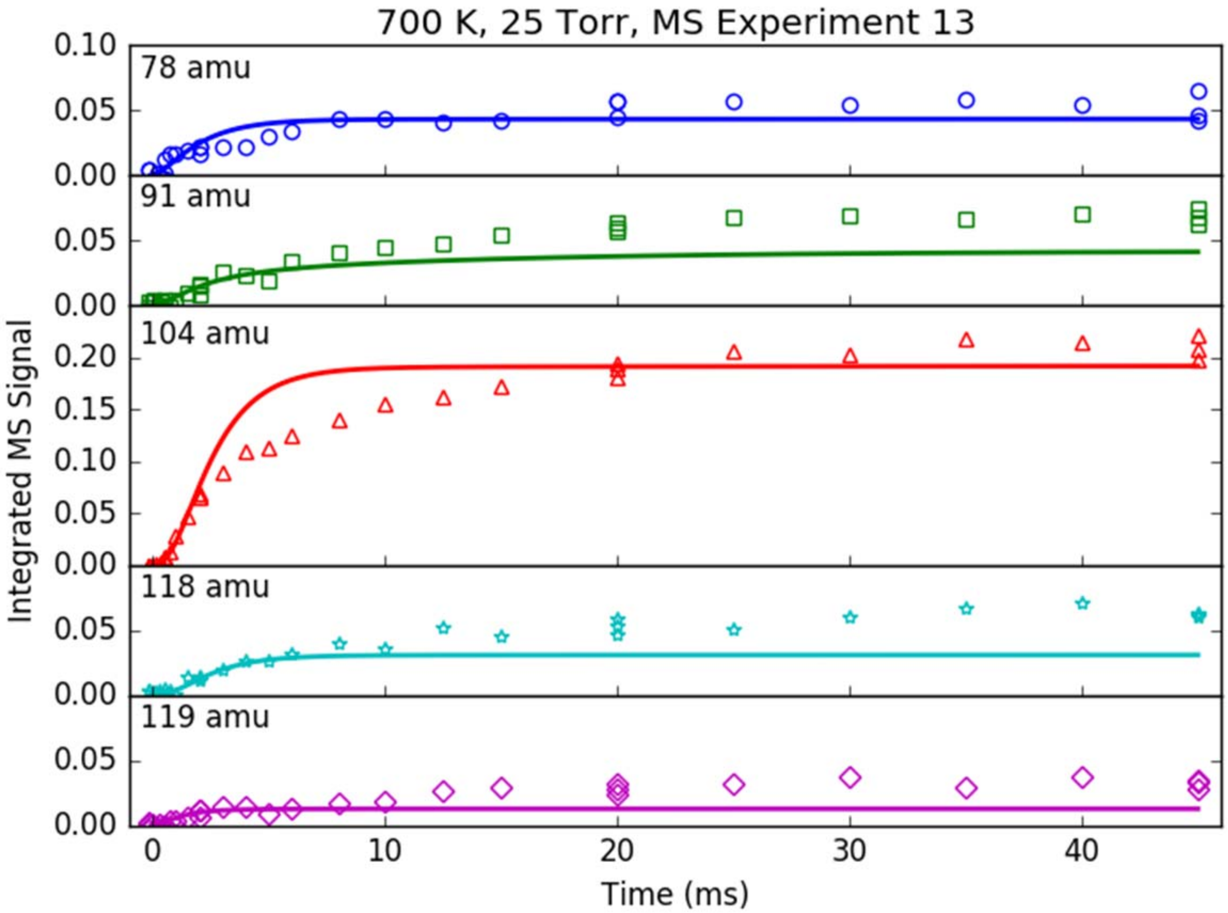

Figure S 30: Time profiles of primary phenyl radical + propene products measured (markers) with MBMS in Experiment 13 (700 K, 25 Torr, "Low" propene). Lines are model results.

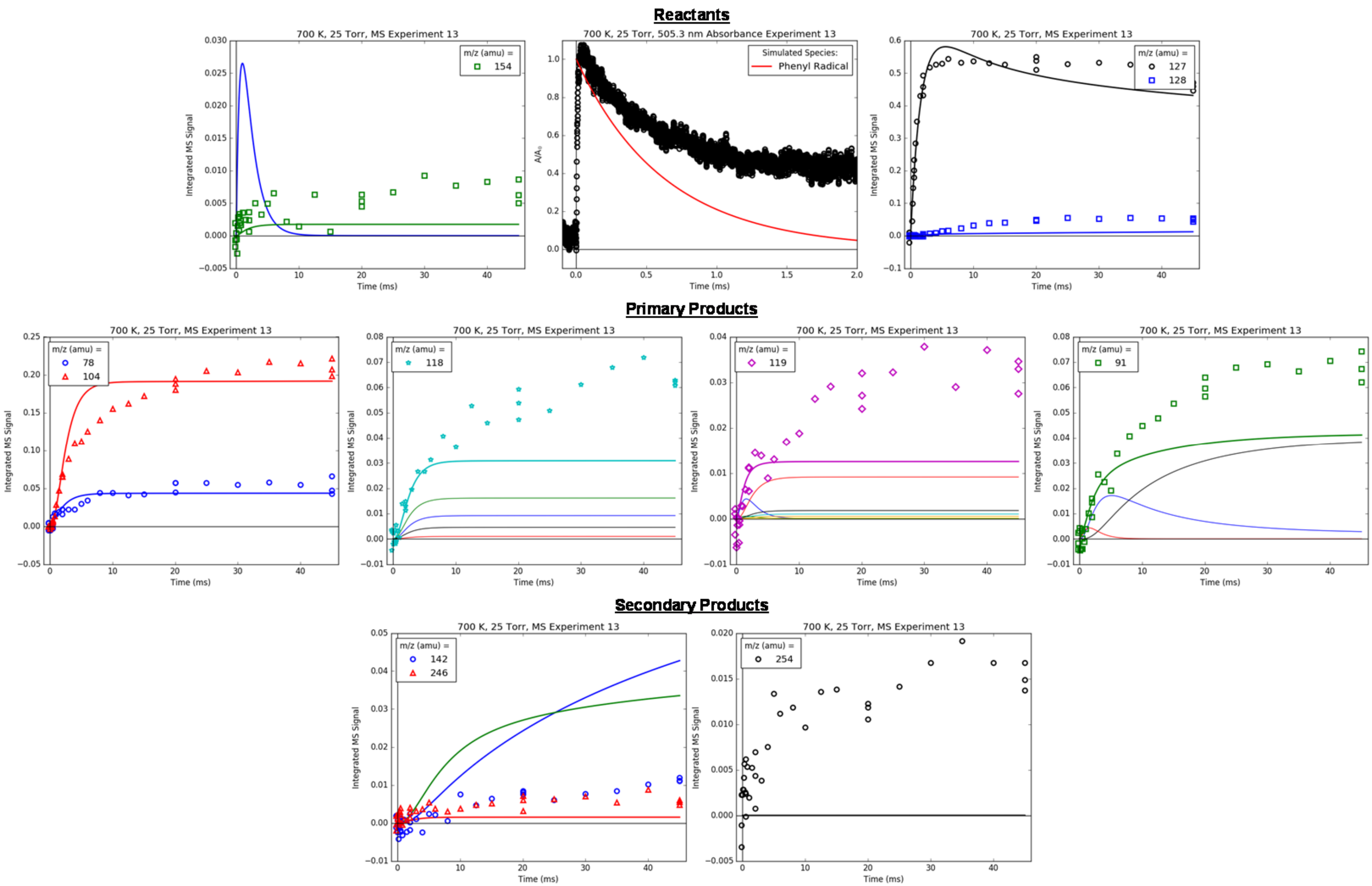

Figure S 31: Summary of all time profiles measured (markers) with MBMS in Experiment 13 (700 K, 25 Torr, "Low" propene). Lines are model results. Simultaneously recorded 505.3 nm absorbance is also shown with model comparison.

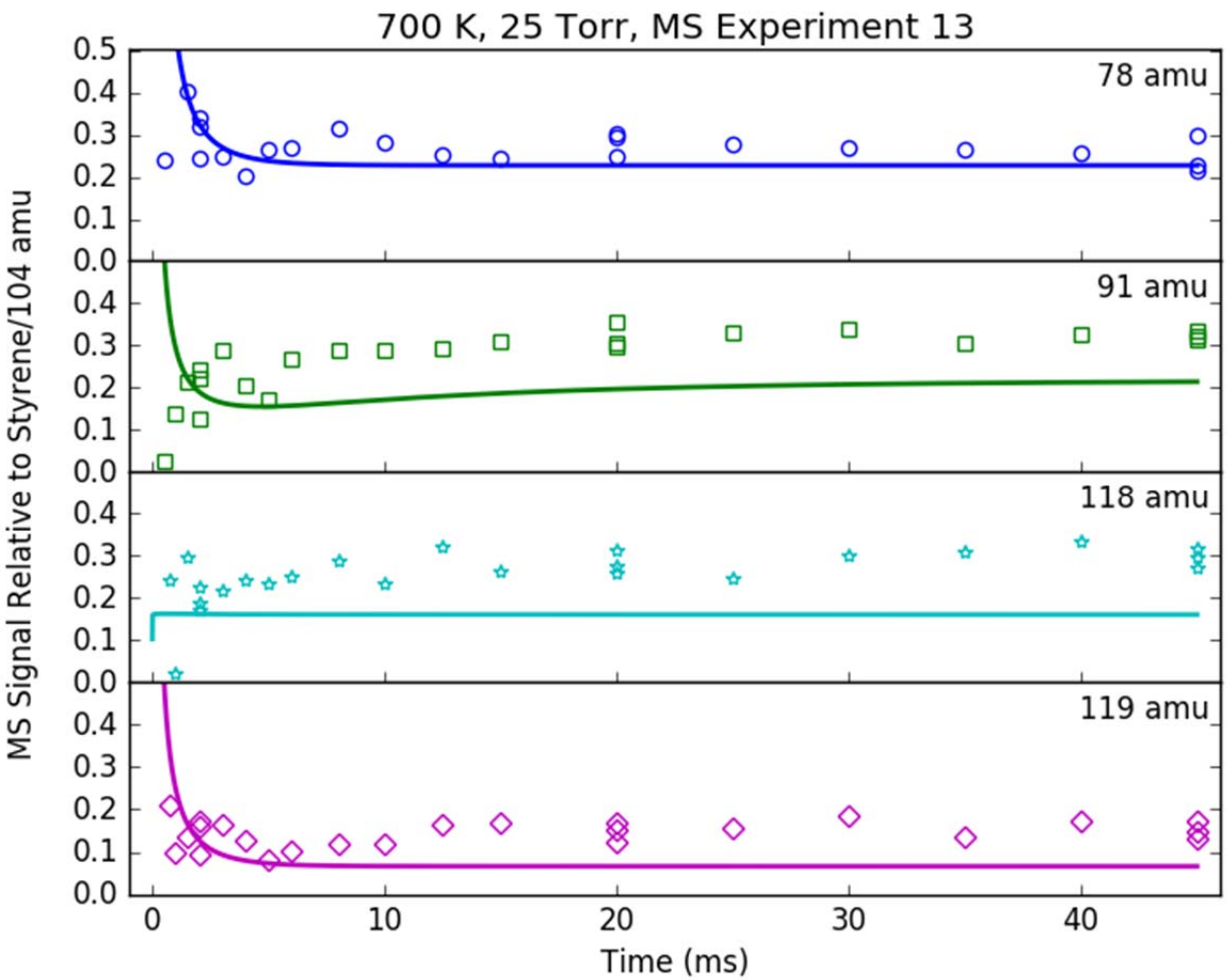

Figure S 32: Time profiles of primary phenyl radical + propene products measured (markers) with MBMS in Experiment 13 (700 K, 25 Torr, "Low" propene). Lines are model results. Both measured and modeled results are plotted relative to the 104 amu/styrene signal at each time point.

S5.14 Experiment 14: 700 K, 50 Torr, No Propene

Experiment #14 was conducted without C_3H_6, and all of the commentary regarding Experiment #1 (also without C_3H_6, but at 600 K and 10 Torr) still applies.

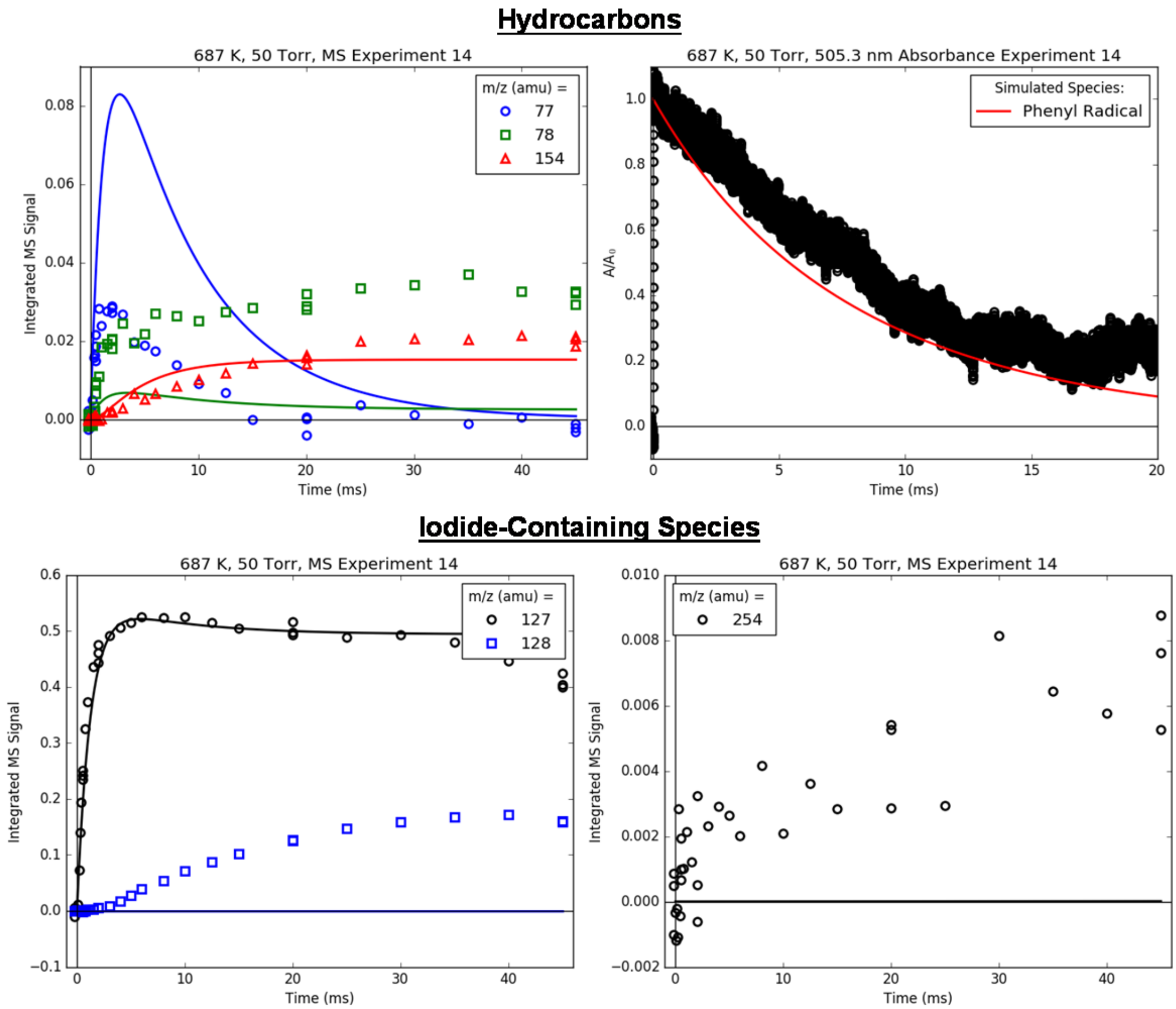

Figure S 33: Summary of all time profiles measured (markers) with MBMS in Experiment 14 (700 K, 50 Torr, no propene). Lines are model results. Simultaneously recorded 505.3 nm absorbance is also shown with model comparison.

S5.15 Experiment 15: 700 K, 50 Torr, Low Propene

Experiment #15 is identical to #7 (and #15) except that the pressure is higher: 50 instead of 10 (or 25) Torr. Figure S 34 is shown in the main text and is reproduced here for convenience. All of the P-dependent trends highlighted for Experiment #13 continue for #15: the time-scale for primary product growth is noticeably slower (and in disagreement with the simple transport model), more CH_3I is observed experimentally (and in closer agreement with the model) and C_3H_5I is still absent. Most importantly, the steady state product branching matches the model satisfactorily, in agreement with the prediction made in Fig. 2 of the main text that at our experimental conditions the product branching would have negligible P-dependence. Figure S 36 shows the instantaneous primary product ratios (relative to styrene/104 amu) such that transport delays largely canceled out. Just as was observed at 25 Torr (Figure S 32), the product ratios are essentially flat after the first few milliseconds, in contrast to the absolute product signals shown in Figure S 34 and Figure S 35 that require ~30 ms to reach steady state. Furthermore, the model matches these ratios well, as expected, again supporting the predicted lack of P-dependence.

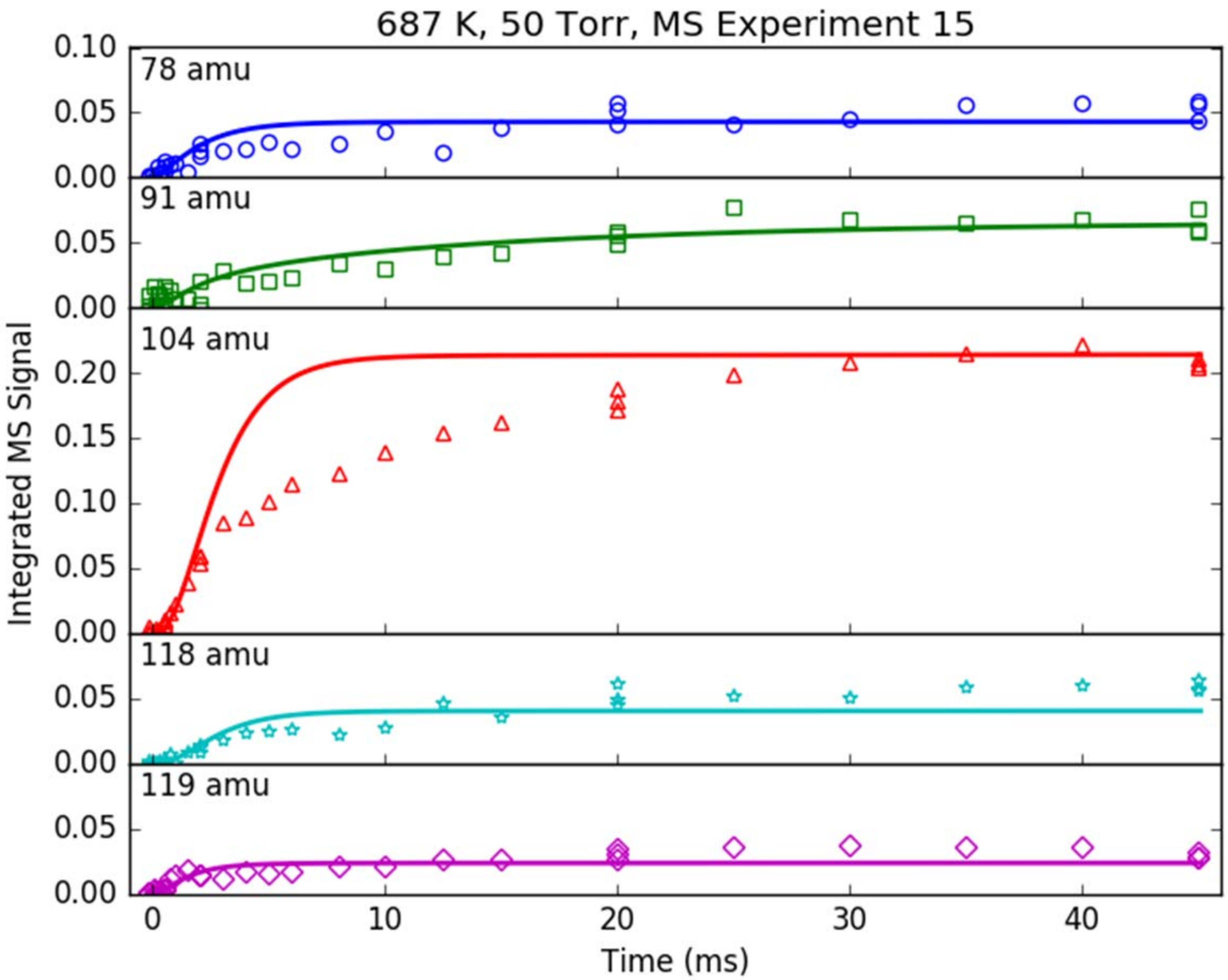

Figure S 34: Time profiles of primary phenyl radical + propene products measured (markers) with MBMS in Experiment 15 (700 K, 50 Torr, "Low" propene). Lines are model results.

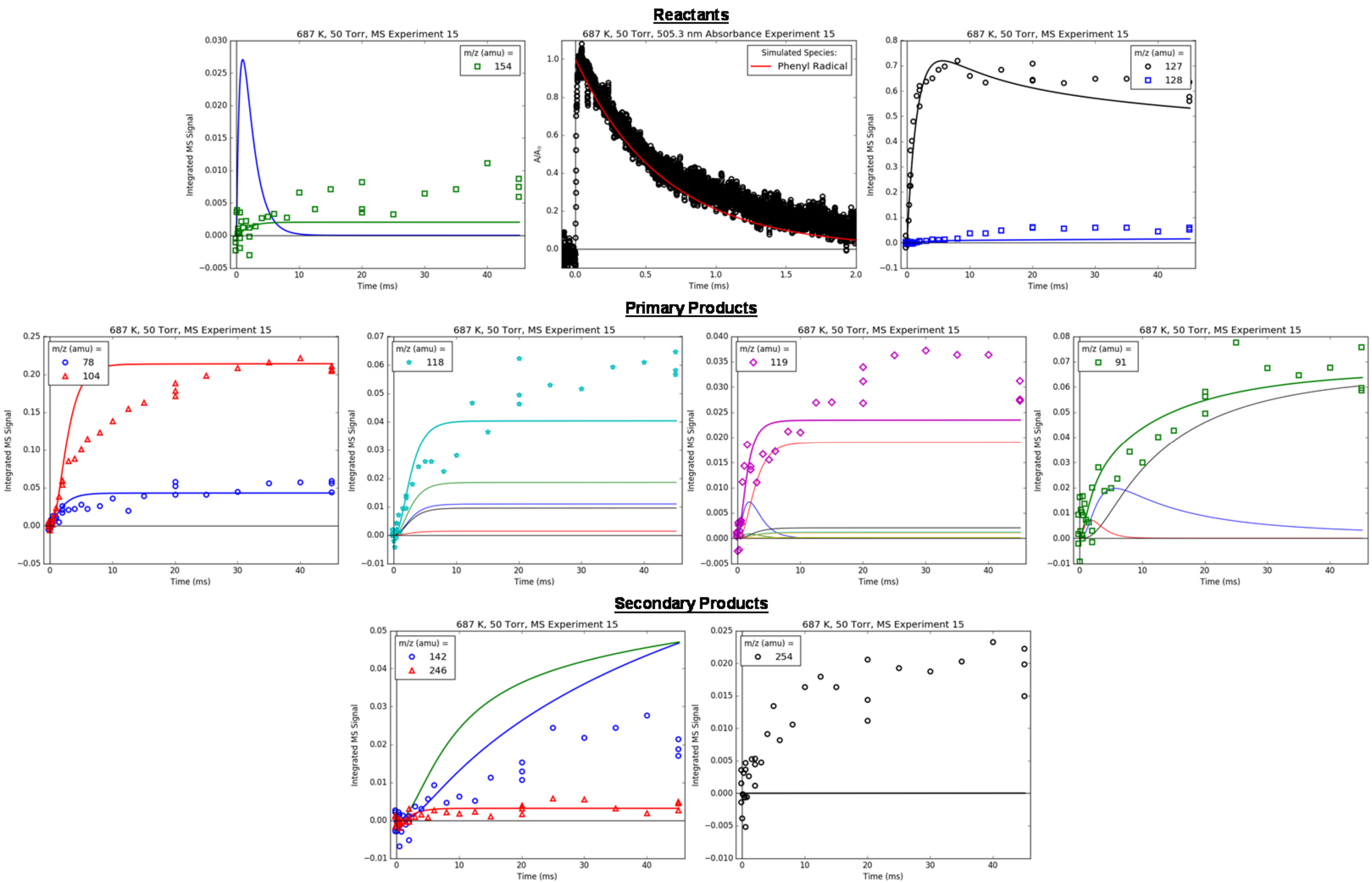

Figure S 35: Summary of all time profiles measured (markers) with MBMS in Experiment 15 (700 K, 50 Torr, "Low" propene). Lines are model results. Simultaneously recorded 505.3 nm absorbance is also shown with model comparison.

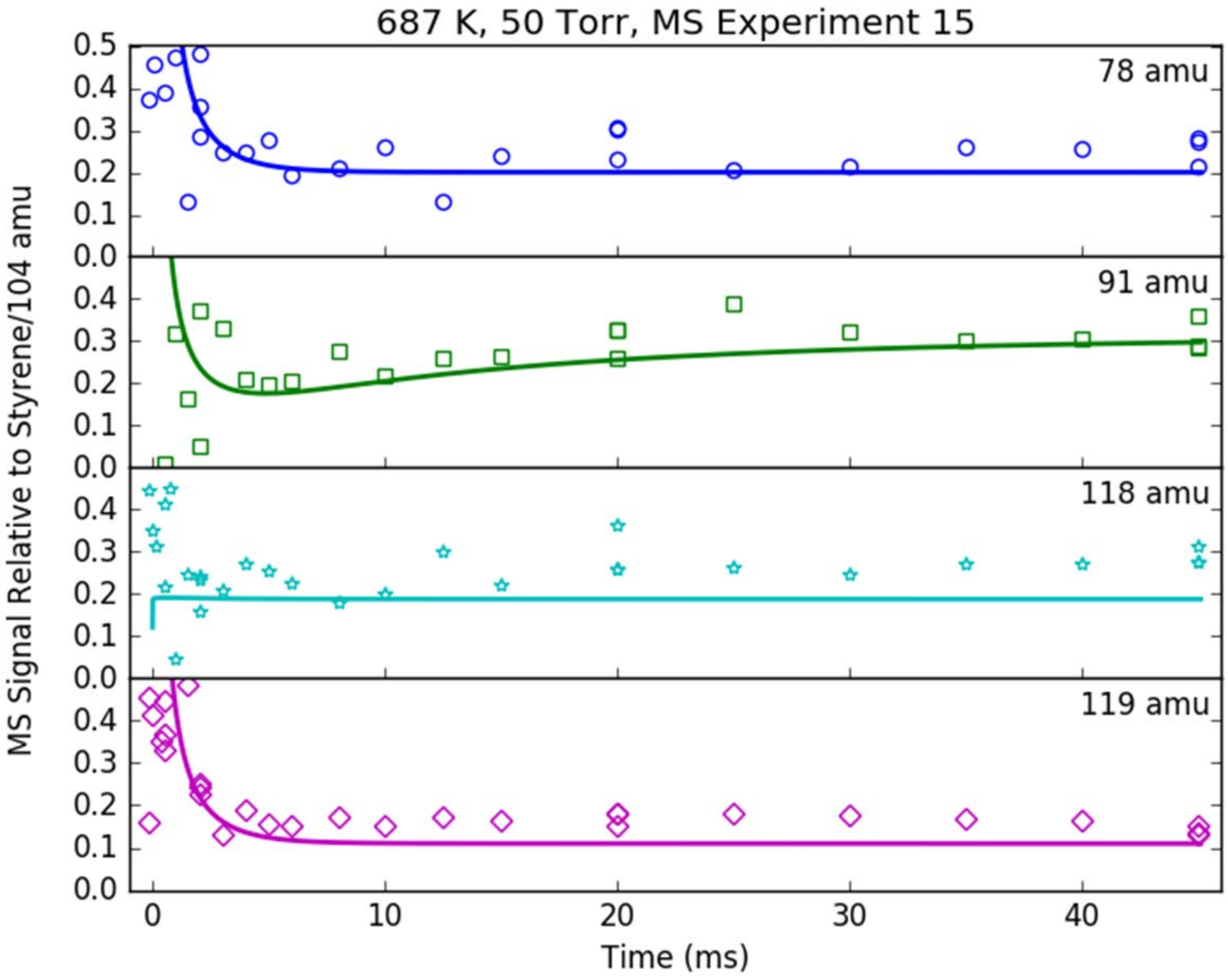

Figure S 36: Time profiles of primary phenyl radical + propene products measured (markers) with MBMS in Experiment 15 (700 K, 50 Torr, "Low" propene). Lines are model results. Both measured and modeled results are plotted relative to the 104 amu/styrene signal at each time point.

S6. Measured 505.3, 447.7 and 408.4 nm Absorbance

S6.1 Experimental Conditions

Table S 4: Conditions of laser absorbance experiments probing for products. Uncertainties represent two standard deviations.

Experiment #	Probe Laser Wavelength (nm)	Nominal T (K)	Real T (K)	P (Torr)	$[C_3H_6]^a$ (10^{15} cm^{-3})	$[C_6H_5I]^a$ (10^{13} cm^{-3})	IR $[I]_0$ (10^{12} cm^{-3})	Photolysis Laser Fluence (mJ cm^{-2})
16	408.4	600	605±8	10	7.5	6.1	4.5±1.5	18
17	408.4	600	605±8	10	15.0	6.1	4.5±1.5	18
18	408.4	600	605±8	10	30.0	6.1	4.5±1.5	18
19	408.4	700	707±11	10	7.5	6.1	3.5±1.2	18
20	408.4	700	707±11	10	15.0	6.1	3.5±1.2	18
21	408.4	700	707±11	10	30.0	6.1	3.5±1.2	18
22	447.7	600	605±8	10	7.5	6.1	4.2±1.4	18
23	447.7	600	605±8	10	15.0	6.1	4.2±1.4	18
24	447.7	600	605±8	10	30.0	6.1	4.2±1.4	18
25	447.7	700	707±11	10	7.5	6.1	4.0±1.3	18
26	447.7	700	707±11	10	15.0	6.1	4.0±1.3	18
27	447.7	700	707±11	10	30.0	6.1	4.0±1.3	18

[a]10% uncertainty in all values due to systematic uncertainty in mass flow controller calibrations.

S6.2 *Model Comparison without $C_3H_5 + I = C_3H_5$*

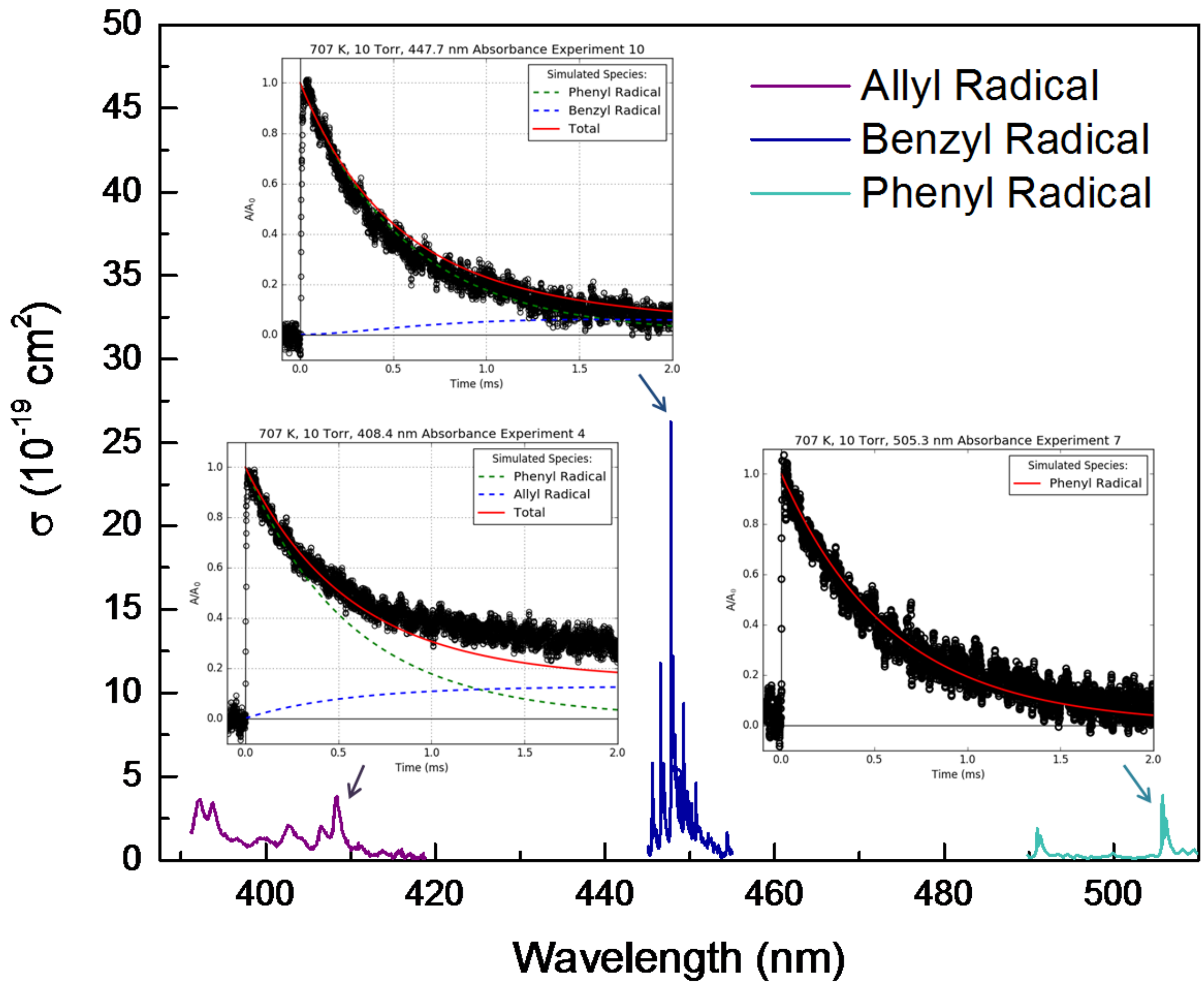

Figure S 37: Room temperature visible absorbance spectra measured by Tonokura *et al*. for allyl,[51] benzyl[52] and phenyl[53] radicals. Insets show representative absorbance traces (markers are measured and lines are modelled) measured in this work at the different wavelengths indicated and otherwise identical conditions (707 K, 10 Torr, $[C_3H_6] = 7.5\times10^{15}$ cm^{-3}). Identical to Fig. 19 in the main text, except the recombination reaction between C_3H_5 and I atom ($C_3H_5 + I \rightarrow C_3H_5I$) has been removed from the model.

S6.3 *Model Comparison with $C_3H_5 + I = C_3H_5$*

Table S 5 compares all of the absorbance traces measured and modeled at three different visible wavelengths: 408.4 nm where allyl radical is known to absorb,[51] 447.7 nm for benzyl radical[52] and 505.3 nm for phenyl radical.[53] In total, six different reactor conditions were explored: 600 and 700 K at "low", "medium" and "high" $[C_3H_6]$ (see Table 3 and Table S 4). As already noted in the main text, C_6H_5 is known to absorb broadly throughout the visible range,[54] so at all three wavelengths the contribution of C_6H_5 had to be included in the model. Generally, the model matches all of the 447.7 and 505.3 nm experiments well, except for the 700 K, high [C_3H_6] experiment where the 447.7 nm absorbance has a negative baseline shift and 505.3 nm has a positive shift, neither of which are matched by the model. Such shifts are usually within $\pm$10% and are irreproducible, indicative of noise or an imperfect background subtraction.

In contrast, there is a clear and reproducible baseline shift at 408.4 nm and 700 K, indicative of absorbance by some relatively long-lived species (most likely allyl radical, C_3H_5). The model does not capture this ~30% shift, but if the recombination reaction between C_3H_5 and I atom is removed from the gas-phase model (Figure S 37) then the measurement and model are within 10% of each other. As discussed in the context of the MBMS results above, C_3H_5I is observed as a product at m/z=168 amu, but it exhibits an unexpected, inverse relationship with pressure. This suggest that perhaps $C_3H_5 + I \rightarrow C_3H_5I$ is not occurring in the gas phase being probed by absorbance, but rather it is occurring on the walls near where MBMS sampling occurs.

Table S 5: Absorbance decays measured at different probe laser wavelengths and otherwise (near) identical conditions while phenyl radical + propene is occurring.

	λ (nm)		
	404.8	447.7	505.3
600 K, "Low" Propene	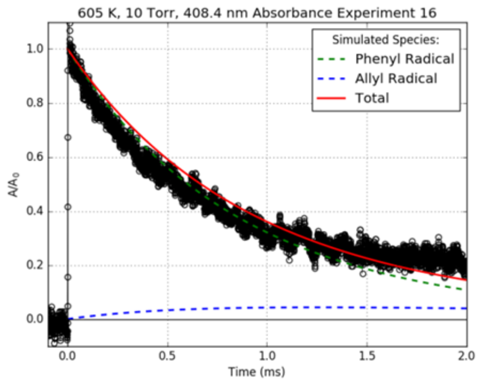	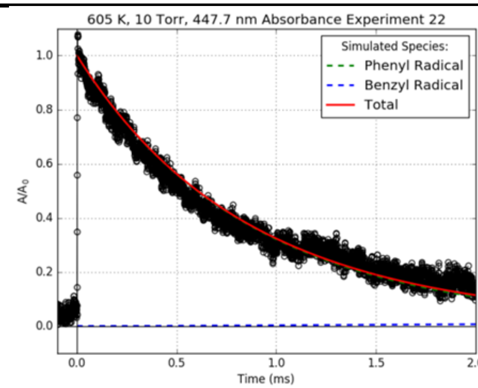	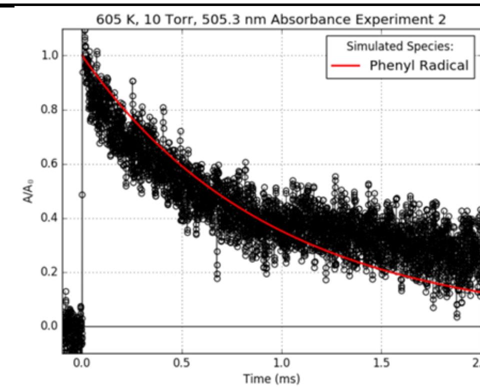
600 K, "Medium" Propene	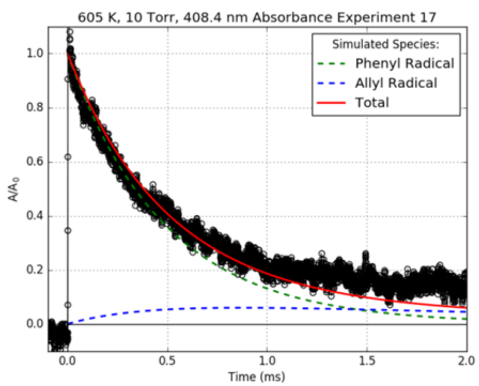	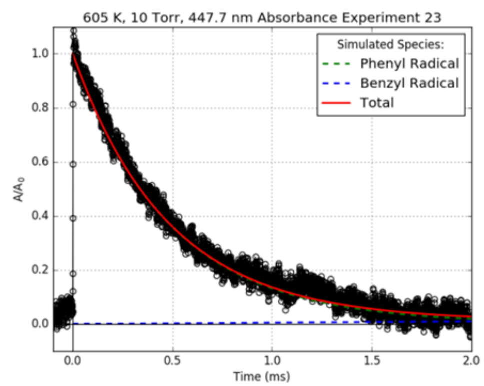	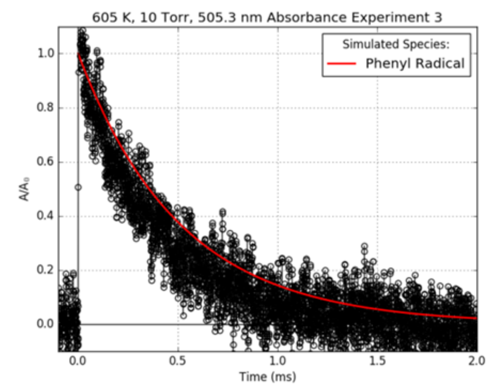

600 K,
“High” Propene

700 K,
“Low” Propene

700 K,
“Medium”
Propene

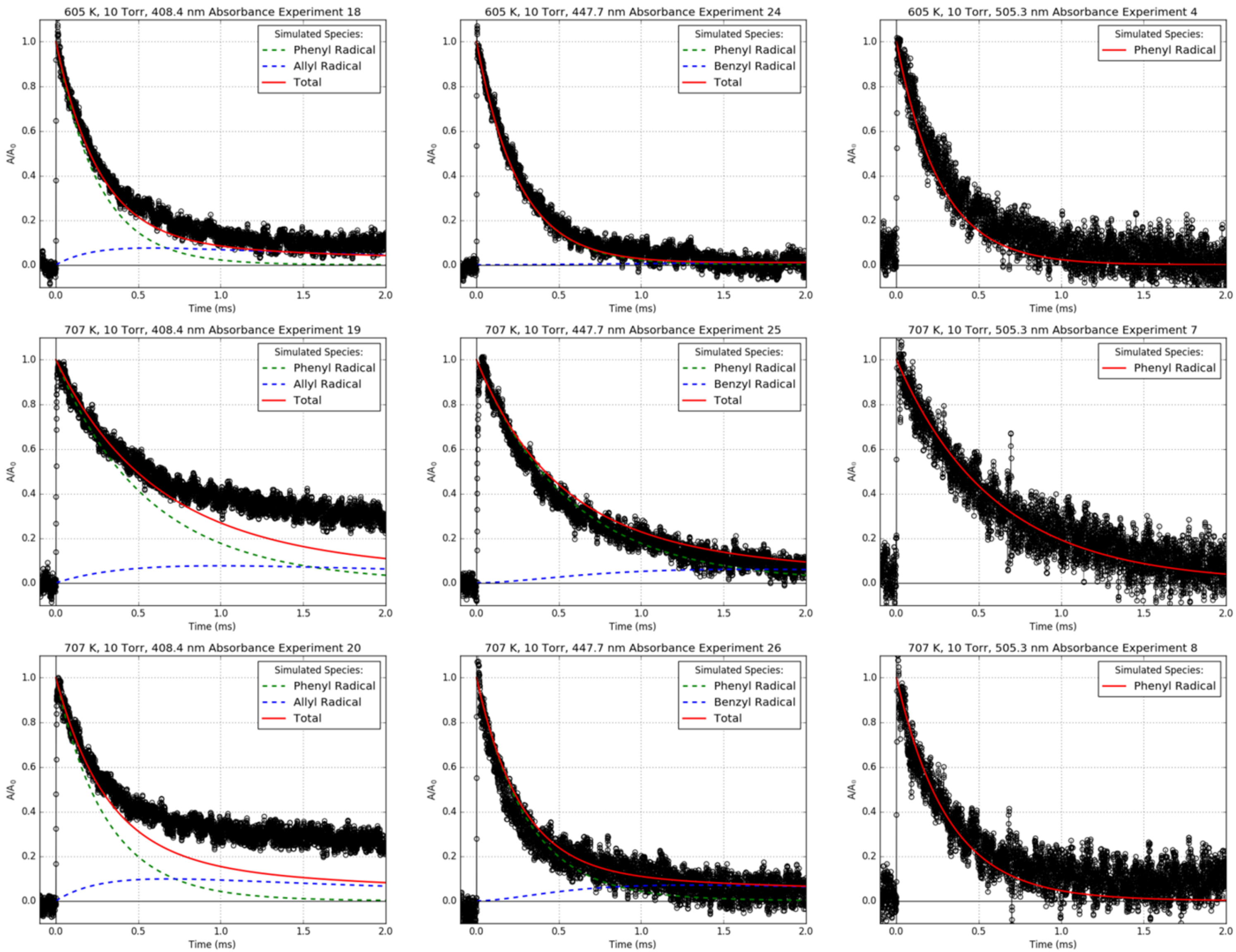

700 K,
“High” Propene

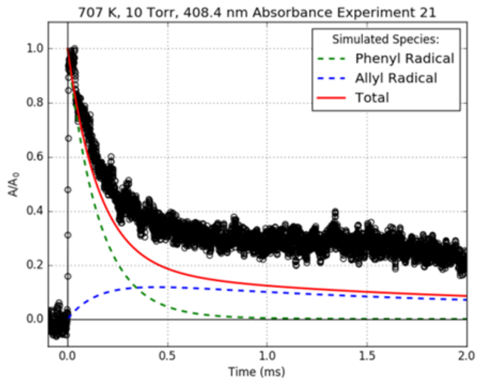

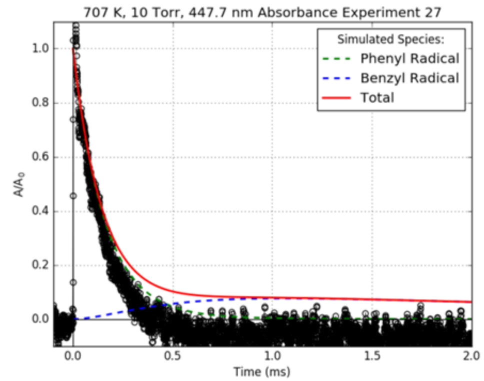

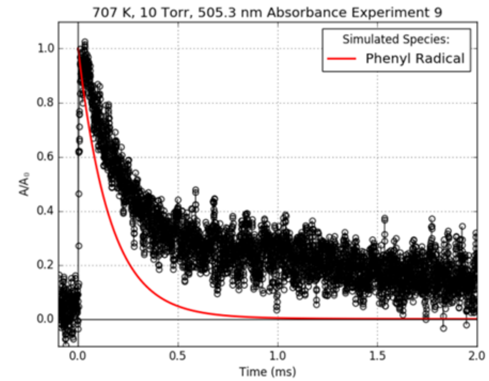

S7. G3(MP2, CC)//B3LYP Calculated Molecular Parameters

Table S 6: Summary of molecular parameters for all calculated stationary points on the C_9H_{11} potential energy surface: B3LYP optimized species structures in Cartesian coordinates; scaled zero-point energy corrections (ZPE) calculated with B3LYP frequencies; CCSD(T), MP2, and G3 calculated energies; external symmetry numbers ($\boldsymbol{\sigma_{ext}}$); numbers of optical isomers (**n**); unscaled vibrational frequencies ($\boldsymbol{v_i}$); and moments of inertia (**I**). **Bolded** frequencies correspond to internal rotations that were modeled as hindered rotors (see Table S 7).

Species	**XYZ Coordinates** (Å)	**Energies** (Hartree)	$\boldsymbol{\sigma_{ext}}$	**n**	$\boldsymbol{v_i}$ (cm^{-1})	**I** (amu*Å^2)
phenyl radical C_6H_5 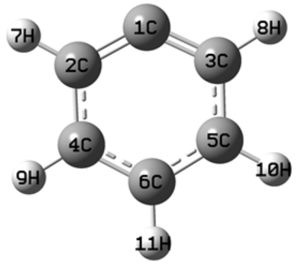 	C 0.000 0.000 1.396 C 0.000 1.224 0.771 C 0.000 -1.224 0.771 C 0.000 1.212 -0.632 C 0.000 -1.212 -0.632 C 0.000 0.000 -1.322 H 0.000 2.158 1.322 H 0.000 -2.158 1.322 H 0.000 2.151 -1.176 H 0.000 -2.151 -1.176 H 0.000 0.000 -2.406	ZPE(B3LYP/6-311G**) = 0.0850 E(CCSD(T)/6-311G**) = -230.9695 E(MP2/6-311G**) = -230.8559 E(MP2/G3large) = -230.9906 E(G3(MP2,CC) = -231.0193	2	1	401, 427, 602, 620, 674, 722, 813, 892, 964, 988, 993, 1016, 1050, 1072, 1175, 1176, 1301, 1323, 1462, 1470, 1573, 1629, 3154, 3160, 3173, 3175, 3187	80.3 89.9 170.2
propene C_3H_6 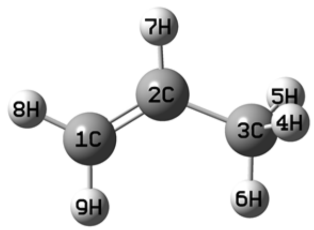 	C 1.291 0.150 0.000 C 0.001 0.472 0.000 C -1.137 -0.505 0.000 H -1.777 -0.364 -0.878 H -1.777 -0.364 0.878 H -0.780 -1.537 0.000 H -0.275 1.526 0.000 H 2.067 0.907 0.000 H 1.618 -0.886 0.000	ZPE(B3LYP/6-311G**) = 0.0774 E(CCSD(T)/6-311G**) = -117.6002 E(MP2/6-311G**) = -117.5435 E(MP2/G3large) = -117.6142 E(G3(MP2,CC) = -117.5934	1	1	229, 433, 600, 923, 947, 953, 1033, 1074, 1190, 1327, 1411, 1450, 1482, 1497, 1701, 3000, 3042, 3079, 3107, 3114, 3194	10.8 54.6 62.3

Species	**XYZ Coordinates** (Å)	**Energies** (Hartree)	**σ_{ext}**	**n**	**ν_i** (cm^{-1})	**I** (amu*Å^2)
i1 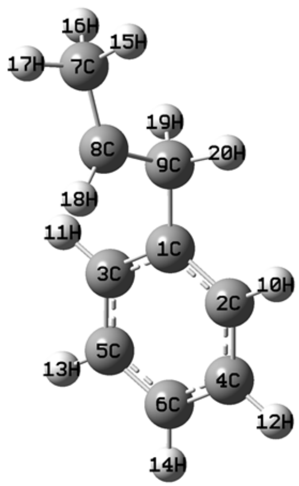 	C -0.040 -0.034 0.074 C 0.015 0.113 1.462 C 1.164 -0.146 -0.632 C 1.238 0.150 2.131 C 2.387 -0.109 0.031 C 2.428 0.039 1.417 C -2.800 -1.608 -2.207 C -1.692 -1.437 -1.225 C -1.365 -0.089 -0.659 H -0.909 0.202 2.025 H 1.137 -0.265 -1.710 H 1.259 0.266 3.209 H 3.309 -0.194 -0.533 H 3.380 0.070 1.935 H -3.792 -1.518 -1.732 H -2.768 -0.842 -2.991 H -2.769 -2.589 -2.688 H -1.272 -2.311 -0.740 H -1.369 0.653 -1.470 H -2.165 0.240 0.026	ZPE(B3LYP/6-311G**) = 0.1654 E(CCSD(T)/6-311G**) = -348.6308 E(MP2/6-311G**) = -348.5035 E(MP2/G3large) = -348.7088 E(G3(MP2,CC) = -348.6707	1	1	**37**, **66**, **93**, 149, 259, 320, 398, 415, 445, 500, 594, 636, 716, 762, 807, 855, 872, 908, 927, 977, 995, 1000, 1018, 1050, 1065, 1116, 1141, 1181, 1201, 1202, 1229, 1300, 1337, 1357, 1384, 1409, 1473, 1481, 1484, 1486, 1524, 1625, 1642, 2947, 3010, 3018, 3053, 3082, 3152, 3154, 3156, 3166, 3174, 3187	113.0 585.2 659.9

Species	XYZ Coordinates (Å)	Energies (Hartree)	σ_{ext}	n	v_i (cm^{-1})	I ($amu*Å^2$)
i2 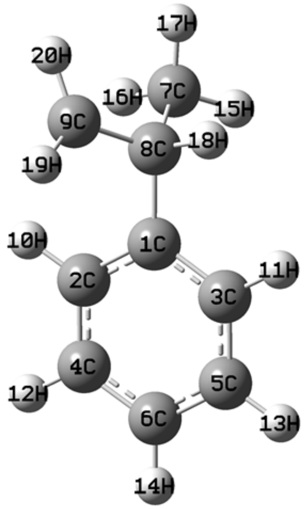	C -0.172 -0.152 -0.127 C 0.376 1.101 0.171 C 0.698 -1.230 -0.310 C 1.754 1.269 0.285 C 2.078 -1.067 -0.197 C 2.610 0.185 0.101 C -2.326 -0.407 1.185 C -1.682 -0.344 -0.218 C -2.344 0.681 -1.082 H -0.284 1.951 0.309 H 0.291 -2.209 -0.547 H 2.160 2.248 0.516 H 2.735 -1.916 -0.347 H 3.683 0.316 0.187 H -1.877 -1.202 1.784 H -2.187 0.538 1.718 H -3.400 -0.600 1.107 H -1.841 -1.333 -0.682 H -1.858 1.038 -1.982 H -3.378 0.958 -0.915	ZPE(B3LYP/6-311G**) = 0.165342 E(CCSD(T)/6-311G**) = - 348.6288 E(MP2/6-311G**) = -348.5027 E(MP2/G3large) = -348.7079 E(G3(MP2,CC) = -348.6687	1	1	**47**, 130, **144**, 209, **257**, 304, 332, 416, 455, 505, 549, 610, 637, 717, 763, 778, 859, 894, 929, 952, 981, 1001, 1015, 1020, 1050, 1102, 1115, 1134, 1181, 1201, 1213, 1286, 1303, 1342, 1364, 1406, 1457, 1484, 1498, 1500, 1526, 1625, 1645, 2915, 3026, 3091, 3102, 3132, 3151, 3157, 3167, 3175, 3187, 3238	147.1 455.6 506.3

Species	**XYZ Coordinates** (Å)	**Energies** (Hartree)	**σ_{ext}**	**n**	***v_i*** (cm^{-1})	**I** (amu*$Å^2$)
i3 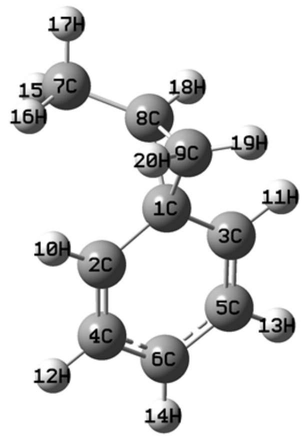	C 0.294 -0.260 0.226 C -0.259 1.091 0.414 C -0.688 -1.282 -0.174 C -1.585 1.356 0.200 C -2.004 -0.973 -0.380 C -2.484 0.344 -0.205 C 2.586 0.732 -0.780 C 1.750 -0.439 -0.319 C 1.481 -0.708 1.118 H 0.404 1.884 0.739 H -0.335 -2.299 -0.309 H -1.954 2.365 0.350 H -2.693 -1.756 -0.681 H -3.529 0.574 -0.372 H 2.284 1.068 -1.776 H 2.512 1.585 -0.102 H 3.642 0.445 -0.828 H 1.840 -1.319 -0.950 H 1.459 -1.731 1.478 H 1.822 0.020 1.846	ZPE(B3LYP/6-311G**) = 0.1663 E(CCSD(T)/6-311G**) = -348.6100 E(MP2/6-311G**) = -348.4578 E(MP2/G3large) = -348.6626 E(G3(MP2,CC) = -348.6485	1	1	82, **153**, 196, 224, 340, 391, 418, 450, 468, 580, 609, 655, 706, 733, 757, 802, 856, 898, 921, 958, 965, 969, 1000, 1011, 1045, 1057, 1105, 1113, 1157, 1189, 1200, 1237, 1328, 1336, 1396, 1418, 1432, 1466, 1481, 1495, 1502, 1540, 1596, 3024, 3077, 3099, 3109, 3126, 3150, 3156, 3168, 3180, 3194, 3197	152.1 402.0 472.0

Species	**XYZ Coordinates** (Å)	**Energies** (Hartree)	σ_{ext}	**n**	ν_i (cm^{-1})	**I** (amu*$Å^2$)
i4 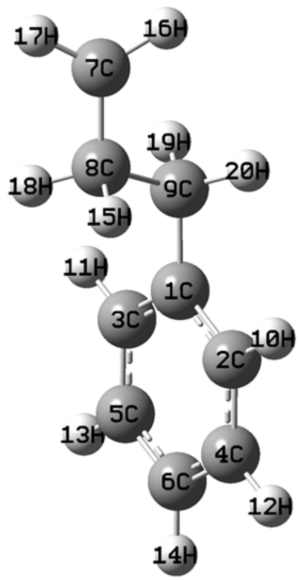 	C -0.059 -0.009 0.372 C -0.744 1.198 0.189 C -0.769 -1.203 0.212 C -2.096 1.211 -0.146 C -2.122 -1.195 -0.123 C -2.790 0.013 -0.304 C 3.770 0.002 -0.255 C 2.313 -0.013 -0.562 C 1.417 -0.022 0.698 H -0.214 2.136 0.317 H -0.258 -2.150 0.358 H -2.609 2.158 -0.279 H -2.654 -2.133 -0.238 H -3.843 0.022 -0.562 H 2.041 0.868 -1.169 H 4.144 0.505 0.630 H 4.495 -0.366 -0.970 H 2.066 -0.876 -1.191 H 1.657 -0.906 1.295 H 1.667 0.850 1.313	ZPE(B3LYP/6-311G**) = 0.1655 E(CCSD(T)/6-311G**) = -348.6273 E(MP2/6-311G**) = -348.5007 E(MP2/G3large) = -348.7061 E(G3(MP2,CC) = -348.6672	1	1	**51**, **90**, 104, **114**, 281, 317, 346, 416, 479, 511, 602, 637, 716, 741, 765, 826, 856, 884, 924, 976, 983, 1000, 1018, 1051, 1070, 1083, 1114, 1171, 1182, 1202, 1226, 1289, 1313, 1341, 1361, 1375, 1461, 1467, 1485, 1500, 1528, 1625, 1647, 2927, 3019, 3028, 3066, 3132, 3151, 3153, 3165, 3174, 3187, 3233	114.2 576.0 644.5

Species	XYZ Coordinates (Å)	Energies (Hartree)	σ_{ext}	n	v_i (cm^{-1})	I (amu*Å^2)
i5 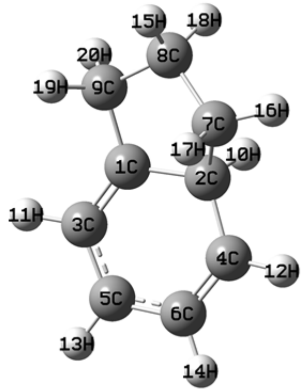	C -0.175 0.745 0.171 C -0.170 -0.745 0.405 C 0.978 1.443 -0.035 C 1.145 -1.396 0.105 C 2.225 0.773 -0.109 C 2.268 -0.646 -0.088 C -1.438 -1.202 -0.363 C -2.448 -0.078 -0.047 C -1.602 1.225 0.037 H -0.397 -0.923 1.479 H 0.943 2.516 -0.203 H 1.199 -2.480 0.111 H 3.136 1.339 -0.260 H 3.221 -1.141 -0.249 H -3.247 -0.010 -0.788 H -1.791 -2.191 -0.059 H -1.217 -1.237 -1.434 H -2.922 -0.278 0.919 H -1.717 1.839 -0.862 H -1.913 1.852 0.881	ZPE(B3LYP/6-311G**) = 0.1686 E(CCSD(T)/6-311G**) = -348.6373 E(MP2/6-311G**) = -348.4834 E(MP2/G3large) = -348.6858 E(G3(MP2,CC) = -348.6712	1	1	74, 177, 214, 341, 392, 478, 509, 547, 606, 638, 680, 742, 764, 813, 867, 889, 910, 915, 965, 996, 999, 1008, 1043, 1070, 1117, 1130, 1163, 1183, 1193, 1228, 1283, 1284, 1293, 1318, 1334, 1342, 1404, 1429, 1477, 1494, 1509, 1540, 1605, 2825, 3013, 3032, 3034, 3044, 3079, 3091, 3143, 3148, 3166, 3190	150.9 341.7 469.0

Species	XYZ Coordinates (Å)	Energies (Hartree)	σ_{ext}	n	ν_i (cm^{-1})	I (amu*$Å^2$)
i6 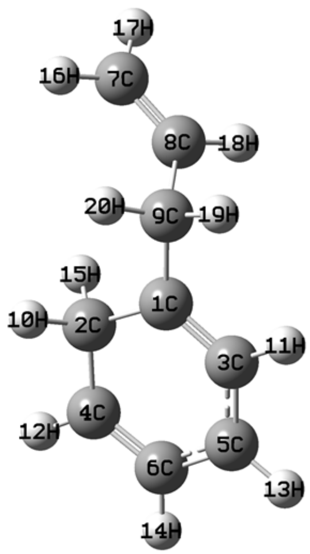 	C 0.021 -0.361 0.311 C -0.339 1.103 0.327 C -0.927 -1.305 0.033 C -1.775 1.388 -0.001 C -2.271 -0.967 -0.258 C -2.666 0.394 -0.271 C 3.414 0.566 -0.327 C 2.413 -0.296 -0.479 C 1.457 -0.723 0.610 H -0.087 1.529 1.316 H -0.641 -2.354 0.036 H -2.091 2.426 -0.013 H -2.992 -1.747 -0.471 H -3.697 0.644 -0.501 H 0.325 1.656 -0.359 H 3.622 1.033 0.631 H 4.066 0.833 -1.151 H 2.235 -0.740 -1.457 H 1.527 -1.809 0.742 H 1.769 -0.263 1.556	ZPE(B3LYP/6-311G**) = 0.1655 E(CCSD(T)/6-311G**) = -348.6103 E(MP2/6-311G**) = -348.4530 E(MP2/G3large) = -348.6586 E(G3(MP2,CC) = -348.6504	1	1	**46**, **80**, 112, 197, 305, 321, 396, 464, 513, 532, 589, 656, 674, 759, 783, 886, 917, 939, 939, 945, 950, 968, 980, 1015, 1035, 1104, 1129, 1174, 1186, 1188, 1235, 1305, 1310, 1325, 1354, 1424, 1431, 1443, 1449, 1473, 1544, 1613, 1701, 2892, 2931, 2994, 3040, 3121, 3129, 3142, 3151, 3170, 3192, 3208	131.6 521.8 609.7

Species	XYZ Coordinates (Å)	Energies (Hartree)	σ_{ext}	n	ν_i (cm^{-1})	I ($amu*Å^2$)
i7 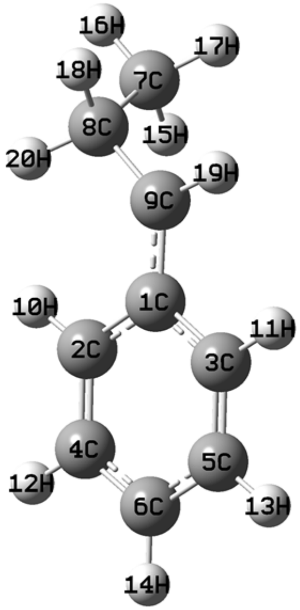	C 0.040 -0.351 -0.171 C 0.425 1.021 -0.205 C 1.079 -1.304 0.045 C 1.746 1.398 -0.038 C 2.395 -0.915 0.209 C 2.744 0.441 0.168 C -3.315 0.300 0.733 C -2.497 0.069 -0.557 C -1.292 -0.790 -0.341 H -0.328 1.784 -0.359 H 0.818 -2.357 0.076 H 2.009 2.451 -0.068 H 3.162 -1.665 0.369 H 3.776 0.745 0.297 H -2.718 0.820 1.485 H -4.206 0.900 0.525 H -3.641 -0.650 1.165 H -3.147 -0.412 -1.298 H -1.467 -1.861 -0.262 H -2.216 1.037 -0.981	ZPE(B3LYP/6-311G**) = 0.1671 E(CCSD(T)/6-311G**) = -348.6458 E(MP2/6-311G**) = -348.4829 E(MP2/G3large) = -348.6888 E(G3(MP2,CC) = -348.6846	1	1	**28**, **81**, 192, 200, **267**, 352, 411, 457, 481, 561, 627, 681, 697, 762, 772, 827, 833, 893, 915, 970, 987, 990, 1029, 1040, 1069, 1090, 1146, 1176, 1190, 1247, 1283, 1330, 1332, 1351, 1404, 1440, 1483, 1490, 1497, 1503, 1514, 1578, 1601, 3011, 3024, 3057, 3089, 3098, 3137, 3155, 3162, 3172, 3184, 3191	124.0 543.4 626.9

Species	**XYZ Coordinates** (Å)	**Energies** (Hartree)	σ_{ext}	**n**	$\boldsymbol{v_i}$ (cm^{-1})	**I** ($amu*Å^2$)
i8 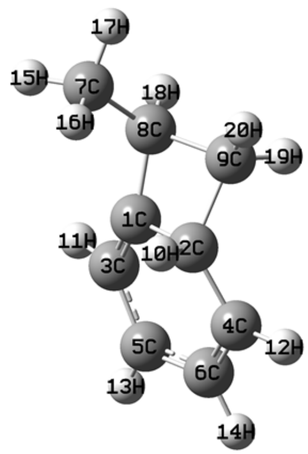 	C -0.238 0.554 -0.064 C 0.033 -0.894 -0.364 C 0.738 1.479 0.129 C 1.460 -1.292 -0.192 C 2.093 1.066 0.011 C 2.414 -0.317 -0.080 C -2.791 0.475 -0.520 C -1.634 0.283 0.466 C -1.158 -1.210 0.623 H -0.306 -1.171 -1.379 H 0.506 2.489 0.457 H 1.740 -2.340 -0.241 H 2.892 1.792 0.104 H 3.460 -0.604 -0.033 H -2.954 1.537 -0.727 H -2.592 -0.023 -1.473 H -3.718 0.064 -0.111 H -1.866 0.793 1.406 H -0.800 -1.418 1.632 H -1.863 -1.984 0.310	ZPE(B3LYP/6-311G**) = 0.1669 E(CCSD(T)/6-311G**) = -348.6006 E(MP2/6-311G**) = -348.4458 E(MP2/G3large) = -348.6480 E(G3(MP2,CC) = -348.6359	1	1	113, 143, **235**, 270, 309, 388, 417, 513, 558, 591, 667, 688, 760, 764, 794, 868, 890, 910, 962, 964, 985, 993, 1036, 1064, 1074, 1112, 1131, 1168, 1183, 1197, 1228, 1258, 1292, 1326, 1348, 1386, 1409, 1425, 1482, 1497, 1499, 1533, 1611, 2900, 3022, 3033, 3046, 3085, 3091, 3113, 3144, 3147, 3165, 3187	143.9 380.3 479.1

Species	**XYZ Coordinates** (Å)	**Energies** (Hartree)	σ_{ext}	**n**	$\boldsymbol{\nu_i}$ (cm^{-1})	**I** (amu*Å^2)
i9 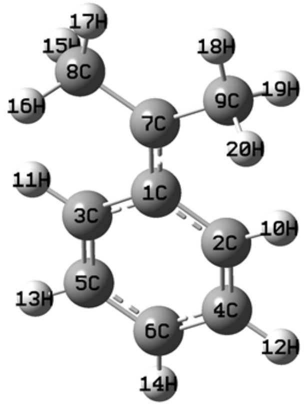 	C 0.000 0.000 -0.186 C 0.000 1.211 0.563 C 0.000 -1.211 0.563 C 0.000 1.205 1.948 C 0.000 -1.205 1.948 C 0.000 0.000 2.656 C 0.000 0.000 -1.613 C 0.000 -1.293 -2.380 C 0.000 1.293 -2.380 H 0.000 2.160 0.043 H 0.000 -2.160 0.043 H 0.000 2.147 2.486 H 0.000 -2.147 2.486 H 0.000 0.000 3.740 H 0.879 -1.909 -2.149 H -0.879 -1.909 -2.149 H 0.000 -1.114 -3.457 H 0.000 1.114 -3.457 H 0.879 1.909 -2.149 H -0.879 1.909 -2.149	ZPE(B3LYP/6-311G**) = 0.1660 E(CCSD(T)/6-311G**) = -348.6486 E(MP2/6-311G**) = -348.4859 E(MP2/G3large) = -348.6925 E(G3(MP2,CC) = -348.6892	1	1	**45**, **69**, **115**, 139, 221, 341, 357, 416, 452, 516, 525, 629, 690, 729, 765, 823, 892, 911, 952, 969, 988, 995, 1004, 1042, 1048, 1104, 1114, 1178, 1202, 1233, 1328, 1356, 1361, 1401, 1419, 1468, 1477, 1488, 1495, 1500, 1511, 1582, 1609, 2987, 2991, 3020, 3021, 3096, 3106, 3158, 3165, 3184, 3193, 3196	149.1 423.0 565.9

Species	XYZ Coordinates (Å)	Energies (Hartree)	σ_{ext}	n	ν_i (cm^{-1})	I ($amu*Å^2$)
i10 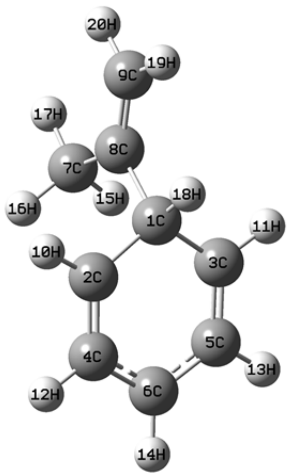	C -0.303 0.000 -0.718 C 0.491 1.253 -0.438 C 0.491 -1.252 -0.439 C 1.770 1.223 0.032 C 1.771 -1.223 0.031 C 2.439 0.000 0.283 C -1.581 -0.001 1.534 C -1.648 0.000 0.029 C -2.801 0.000 -0.639 H -0.004 2.199 -0.630 H -0.004 -2.199 -0.631 H 2.293 2.157 0.214 H 2.293 -2.157 0.213 H 3.455 0.000 0.657 H -1.039 -0.879 1.900 H -1.038 0.876 1.901 H -2.579 -0.001 1.976 H -0.572 0.001 -1.790 H -2.830 0.001 -1.724 H -3.756 0.000 -0.124	ZPE(B3LYP/6-311G**) = 0.1655 E(CCSD(T)/6-311G**) = -348.6122 E(MP2/6-311G**) = -348.4552 E(MP2/G3large) = -348.6607 E(G3(MP2,CC) = -348.6522	1	1	**61**, 73, 184, **185**, 269, 361, 396, 450, 543, 545, 593, 626, 667, 730, 754, 782, 839, 900, 927, 963, 970, 977, 990, 1017, 1019, 1028, 1075, 1115, 1171, 1193, 1224, 1288, 1290, 1347, 1397, 1409, 1444, 1449, 1478, 1496, 1539, 1598, 1705, 2911, 3022, 3069, 3106, 3125, 3149, 3151, 3169, 3170, 3194, 3204	157.9 428.0 458.5

Species	XYZ Coordinates (Å)	Energies (Hartree)	σ_{ext}	n	ν_i (cm^{-1})	I (amu*Å^2)
i11 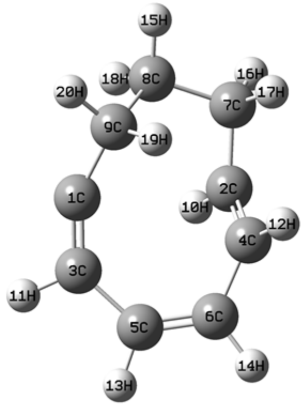	C -0.105 1.636 -0.015 C 0.377 -1.272 -0.495 C -1.365 1.405 -0.338 C -0.561 -1.442 0.438 C -2.263 0.241 -0.128 C -1.952 -1.020 0.223 C 1.834 -1.115 -0.203 C 2.148 0.405 -0.208 C 1.165 1.265 0.638 H 0.056 -0.968 -1.490 H -1.878 2.234 -0.836 H -0.278 -1.767 1.440 H -3.315 0.476 -0.275 H -2.762 -1.724 0.400 H 3.159 0.558 0.182 H 2.472 -1.613 -0.942 H 2.074 -1.536 0.779 H 2.147 0.778 -1.236 H 0.959 0.754 1.590 H 1.687 2.192 0.910	ZPE(B3LYP/6-311G**) = 0.1667 E(CCSD(T)/6-311G**) = -348.5490 E(MP2/6-311G**) = -348.3759 E(MP2/G3large) = -348.5781 E(G3(MP2,CC) = -348.5845	1	1	115, 175, 199, 242, 285, 311, 366, 419, 488, 522, 585, 683, 748, 779, 828, 837, 860, 883, 914, 941, 988, 996, 1007, 1030, 1071, 1100, 1163, 1216, 1236, 1249, 1314, 1321, 1326, 1343, 1350, 1366, 1424, 1465, 1486, 1494, 1643, 1709, 1721, 2978, 3003, 3019, 3035, 3036, 3057, 3076, 3095, 3120, 3127, 3143	198.2 323.4 471.5

Species	XYZ Coordinates (Å)	Energies (Hartree)	σ_{ext}	n	v_i (cm^{-1})	I (amu*Å^2)
i12 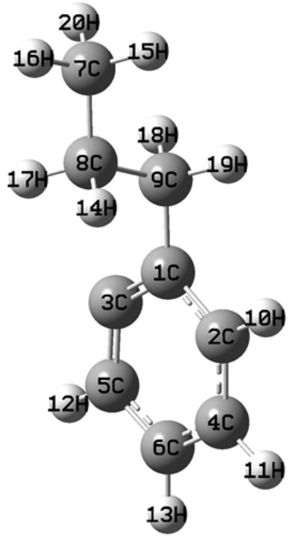	C -0.074 0.014 0.369 C -0.789 1.220 0.256 C -0.815 -1.121 0.115 C -2.141 1.230 -0.085 C -2.145 -1.182 -0.222 C -2.825 0.040 -0.325 C 3.790 -0.170 -0.194 C 2.300 -0.132 -0.541 C 1.400 -0.019 0.705 H -0.273 2.157 0.446 H -2.666 2.176 -0.160 H -2.654 -2.123 -0.399 H -3.877 0.052 -0.588 H 2.094 0.713 -1.207 H 4.099 0.738 0.334 H 4.405 -0.256 -1.094 H 2.023 -1.034 -1.096 H 1.601 -0.867 1.368 H 1.663 0.887 1.261 H 4.025 -1.023 0.451	ZPE(B3LYP/6-311G**) = 0.1676 E(CCSD(T)/6-311G**) = -348.6129 E(MP2/6-311G**) = -348.4499 E(MP2/G3large) = -348.6501 E(G3(MP2,CC) = -348.6455	1	1	**34**, **83**, 100, **238**, 274, 309, 331, 419, 509, 588, 633, 704, 744, 748, 816, 853, 876, 899, 939, 983, 990, 1038, 1043, 1070, 1108, 1141, 1173, 1216, 1239, 1286, 1313, 1321, 1333, 1380, 1411, 1449, 1475, 1489, 1497, 1500, 1512, 1574, 1634, 3018, 3019, 3027, 3043, 3065, 3085, 3088, 3145, 3159, 3172, 3184	109.4 599.7 664.9

Species	XYZ Coordinates (Å)	Energies (Hartree)	σ_{ext}	n	ν_i (cm^{-1})	I ($amu*Å^2$)
TS 1-propenyl 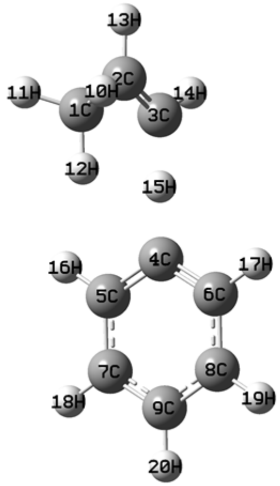	C -1.717 -2.839 0.000 C -2.747 -1.745 0.000 C -2.510 -0.445 0.000 C -0.001 0.478 0.000 C 0.619 0.725 -1.214 C 0.619 0.725 1.214 C 1.918 1.242 -1.210 C 1.918 1.242 1.210 C 2.563 1.499 0.000 H -1.835 -3.482 0.879 H -1.835 -3.482 -0.879 H -0.703 -2.437 0.000 H -3.789 -2.079 0.000 H -3.247 0.351 0.000 H -1.259 0.003 0.000 H 0.110 0.524 -2.151 H 0.110 0.524 2.151 H 2.423 1.444 -2.148 H 2.423 1.444 2.148 H 3.570 1.900 0.000	ZPE(B3LYP/6-311G**) = 0.1581 E(CCSD(T)/6-311G**) = -348.5504 E(MP2/6-311G**) = -348.3728 E(MP2/G3large) = -348.5799 E(G3(MP2,CC) = -348.5994	1	1	1580i, **23**, 51, 71, 140, **174**, 269, 320, 403, 428, 505, 618, 635, 665, 700, 731, 846, 906, 919, 922, 962, 972, 1000, 1011, 1028, 1063, 1067, 1075, 1167, 1177, 1186, 1207, 1274, 1326, 1326, 1343, 1410, 1474, 1485, 1488, 1498, 1603, 1627, 1687, 3017, 3054, 3061, 3114, 3152, 3157, 3167, 3172, 3174, 3185	145.3 694.6 730.3

Species	**XYZ Coordinates** (Å)	**Energies** (Hartree)	**σ_{ext}**	**n**	**v_i** (cm^{-1})	**I** (amu*Å^2)
TS 2-propenyl 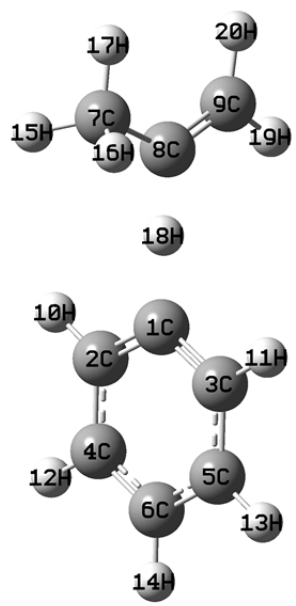	C 0.240 0.000 0.026 C 0.907 1.209 0.128 C 0.903 -1.208 -0.105 C 2.304 1.206 0.095 C 2.301 -1.202 -0.137 C 2.996 0.002 -0.037 C -3.110 0.192 -1.209 C -2.441 -0.015 0.106 C -2.956 -0.211 1.307 H 0.361 2.141 0.235 H 0.355 -2.142 -0.181 H 2.849 2.141 0.174 H 2.844 -2.137 -0.238 H 4.080 0.003 -0.062 H -2.828 1.156 -1.647 H -2.817 -0.581 -1.927 H -4.200 0.169 -1.106 H -1.143 -0.002 0.052 H -2.330 -0.347 2.182 H -4.034 -0.242 1.468	ZPE(B3LYP/6-311G**) = 0.1581 E(CCSD(T)/6-311G**) = -348.5531 E(MP2/6-311G**) = -348.3761 E(MP2/G3large) = -348.5835 E(G3(MP2,CC) = -348.6025	1	1	1527i, **20**, 52, 63, **158**, 164, 225, 306, 402, 435, 438, 617, 630, 665, 699, 730, 844, 907, 917, 922, 964, 971, 1000, 1011, 1026, 1054, 1061, 1077, 1175, 1177, 1186, 1218, 1290, 1325, 1342, 1401, 1432, 1467, 1474, 1484, 1497, 1601, 1626, 1714, 3005, 3067, 3069, 3086, 3151, 3156, 3166, 3171, 3179, 3184	144.9 691.5 729.0

Species	**XYZ Coordinates** (Å)	**Energies** (Hartree)	**σ_{ext}**	**n**	$\boldsymbol{v_i}$ (cm^{-1})	**I** ($amu*Å^2$)
TS allyl 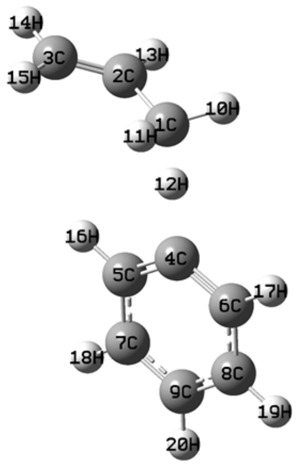	C 2.241 1.121 -0.069 C 3.085 0.031 0.454 C 3.805 -0.814 -0.293 C -0.403 0.350 -0.015 C -0.646 -1.009 0.017 C -1.403 1.303 -0.039 C -1.978 -1.439 0.025 C -2.731 0.861 -0.030 C -3.013 -0.505 0.002 H 2.259 2.028 0.538 H 2.415 1.350 -1.122 H 1.061 0.782 -0.021 H 3.087 -0.100 1.535 H 4.389 -1.610 0.153 H 3.838 -0.727 -1.375 H 0.168 -1.727 0.034 H -1.177 2.364 -0.064 H -2.203 -2.500 0.049 H -3.541 1.583 -0.048 H -4.043 -0.842 0.008	ZPE(B3LYP/6-311G**) = 0.1589 E(CCSD(T)/6-311G**) = -348.5583 E(MP2/6-311G**) = -348.3814 E(MP2/G3large) = -348.5888 E(G3(MP2,CC) = -348.6068	1	1	1083i, **26**, 40, 66, **117**, 178, 358, 401, 424, 435, 528, 614, 631, 692, 729, 730, 837, 904, 925, 948, 969, 973, 998, 1013, 1022, 1036, 1072, 1079, 1093, 1178, 1183, 1199, 1318, 1320, 1326, 1362, 1413, 1441, 1471, 1478, 1493, 1593, 1626, 1673, 3057, 3116, 3127, 3135, 3150, 3155, 3165, 3170, 3184, 3213	131.3 724.6 837.0

Species	XYZ Coordinates (Å)	Energies (Hartree)	σ_{ext}	n	ν_i (cm^{-1})	I (amu*Å^2)
TS i1 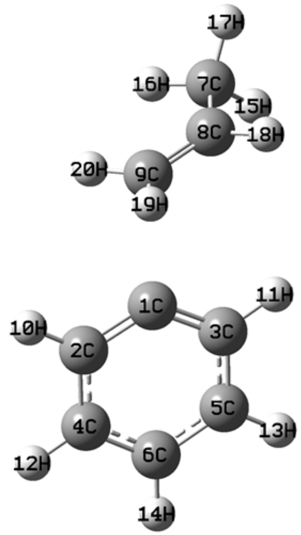	C 0.286 0.327 -0.177 C 1.207 1.299 0.152 C 0.594 -1.005 -0.343 C 2.538 0.900 0.326 C 1.929 -1.390 -0.166 C 2.894 -0.439 0.168 C -3.418 -0.589 0.807 C -2.822 -0.039 -0.452 C -2.020 1.043 -0.515 H 0.925 2.340 0.273 H -0.165 -1.736 -0.602 H 3.293 1.636 0.585 H 2.211 -2.431 -0.288 H 3.925 -0.743 0.304 H -3.061 -1.607 1.004 H -3.167 0.030 1.672 H -4.510 -0.651 0.734 H -3.030 -0.590 -1.367 H -1.688 1.439 -1.467 H -1.865 1.671 0.355	ZPE(B3LYP/6-311G**) = 0.1670 E(CCSD(T)/6-311G**) = -348.5671 E(MP2/6-311G**) = -348.3886 E(MP2/G3large) = -348.5949 E(G3(MP2,CC) = -348.6103	1	1	194i, **16**, **49**, 77, 119, 149, 248, 400, 424, 432, 581, 611, 646, 689, 725, 831, 877, 897, 922, 943, 964, 987, 993, 998, 1018, 1050, 1053, 1076, 1176, 1178, 1189, 1305, 1312, 1323, 1407, 1439, 1463, 1475, 1479, 1492, 1579, 1624, 1627, 3006, 3046, 3092, 3129, 3135, 3147, 3152, 3163, 3168, 3183, 3223	139.1 644.4 729.6

Species	**XYZ Coordinates** (Å)	**Energies** (Hartree)	σ_{ext}	**n**	ν_i (cm^{-1})	**I** ($amu*Å^2$)
TS i2 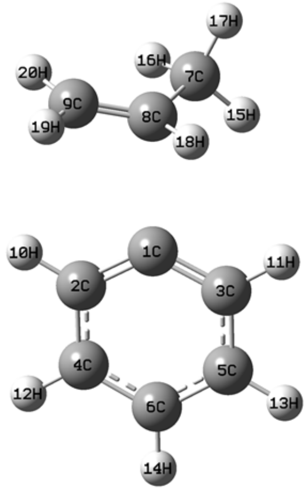 	C 0.074 -0.026 -0.158 C 0.653 1.174 0.194 C 0.787 -1.185 -0.386 C 2.044 1.210 0.340 C 2.179 -1.135 -0.239 C 2.801 0.059 0.124 C -2.596 -0.968 0.843 C -2.280 -0.152 -0.386 C -2.645 1.144 -0.528 H 0.052 2.064 0.353 H 0.299 -2.113 -0.668 H 2.534 2.138 0.620 H 2.771 -2.029 -0.409 H 3.879 0.092 0.236 H -1.825 -1.711 1.054 H -2.703 -0.330 1.724 H -3.540 -1.506 0.701 H -2.031 -0.714 -1.282 H -2.527 1.666 -1.470 H -3.016 1.721 0.314	ZPE(B3LYP/6-311G**) = 0.1632 E(CCSD(T)/6-311G**) = -348.5653 E(MP2/6-311G**) = -348.3864 E(MP2/G3large) = -348.5927 E(G3(MP2,CC) = -348.6084	1	1	272i, **27**, 67, 98, **160**, 200, 254, 401, 420, 440, 518, 605, 612, 691, 726, 833, 865, 898, 900, 942, 952, 966, 994, 1004, 1021, 1046, 1059, 1078, 1176, 1180, 1184, 1292, 1314, 1324, 1409, 1439, 1463, 1476, 1486, 1496, 1578, 1599, 1627, 3019, 3079, 3108, 3128, 3140, 3145, 3153, 3163, 3169, 3184, 3217	151.1 541.6 636.3

Species	**XYZ Coordinates** (Å)	**Energies** (Hartree)	σ_{ext}	**n**	$\boldsymbol{v_i}$ (cm^{-1})	**I** (amu*Å^2)
TS i1-i3 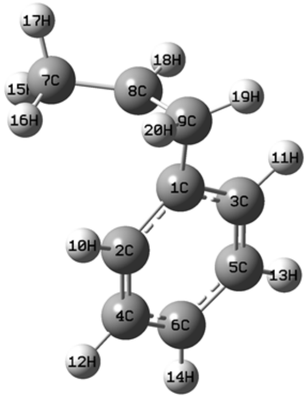	C 0.220 -0.326 0.421 C -0.296 1.005 0.634 C -0.716 -1.303 -0.085 C -1.574 1.340 0.244 C -1.988 -0.939 -0.465 C -2.434 0.388 -0.328 C 2.520 0.833 -0.840 C 1.824 -0.421 -0.408 C 1.541 -0.759 1.005 H 0.336 1.746 1.111 H -0.394 -2.336 -0.175 H -1.929 2.353 0.404 H -2.661 -1.693 -0.858 H -3.437 0.664 -0.628 H 2.171 1.174 -1.818 H 2.373 1.650 -0.129 H 3.603 0.664 -0.919 H 1.794 -1.237 -1.121 H 1.607 -1.803 1.301 H 1.954 -0.090 1.757	ZPE(B3LYP/6-311G**) = 0.1652 E(CCSD(T)/6-311G**) = -348.6036 E(MP2/6-311G**) = -348.4452 E(MP2/G3large) = -348.6508 E(G3(MP2,CC) = -348.6439	1	1	495i, **100**, 116, 161, 219, 329, 406, 425, 437, 493, 622, 664, 701, 741, 782, 804, 829, 880, 938, 959, 969, 986, 993, 1020, 1038, 1111, 1135, 1164, 1168, 1190, 1195, 1232, 1330, 1345, 1392, 1417, 1458, 1478, 1480, 1489, 1497, 1546, 1595, 2993, 3058, 3077, 3098, 3146, 3150, 3156, 3168, 3170, 3176, 3192	159.0 403.8 468.7

Species	XYZ Coordinates (Å)	Energies (Hartree)	σ_{ext}	n	v_i (cm^{-1})	I (amu*Å^2)
TS i1-i4 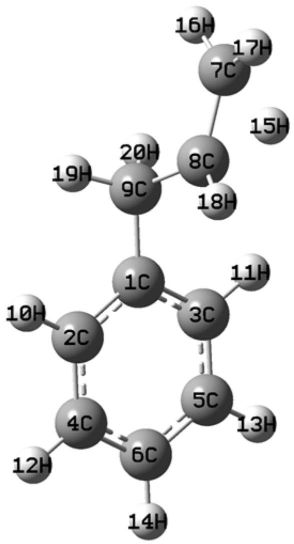	C 0.002 -0.002 -0.003 C -0.002 -0.001 1.394 C 1.235 -0.001 -0.665 C 1.192 0.000 2.115 C 2.430 -0.002 0.050 C 2.412 -0.001 1.444 C -2.583 1.409 -2.565 C -1.577 1.328 -1.466 C -1.294 0.014 -0.787 H -0.949 -0.005 1.923 H 1.257 0.001 -1.750 H 1.167 -0.001 3.199 H 3.376 -0.006 -0.481 H 3.342 -0.003 2.002 H -1.289 1.449 -2.725 H -3.024 0.496 -2.945 H -3.064 2.352 -2.785 H -1.366 2.244 -0.926 H -2.128 -0.239 -0.113 H -1.277 -0.784 -1.541	ZPE(B3LYP/6-311G**) = 0.1617 E(CCSD(T)/6-311G**) = -348.5586 E(MP2/6-311G**) = -348.4317 E(MP2/G3large) = -348.6399 E(G3(MP2,CC) = -348.6050	1	1	1921i, **42**, **78**, 142, 241, 334, 369, 411, 416, 494, 603, 637, 705, 717, 724, 760, 818, 858, 892, 926, 932, 979, 1001, 1018, 1049, 1060, 1104, 1149, 1181, 1202, 1216, 1237, 1257, 1332, 1342, 1359, 1370, 1429, 1479, 1486, 1527, 1626, 1646, 2194, 2952, 3045, 3144, 3153, 3155, 3159, 3167, 3175, 3187, 3260	113.8 577.9 651.8

Species	XYZ Coordinates (Å)	Energies (Hartree)	σ_{ext}	n	ν_i (cm^{-1})	I (amu*Å^2)
TS i1-i6 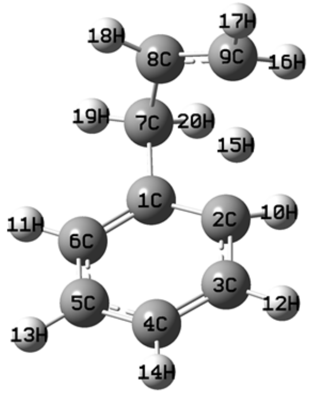	C 0.114 -0.534 0.490 C -0.132 0.891 0.598 C -1.441 1.368 0.238 C -2.385 0.520 -0.298 C -2.110 -0.852 -0.429 C -0.862 -1.357 -0.044 C 1.557 -0.983 0.639 C 2.267 -0.349 -0.534 C 2.347 1.035 -0.581 H 0.345 1.408 1.436 H -0.649 -2.414 -0.178 H -1.675 2.417 0.389 H -2.863 -1.521 -0.830 H -3.355 0.905 -0.594 H 0.884 1.287 -0.264 H 2.624 1.580 0.322 H 2.643 1.524 -1.505 H 2.312 -0.927 -1.452 H 1.632 -2.072 0.624 H 1.975 -0.619 1.587	ZPE(B3LYP/6-311G**) = 0.1619 E(CCSD(T)/6-311G**) = -348.5594 E(MP2/6-311G**) = -348.3883 E(MP2/G3large) = -348.5937 E(G3(MP2,CC) = -348.6029	1	1	1940i, 117, 181, 267, 358, 373, 431, 461, 507, 541, 620, 632, 709, 732, 790, 810, 861, 902, 922, 942, 956, 972, 999, 1027, 1046, 1085, 1100, 1170, 1178, 1183, 1208, 1255, 1275, 1292, 1341, 1345, 1395, 1421, 1458, 1482, 1494, 1541, 1548, 1619, 2989, 3029, 3067, 3089, 3148, 3150, 3158, 3173, 3176, 3187	158.7 396.8 486.9

Species	XYZ Coordinates (Å)	Energies (Hartree)	σ_{ext}	n	v_i (cm^{-1})	I (amu*Å^2)
TS i1-i7 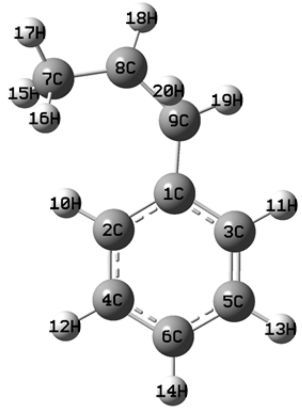	C -0.028 -0.456 -0.076 C -0.263 0.935 -0.155 C -1.161 -1.294 0.055 C -1.553 1.449 -0.087 C -2.444 -0.775 0.117 C -2.654 0.606 0.053 C 3.005 0.944 0.194 C 2.655 -0.485 -0.093 C 1.285 -1.082 -0.134 H 0.564 1.617 -0.293 H -1.015 -2.368 0.110 H -1.699 2.522 -0.155 H -3.289 -1.448 0.216 H -3.657 1.013 0.104 H 2.873 1.592 -0.685 H 2.397 1.369 0.997 H 4.052 1.023 0.496 H 3.432 -1.134 -0.478 H 1.287 -2.114 -0.470 H 1.997 -1.122 0.910	ZPE(B3LYP/6-311G**) = 0.1624 E(CCSD(T)/6-311G**) = -348.5630 E(MP2/6-311G**) = -348.4002 E(MP2/G3large) = -348.6091 E(G3(MP2,CC) = -348.6095	1	1	1847i, **34**, 145, 163, **239**, 273, 308, 415, 451, 477, 575, 627, 643, 701, 750, 773, 833, 849, 899, 916, 968, 986, 1006, 1024, 1046, 1075, 1107, 1150, 1178, 1205, 1230, 1279, 1338, 1355, 1380, 1420, 1431, 1482, 1486, 1501, 1526, 1594, 1628, 2170, 2965, 3050, 3088, 3146, 3152, 3160, 3170, 3171, 3187, 3216	132.4 496.0 619.2

Species	**XYZ Coordinates** (Å)	**Energies** (Hartree)	**σ_{ext}**	**n**	***ν_i*** (cm^{-1})	**I** (amu*Å^2)
TS i1-i12 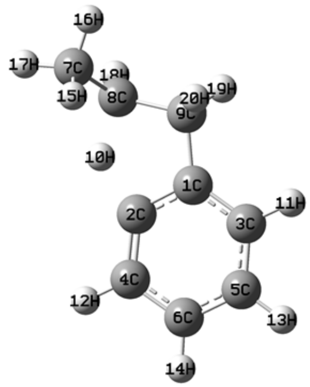	C 0.023 -0.136 -0.261 C -0.157 -0.008 1.109 C 1.322 -0.073 -0.770 C 0.878 0.178 2.005 C 2.390 0.116 0.109 C 2.175 0.241 1.484 C -3.430 0.727 0.030 C -2.381 -0.360 0.063 C -1.283 -0.330 -1.013 H -1.570 -0.160 1.084 H 1.505 -0.170 -1.836 H 0.706 0.273 3.072 H 3.401 0.165 -0.280 H 3.019 0.387 2.150 H -2.970 1.720 -0.005 H -4.071 0.633 -0.857 H -4.082 0.686 0.908 H -2.790 -1.355 0.247 H -1.268 -1.252 -1.603 H -1.449 0.491 -1.720	ZPE(B3LYP/6-311G**) = 0.1622 E(CCSD(T)/6-311G**) = -348.5799 E(MP2/6-311G**) = -348.4133 E(MP2/G3large) = -348.6182 E(G3(MP2,CC) = -348.6226	1	1	1752i, 41, 156, 191, **207**, 318, 391, 415, 472, 489, 607, 660, 704, 745, 797, 831, 866, 884, 912, 947, 990, 1002, 1038, 1071, 1096, 1115, 1130, 1174, 1206, 1220, 1247, 1286, 1307, 1332, 1360, 1408, 1466, 1476, 1485, 1490, 1492, 1602, 1628, 1683, 2994, 3017, 3045, 3054, 3079, 3095, 3147, 3155, 3168, 3180	129.4 493.5 591.7

Species	XYZ Coordinates (Å)	Energies (Hartree)	σ_{ext}	n	v_i (cm^{-1})	I ($amu*Å^2$)
TS i1-p2 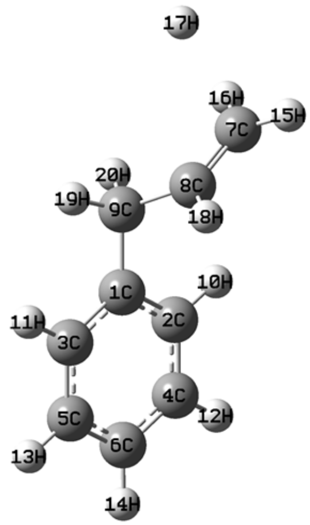	C 0.075 -0.301 -0.278 C 0.477 1.039 -0.291 C 1.033 -1.282 -0.010 C 1.802 1.388 -0.050 C 2.362 -0.936 0.234 C 2.750 0.400 0.214 C -3.379 0.629 0.255 C -2.323 -0.150 0.498 C -1.375 -0.673 -0.548 H -0.257 1.814 -0.488 H 0.738 -2.326 0.003 H 2.096 2.432 -0.068 H 3.091 -1.712 0.439 H 3.783 0.672 0.403 H -4.019 0.984 1.054 H -3.613 0.972 -0.748 H -5.112 -1.008 -0.145 H -2.109 -0.453 1.522 H -1.455 -1.765 -0.588 H -1.680 -0.300 -1.532	ZPE(B3LYP/6-311G**) = 0.1580 E(CCSD(T)/6-311G**) = -348.5659 E(MP2/6-311G**) = -348.4386 E(MP2/G3large) = -348.6463 E(G3(MP2,CC) = -348.6156	1	1	118i, **28**, 73, 104, 143, 190, 291, 324, 400, 415, 502, 549, 636, 677, 716, 760, 835, 857, 912, 927, 943, 949, 978, 1001, 1018, 1027, 1051, 1097, 1126, 1181, 1203, 1214, 1232, 1311, 1324, 1342, 1362, 1451, 1477, 1486, 1528, 1626, 1645, 1679, 3015, 3052, 3128, 3135, 3154, 3158, 3168, 3176, 3188, 3216	122.2 548.3 634.7

Species	XYZ Coordinates (Å)	Energies (Hartree)	σ_{ext}	n	ν_i (cm^{-1})	I ($amu*Å^2$)
TS i1-p3 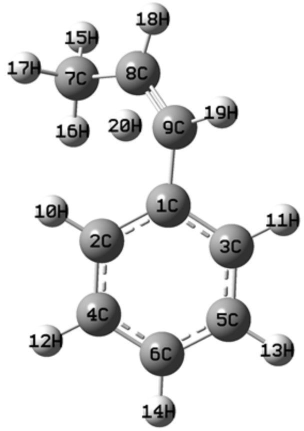	C 0.026 -0.423 0.216 C -0.306 0.917 0.461 C -0.993 -1.291 -0.203 C -1.605 1.377 0.265 C -2.290 -0.831 -0.404 C -2.601 0.508 -0.175 C 2.780 0.921 -0.650 C 2.560 -0.418 -0.019 C 1.393 -0.964 0.398 H 0.450 1.594 0.840 H -0.759 -2.336 -0.380 H -1.842 2.416 0.467 H -3.060 -1.519 -0.735 H -3.613 0.867 -0.325 H 3.518 0.842 -1.454 H 1.864 1.346 -1.061 H 3.187 1.637 0.076 H 3.456 -1.012 0.144 H 1.429 -2.001 0.721 H 1.581 -0.611 2.383	ZPE(B3LYP/6-311G**) = 0.1587 E(CCSD(T)/6-311G**) = -348.5658 E(MP2/6-311G**) = -348.3949 E(MP2/G3large) = -348.6032 E(G3(MP2,CC) = -348.6153	1	1	553i, **54**, 122, **162**, 209, 257, 290, 359, 417, 430, 478, 550, 634, 670, 715, 735, 782, 819, 857, 932, 936, 981, 999, 1004, 1017, 1050, 1053, 1091, 1110, 1182, 1203, 1205, 1269, 1333, 1355, 1403, 1436, 1474, 1486, 1493, 1527, 1614, 1640, 1645, 3003, 3056, 3110, 3131, 3149, 3158, 3164, 3175, 3186, 3194	142.5 477.0 569.6

Species	**XYZ Coordinates** (Å)	**Energies** (Hartree)	σ_{ext}	**n**	v_i (cm^{-1})	**I** (amu*Å^2)
TS i2-i3 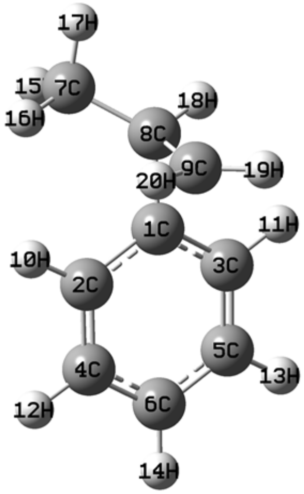 	C 0.274 -0.191 -0.033 C -0.265 1.132 0.163 C -0.680 -1.235 -0.320 C -1.626 1.347 0.178 C -2.034 -0.991 -0.299 C -2.532 0.296 -0.035 C 2.686 0.658 -0.662 C 1.752 -0.454 -0.219 C 1.505 -0.675 1.224 H 0.411 1.966 0.310 H -0.308 -2.230 -0.545 H -2.001 2.352 0.342 H -2.724 -1.802 -0.508 H -3.600 0.480 -0.023 H 2.507 0.929 -1.705 H 2.570 1.557 -0.053 H 3.725 0.331 -0.565 H 1.922 -1.372 -0.781 H 1.328 -1.665 1.617 H 1.687 0.125 1.930	ZPE(B3LYP/6-311G**) = 0.1651 E(CCSD(T)/6-311G**) = -348.6026 E(MP2/6-311G**) = -348.4440 E(MP2/G3large) = -348.6496 E(G3(MP2,CC) = -348.6431	1	1	535i, 120, 143, **219**, 234, 335, 401, 410, 442, 525, 620, 660, 681, 694, 737, 791, 798, 841, 877, 925, 958, 970, 986, 1020, 1028, 1077, 1122, 1163, 1170, 1196, 1214, 1231, 1324, 1346, 1394, 1418, 1459, 1467, 1480, 1498, 1504, 1550, 1595, 3030, 3079, 3091, 3105, 3146, 3151, 3158, 3169, 3183, 3193, 3256	145.8 414.1 484.2

Species	**XYZ Coordinates** (Å)	**Energies** (Hartree)	σ_{ext}	**n**	$\boldsymbol{v_i}$ (cm^{-1})	**I** (amu*Å^2)
TS i2-i8 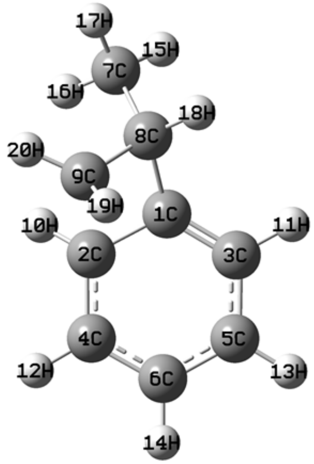	C -0.224 0.471 -0.154 C 0.113 -0.926 -0.362 C 0.744 1.407 0.095 C 1.494 -1.294 -0.310 C 2.109 1.028 0.083 C 2.456 -0.317 -0.078 C -2.759 0.334 -0.687 C -1.644 0.393 0.363 C -1.330 -0.960 1.022 H -0.526 -1.524 -1.010 H 0.465 2.418 0.374 H 1.790 -2.322 -0.485 H 2.880 1.770 0.254 H 3.503 -0.600 -0.049 H -2.849 1.289 -1.212 H -2.568 -0.441 -1.435 H -3.721 0.113 -0.215 H -1.868 1.189 1.081 H -0.847 -0.918 1.992 H -2.016 -1.794 0.885	ZPE(B3LYP/6-311G**) = 0.1652 E(CCSD(T)/6-311G**) = -348.5774 E(MP2/6-311G**) = -348.4123 E(MP2/G3large) = -348.6164 E(G3(MP2,CC) = -348.6163	1	1	653i, 129, 154, **231**, 295, 307, 403, 439, 559, 585, 596, 643, 719, 732, 789, 816, 846, 864, 907, 926, 956, 967, 994, 1017, 1026, 1076, 1093, 1158, 1163, 1177, 1200, 1233, 1304, 1335, 1361, 1406, 1444, 1451, 1489, 1498, 1501, 1536, 1611, 3024, 3025, 3083, 3086, 3093, 3098, 3152, 3156, 3175, 3187, 3196	143.6 400.3 475.8

Species	XYZ Coordinates (Å)	Energies (Hartree)	σ_{ext}	n	ν_i (cm^{-1})	I (amu*Å^2)
TS i2-i9 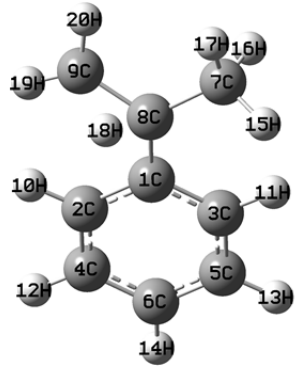	C 0.169 0.029 0.044 C -0.599 1.216 0.034 C -0.540 -1.191 0.007 C -1.986 1.179 0.003 C -1.929 -1.221 -0.032 C -2.666 -0.038 -0.031 C 2.422 -1.235 -0.030 C 1.635 0.049 0.098 C 2.407 1.306 -0.127 H -0.109 2.181 0.063 H 0.000 -2.129 -0.004 H -2.542 2.110 0.000 H -2.438 -2.178 -0.067 H -3.749 -0.064 -0.060 H 2.054 -2.021 0.631 H 2.380 -1.611 -1.060 H 3.474 -1.067 0.212 H 2.056 0.744 1.062 H 1.915 2.248 -0.307 H 3.476 1.233 -0.262	ZPE(B3LYP/6-311G**) = 0.1620 E(CCSD(T)/6-311G**) = -348.5675 E(MP2/6-311G**) = -348.4059 E(MP2/G3large) = -348.6166 E(G3(MP2,CC) = -348.6162	1	1	1821i, **43**, 145, **190**, 252, 358, 379, 406, 419, 444, 510, 544, 634, 638, 700, 733, 768, 826, 891, 915, 965, 979, 988, 1009, 1038, 1050, 1107, 1122, 1181, 1209, 1224, 1241, 1332, 1359, 1365, 1415, 1444, 1477, 1491, 1506, 1530, 1600, 1633, 2175, 3003, 3073, 3101, 3158, 3165, 3171, 3184, 3192, 3197, 3288	145.1 429.3 567.9

Species	XYZ Coordinates (Å)	Energies (Hartree)	σ_{ext}	n	ν_i (cm^{-1})	I (amu*Å^2)
TS i2-i10 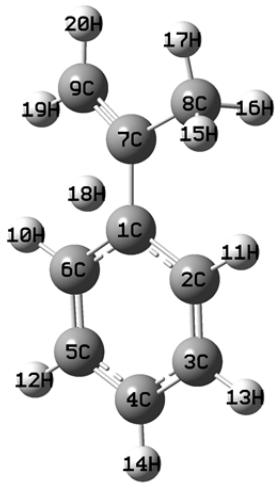	C 0.193 0.054 0.096 C -0.504 -1.197 -0.022 C -1.885 -1.241 -0.071 C -2.652 -0.071 -0.046 C -1.994 1.164 0.012 C -0.617 1.243 0.065 C 1.699 0.124 0.036 C 2.451 -1.192 0.005 C 2.392 1.299 -0.166 H -0.142 2.213 0.116 H 0.056 -2.121 -0.071 H -2.572 2.082 0.003 H -2.376 -2.205 -0.150 H -3.733 -0.119 -0.087 H 2.123 -1.887 0.782 H 2.310 -1.687 -0.962 H 3.518 -1.016 0.143 H 0.943 0.093 1.226 H 1.906 2.256 -0.293 H 3.473 1.291 -0.168	ZPE(B3LYP/6-311G**) = 0.1606 E(CCSD(T)/6-311G**) = -348.5486 E(MP2/6-311G**) = -348.3851 E(MP2/G3large) = -348.5955 E(G3(MP2,CC) = -348.5985	1	1	1615i, 95, 135, 215, **254**, 355, 400, 413, 457, 517, 525, 587, 625, 677, 711, 723, 775, 787, 859, 929, 962, 978, 985, 1010, 1018, 1036, 1083, 1109, 1117, 1177, 1210, 1259, 1305, 1355, 1388, 1413, 1437, 1468, 1494, 1495, 1505, 1557, 1563, 1626, 3021, 3078, 3115, 3159, 3160, 3165, 3191, 3200, 3205, 3248	144.9 427.3 564.6

Species	XYZ Coordinates (Å)	Energies (Hartree)	σ_{ext}	n	v_i (cm^{-1})	I (amu*Å^2)
TS i2-p1 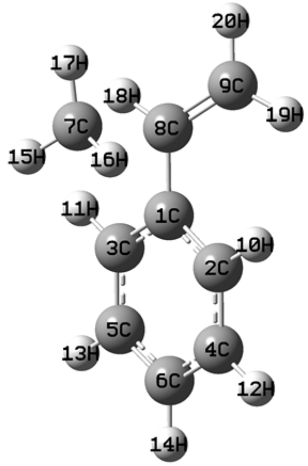	C -0.164 -0.053 -0.300 C 0.404 1.118 0.222 C 0.682 -1.140 -0.554 C 1.770 1.201 0.467 C 2.051 -1.059 -0.312 C 2.602 0.114 0.199 C -2.325 -0.770 1.484 C -1.614 -0.172 -0.597 C -2.405 0.881 -0.969 H -0.230 1.967 0.451 H 0.261 -2.058 -0.954 H 2.188 2.115 0.873 H 2.687 -1.912 -0.523 H 3.666 0.180 0.392 H -1.701 -1.640 1.649 H -2.066 0.122 2.040 H -3.381 -0.949 1.320 H -1.931 -1.164 -0.902 H -2.079 1.910 -0.873 H -3.418 0.717 -1.314	ZPE(B3LYP/6-311G**) = 0.1618 E(CCSD(T)/6-311G**) = -348.5770 E(MP2/6-311G**) = -348.3996 E(MP2/G3large) = -348.6073 E(G3(MP2,CC) = -348.6229	1	1	474 i, **54**, 101, **113**, 197, 224, 290, 415, 431, 469, 526, 545, 575, 594, 636, 712, 774, 786, 815, 852, 876, 925, 977, 990, 999, 1015, 1035, 1053, 1106, 1181, 1201, 1210, 1280, 1325, 1354, 1419, 1422, 1431, 1480, 1525, 1557, 1624, 1644, 3083, 3140, 3145, 3155, 3161, 3171, 3178, 3189, 3231, 3240, 3247	169.8 472.6 510.7

Species	XYZ Coordinates (Å)	Energies (Hartree)	σ_{ext}	n	ν_i (cm^{-1})	I (amu*Å^2)
TS i2-p4 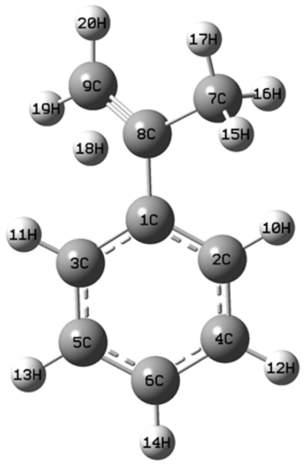	C -0.002 -0.002 0.003 C -0.001 0.041 1.404 C 1.236 -0.040 -0.656 C 1.194 0.073 2.119 C 2.429 -0.011 0.057 C 2.414 0.049 1.450 C -2.540 -0.476 -0.064 C -1.285 0.009 -0.766 C -1.388 0.716 -1.921 H -0.938 0.063 1.946 H 1.260 -0.123 -1.736 H 1.169 0.114 3.203 H 3.373 -0.049 -0.475 H 3.344 0.067 2.007 H -2.380 -1.429 0.443 H -2.860 0.254 0.687 H -3.356 -0.596 -0.778 H -0.998 -1.698 -1.600 H -0.535 1.209 -2.369 H -2.329 0.774 -2.455	ZPE(B3LYP/6-311G**) = 0.1627 E(CCSD(T)/6-311G**) = -348.5652 E(MP2/6-311G**) = -348.4269 E(MP2/G3large) = -348.6333 E(G3(MP2,CC) = -348.6090	1	1	780i, **60**, 137, 201, **236**, 332, 380, 416, 429, 500, 534, 541, 578, 636, 667, 714, 746, 787, 856, 897, 925, 937, 982, 1003, 1017, 1022, 1050, 1058, 1107, 1136, 1183, 1207, 1295, 1326, 1353, 1409, 1427, 1475, 1483, 1496, 1526, 1599, 1624, 1643, 3028, 3091, 3117, 3141, 3161, 3169, 3180, 3186, 3192, 3229	145.3 430.5 547.4

Species	**XYZ Coordinates** (Å)	**Energies** (Hartree)	σ_{ext}	**n**	ν_i (cm^{-1})	**I** (amu*Å^2)
TS i4-i5 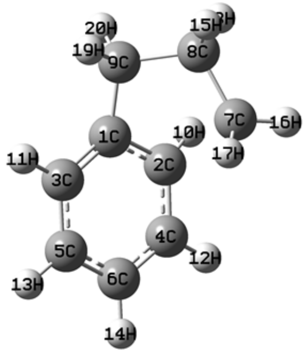	C -0.060 0.137 -0.028 C -0.105 0.120 1.405 C 1.132 -0.125 -0.674 C 1.103 -0.083 2.125 C 2.313 -0.356 0.051 C 2.285 -0.347 1.449 C -1.526 -1.466 1.271 C -2.341 -0.780 0.199 C -1.411 0.122 -0.693 H -0.900 0.666 1.907 H 1.150 -0.183 -1.759 H 1.095 -0.027 3.208 H 3.241 -0.552 -0.474 H 3.198 -0.524 2.008 H -2.866 -1.510 -0.427 H -1.966 -1.587 2.256 H -0.885 -2.288 0.966 H -3.116 -0.165 0.666 H -1.333 -0.266 -1.712 H -1.836 1.128 -0.771	ZPE(B3LYP/6-311G**) = 0.1664 E(CCSD(T)/6-311G**) = -348.5997 E(MP2/6-311G**) = -348.4358 E(MP2/G3large) = -348.6402 E(G3(MP2,CC) -348.6378	1	1	536i, 51, 146, 213, 327, 404, 464, 506, 586, 618, 640, 709, 732, 768, 813, 843, 849, 876, 904, 936, 964, 975, 1017, 1032, 1039, 1067, 1105, 1172, 1183, 1188, 1216, 1230, 1296, 1329, 1337, 1355, 1455, 1468, 1483, 1505, 1512, 1568, 1606, 3016, 3026, 3056, 3078, 3109, 3117, 3150, 3159, 3174, 3186, 3198	155.5 364.9 460.4

Species	**XYZ Coordinates** (Å)	**Energies** (Hartree)	**σ_{ext}**	**n**	***v_i*** (cm^{-1})	**I** (amu*$Å^2$)
TS i4-p2 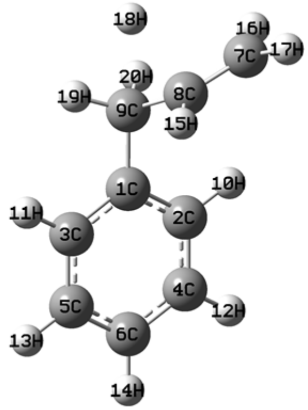	C 0.000 -0.002 -0.007 C -0.011 0.013 1.392 C 1.234 -0.015 -0.663 C 1.179 0.022 2.115 C 2.428 -0.010 0.057 C 2.404 0.010 1.448 C -3.182 -1.483 0.037 C -2.041 -1.325 -0.656 C -1.301 -0.012 -0.793 H -0.960 0.015 1.918 H 1.260 -0.024 -1.748 H 1.151 0.038 3.199 H 3.375 -0.018 -0.471 H 3.331 0.016 2.011 H -1.500 -2.207 -0.989 H -3.719 -0.632 0.444 H -3.631 -2.460 0.173 H -2.815 -1.419 -2.523 H -1.079 0.177 -1.846 H -1.950 0.802 -0.454	ZPE(B3LYP/6-311G**) = 0.1588 E(CCSD(T)/6-311G**) = -348.5616 E(MP2/6-311G**) = -348.4298 E(MP2/G3large) = -348.6375 E(G3(MP2,CC) = -348.6104	1	1	574i, **43**, **72**, 111, 282, 318, 348, 374, 395, 415, 505, 560, 635, 637, 715, 760, 831, 854, 905, 917, 924, 940, 976, 1001, 1018, 1027, 1051, 1087, 1127, 1182, 1203, 1218, 1225, 1308, 1324, 1340, 1360, 1446, 1477, 1485, 1528, 1626, 1634, 1648, 3007, 3065, 3129, 3140, 3151, 3158, 3168, 3176, 3188, 3218	131.0 516.9 605.9

Species	XYZ Coordinates (Å)	Energies (Hartree)	σ_{ext}	n	ν_i (cm^{-1})	I (amu*Å^2)
TS i4-p10 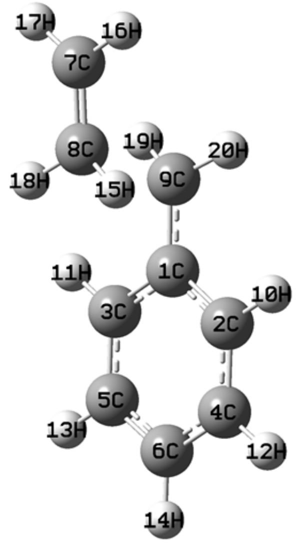	C -0.052 0.102 -0.022 C -0.039 0.065 1.390 C 1.191 0.043 -0.690 C 1.155 -0.015 2.094 C 2.382 -0.037 0.018 C 2.373 -0.067 1.414 C -3.062 -1.972 -1.783 C -1.885 -1.922 -1.082 C -1.293 0.145 -0.756 H -0.981 0.110 1.928 H 1.209 0.072 -1.775 H 1.139 -0.034 3.179 H 3.325 -0.073 -0.517 H 3.305 -0.128 1.966 H -1.886 -2.120 -0.016 H -4.022 -1.934 -1.280 H -3.077 -1.956 -2.867 H -0.950 -2.141 -1.585 H -1.257 0.438 -1.798 H -2.186 0.456 -0.228	ZPE(B3LYP/6-311G**) = 0.1634 E(CCSD(T)/6-311G**) = -348.5859 E(MP2/6-311G**) = -348.4104 E(MP2/G3large) = -348.6181 E(G3(MP2,CC) = -348.6302	1	1	542i, **51**, 78, 81, 238, 241, 347, 407, 417, 504, 549, 633, 702, 720, 768, 798, 814, 834, 845, 863, 911, 975, 994, 1006, 1007, 1015, 1017, 1044, 1117, 1179, 1195, 1237, 1246, 1277, 1332, 1355, 1464, 1480, 1486, 1515, 1555, 1599, 1622, 3123, 3133, 3136, 3154, 3156, 3169, 3175, 3189, 3198, 3223, 3227	132.1 601.0 656.2

Species	XYZ Coordinates (Å)	Energies (Hartree)	σ_{ext}	n	ν_i (cm^{-1})	I ($amu*Å^2$)
TS i5-i11 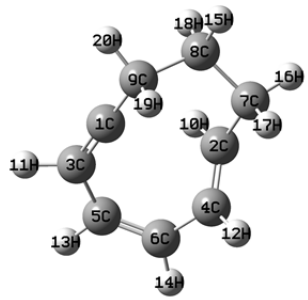	C 0.068 1.419 0.114 C 0.215 -1.215 -0.376 C -1.221 1.522 -0.115 C -0.838 -1.436 0.420 C -2.255 0.460 -0.224 C -2.136 -0.850 0.078 C 1.668 -1.265 -0.031 C 2.254 0.142 -0.302 C 1.491 1.297 0.405 H 0.002 -0.796 -1.359 H -1.660 2.529 -0.160 H -0.718 -1.921 1.389 H -3.248 0.837 -0.459 H -3.036 -1.459 0.126 H 3.302 0.181 0.010 H 2.213 -1.990 -0.648 H 1.812 -1.551 1.016 H 2.238 0.325 -1.382 H 1.595 1.171 1.492 H 2.021 2.233 0.167	ZPE(B3LYP/6-311G**) = 0.1654 E(CCSD(T)/6-311G**) = -348.5438 E(MP2/6-311G**) = -348.3696 E(MP2/G3large) = -348.5723 E(G3(MP2,CC) = -348.5812	1	1	149i, 158, 191, 195, 279, 301, 350, 382, 417, 512, 539, 686, 741, 766, 815, 833, 850, 870, 910, 948, 984, 993, 1014, 1022, 1069, 1111, 1164, 1199, 1230, 1256, 1300, 1315, 1328, 1345, 1362, 1369, 1423, 1450, 1485, 1491, 1617, 1695, 1768, 2940, 2966, 2998, 3010, 3028, 3052, 3070, 3105, 3119, 3121, 3146	189.5 335.4 489.7

Species	**XYZ Coordinates** (Å)	**Energies** (Hartree)	**σ_{ext}**	**n**	**ν_i** (cm^{-1})	**I** (amu*$Å^2$)
TS i5-p5 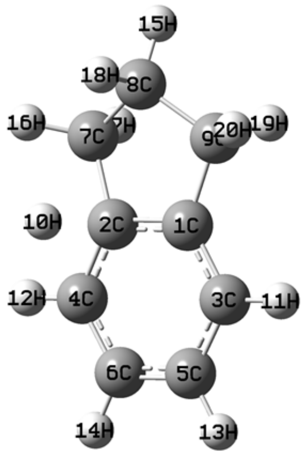	C -0.145 0.719 -0.013 C -0.148 -0.696 0.047 C 1.052 1.419 -0.001 C 1.071 -1.398 -0.040 C 2.258 0.712 0.014 C 2.264 -0.687 -0.024 C -1.555 -1.209 -0.214 C -2.439 0.001 0.162 C -1.559 1.246 -0.118 H -0.323 -0.824 1.869 H 1.058 2.504 -0.016 H 1.076 -2.482 -0.072 H 3.198 1.252 0.030 H 3.209 -1.218 -0.047 H -3.385 0.022 -0.382 H -1.804 -2.112 0.347 H -1.654 -1.446 -1.281 H -2.670 -0.046 1.230 H -1.737 1.633 -1.129 H -1.760 2.069 0.574	ZPE(B3LYP/6-311G**) = 0.1621 E(CCSD(T)/6-311G**) = -348.5912 E(MP2/6-311G**) = -348.4332 E(MP2/G3large) = -348.6379 E(G3(MP2,CC) = -348.6339	1	1	792i, 153, 188, 254, 358, 411, 457, 507, 528, 535, 603, 628, 712, 745, 766, 838, 861, 874, 905, 918, 947, 987, 1007, 1042, 1060, 1103, 1151, 1176, 1178, 1198, 1216, 1241, 1290, 1293, 1331, 1344, 1349, 1474, 1483, 1484, 1498, 1504, 1596, 1628, 3006, 3011, 3046, 3061, 3085, 3097, 3157, 3163, 3175, 3187	147.1 343.3 471.1

Species	**XYZ Coordinates** (Å)	**Energies** (Hartree)	**σ_{ext}**	**n**	**ν_i** (cm^{-1})	**I** (amu*$Å^2$)
TS i6-p2 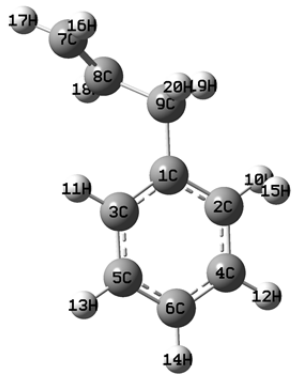	C -0.008 0.017 0.005 C 0.001 -0.006 1.418 C 1.214 0.026 -0.665 C 1.217 0.085 2.123 C 2.419 0.055 0.038 C 2.421 0.094 1.435 C -1.610 0.397 -3.208 C -1.385 0.828 -1.970 C -1.324 -0.049 -0.748 H -0.933 0.131 1.953 H 1.224 0.024 -1.749 H 1.204 0.125 3.206 H 3.357 0.063 -0.505 H 3.358 0.143 1.977 H -0.413 -1.833 1.674 H -1.763 -0.656 -3.425 H -1.656 1.081 -4.048 H -1.232 1.891 -1.796 H -2.130 0.235 -0.062 H -1.522 -1.090 -1.035	ZPE(B3LYP/6-311G**) = 0.1588 E(CCSD(T)/6-311G**) = -348.5595 E(MP2/6-311G**) = -348.3981 E(MP2/G3large) = -348.6055 E(G3(MP2,CC) = -348.6081	1	1	743i, **27**, **87**, 151, 260, 311, 321, 387, 396, 460, 515, 545, 632, 665, 733, 753, 830, 872, 913, 936, 945, 951, 987, 1007, 1018, 1029, 1050, 1088, 1122, 1181, 1196, 1209, 1231, 1310, 1325, 1336, 1360, 1450, 1469, 1479, 1522, 1604, 1624, 1703, 3011, 3046, 3123, 3135, 3155, 3162, 3170, 3180, 3190, 3209	124.2 527.3 623.3

Species	XYZ Coordinates (Å)	Energies (Hartree)	σ_{ext}	n	ν_i (cm^{-1})	I (amu*Å^2)
TS i7-p1 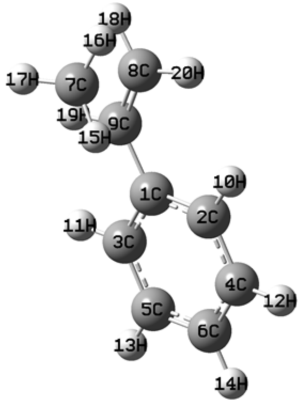	C 0.094 -0.421 -0.214 C 0.411 0.934 -0.432 C 1.125 -1.270 0.229 C 1.698 1.410 -0.220 C 2.414 -0.793 0.440 C 2.708 0.550 0.216 C -3.497 0.677 1.048 C -2.339 -0.319 -0.876 C -1.240 -0.974 -0.425 H -0.358 1.620 -0.767 H 0.903 -2.317 0.407 H 1.917 2.457 -0.394 H 3.189 -1.470 0.781 H 3.711 0.926 0.380 H -2.679 1.280 1.416 H -4.295 1.171 0.508 H -3.735 -0.230 1.586 H -3.251 -0.863 -1.081 H -1.352 -2.021 -0.150 H -2.285 0.685 -1.277	ZPE(B3LYP/6-311G**) = 0.1615 E(CCSD(T)/6-311G**) = -348.5826 E(MP2/6-311G**) = -348.4033 E(MP2/G3large) = -348.6115 E(G3(MP2,CC) = -348.6292	1	1	313i, **35**, 61, **85**, 164, 235, 286, 411, 415, 437, 458, 485, 562, 634, 685, 711, 731, 790, 799, 844, 898, 919, 973, 977, 998, 1012, 1043, 1057, 1111, 1181, 1200, 1227, 1304, 1333, 1356, 1412, 1418, 1443, 1481, 1524, 1587, 1617, 1639, 3094, 3135, 3153, 3157, 3163, 3173, 3182, 3190, 3236, 3257, 3266	151.4 567.2 637.2

Species	**XYZ Coordinates** (Å)	**Energies** (Hartree)	σ_{ext}	**n**	ν_i (cm^{-1})	**I** (amu*Å^2)
TS i7-p6 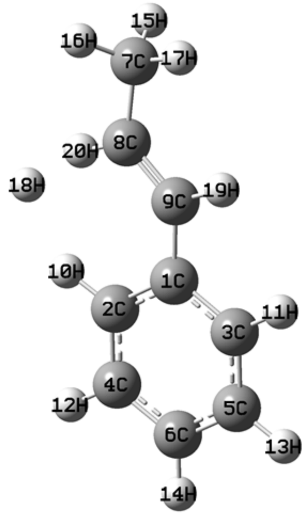	C -0.096 -0.219 0.010 C -0.610 1.089 -0.028 C -1.012 -1.283 0.034 C -1.980 1.316 -0.052 C -2.384 -1.056 0.009 C -2.876 0.246 -0.035 C 3.809 -0.061 -0.129 C 2.364 0.342 -0.086 C 1.340 -0.522 0.028 H 0.066 1.935 -0.031 H -0.636 -2.301 0.069 H -2.353 2.334 -0.079 H -3.070 -1.896 0.026 H -3.944 0.428 -0.052 H 4.235 0.137 -1.119 H 4.405 0.509 0.591 H 3.936 -1.124 0.088 H 2.283 1.049 2.108 H 1.581 -1.576 0.151 H 2.161 1.396 -0.257	ZPE(B3LYP/6-311G**) = 0.1581 E(CCSD(T)/6-311G**) = -348.5713 E(MP2/6-311G**) = -348.3987 E(MP2/G3large) = -348.6074 E(G3(MP2,CC) = -348.6219	1	1	239i, **37**, 109, 152, **168**, 238, 263, 295, 352, 413, 416, 508, 626, 635, 704, 754, 832, 838, 851, 926, 956, 976, 991, 1004, 1015, 1051, 1059, 1098, 1123, 1183, 1205, 1233, 1308, 1329, 1353, 1366, 1415, 1479, 1481, 1495, 1528, 1617, 1642, 1679, 3013, 3061, 3097, 3121, 3144, 3157, 3164, 3174, 3184, 3191	106.2 596.9 690.1

Species	XYZ Coordinates (Å)	Energies (Hartree)	σ_{ext}	n	ν_i (cm^{-1})	I ($amu*Å^2$)
TS i8-p7 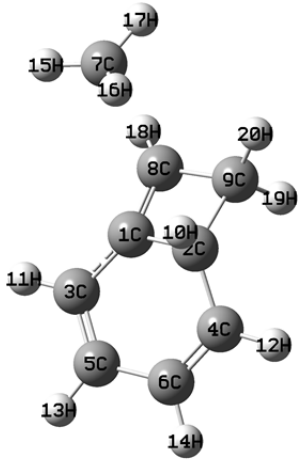	C -0.184 0.499 0.207 C 0.066 -0.871 -0.380 C 0.806 1.534 0.176 C 1.508 -1.264 -0.295 C 2.085 1.128 -0.049 C 2.432 -0.287 -0.193 C -3.251 0.605 -0.729 C -1.322 0.128 0.865 C -1.107 -1.356 0.566 H -0.266 -0.954 -1.428 H 0.572 2.566 0.416 H 1.806 -2.301 -0.413 H 2.894 1.850 -0.040 H 3.487 -0.540 -0.212 H -3.247 1.685 -0.679 H -2.818 0.130 -1.598 H -4.000 0.064 -0.165 H -1.955 0.632 1.583 H -0.731 -1.914 1.427 H -1.925 -1.917 0.104	ZPE(B3LYP/6-311G**) = 0.1606 E(CCSD(T)/6-311G**) = -348.5183 E(MP2/6-311G**) = -348.3432 E(MP2/G3large) = -348.5465 E(G3(MP2,CC) = -348.5609	1	1	302i, 73, **83**, 90, 202, 214, 360, 373, 399, 413, 511, 552, 600, 666, 698, 710, 773, 802, 818, 877, 935, 952, 958, 979, 990, 1004, 1082, 1111, 1146, 1156, 1196, 1209, 1219, 1288, 1331, 1385, 1408, 1411, 1428, 1479, 1520, 1570, 1651, 2938, 3032, 3085, 3097, 3143, 3157, 3165, 3181, 3199, 3264, 3269	163.1 421.6 517.8

Species	XYZ Coordinates (Å)	Energies (Hartree)	σ_{ext}	n	v_i (cm^{-1})	I (amu*$Å^2$)
TS i8-p8 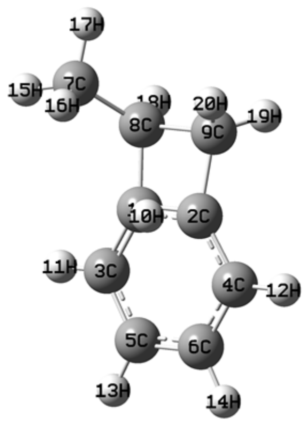 	C -0.209 -0.472 -0.182 C 0.124 0.876 0.053 C 0.739 -1.476 -0.193 C 1.463 1.288 0.129 C 2.069 -1.077 0.008 C 2.421 0.275 0.146 C -2.713 -0.683 0.522 C -1.675 -0.164 -0.471 C -1.276 1.364 -0.337 H -0.186 0.946 1.874 H 0.494 -2.518 -0.374 H 1.748 2.330 0.217 H 2.854 -1.826 0.021 H 3.469 0.534 0.253 H -2.795 -1.773 0.469 H -2.440 -0.414 1.546 H -3.700 -0.262 0.308 H -1.970 -0.428 -1.492 H -1.301 1.905 -1.287 H -1.830 1.931 0.413	ZPE(B3LYP/6-311G**) = 0.1600 E(CCSD(T)/6-311G**) = -348.5480 E(MP2/6-311G**) = -348.3893 E(MP2/G3large) = -348.5941 E(G3(MP2,CC) = -348.5928	1	1	767i, 115, 175, **228**, 277, 344, 388, 426, 461, 522, 542, 571, 644, 735, 749, 782, 787, 866, 882, 902, 946, 989, 1012, 1022, 1067, 1088, 1106, 1150, 1169, 1180, 1200, 1219, 1235, 1300, 1328, 1364, 1407, 1465, 1478, 1486, 1496, 1499, 1602, 1624, 3021, 3027, 3051, 3083, 3093, 3102, 3158, 3167, 3177, 3186	147.6 375.5 484.7

Species	**XYZ Coordinates** (Å)	**Energies** (Hartree)	**σ_{ext}**	**n**	***v_i*** (cm^{-1})	**I** ($amu*Å^2$)
TS i10-p4 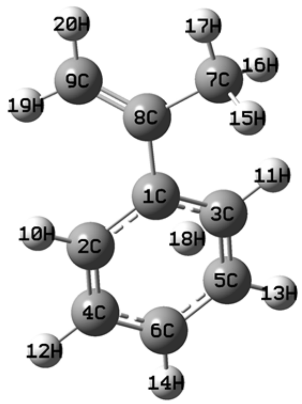	C 0.204 0.037 0.130 C -0.604 1.201 0.262 C -0.462 -1.175 -0.201 C -1.983 1.128 0.184 C -1.844 -1.235 -0.280 C -2.616 -0.091 -0.078 C 2.526 -1.065 0.304 C 1.690 0.143 -0.041 C 2.257 1.256 -0.518 H -0.126 2.146 0.490 H 0.119 -2.072 -0.371 H -2.575 2.025 0.328 H -2.326 -2.179 -0.511 H -3.697 -0.143 -0.136 H 2.302 -1.422 1.314 H 2.336 -1.896 -0.383 H 3.590 -0.829 0.245 H 0.353 -0.260 1.906 H 1.678 2.118 -0.823 H 3.332 1.325 -0.637	ZPE(B3LYP/6-311G**) = 0.1590 E(CCSD(T)/6-311G**) = -348.5618 E(MP2/6-311G**) = -348.3909 E(MP2/G3large) = -348.5992 E(G3(MP2,CC) = -348.6111	1	1	901i, **63**, 141, **181**, 226, 355, 378, 401, 444, 501, 525, 550, 579, 628, 689, 718, 741, 800, 841, 921, 928, 938, 980, 998, 1005, 1022, 1043, 1067, 1112, 1125, 1180, 1207, 1289, 1319, 1353, 1410, 1441, 1471, 1483, 1499, 1509, 1587, 1624, 1691, 3022, 3070, 3111, 3142, 3163, 3170, 3185, 3193, 3199, 3223	145.7 428.1 544.3

Species	XYZ Coordinates (Å)	Energies (Hartree)	σ_{ext}	n	v_i (cm^{-1})	I ($amu*Å^2$)
TS i12-i4 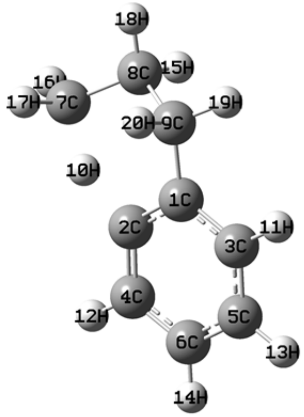	C 0.106 -0.126 -0.082 C 0.199 -0.496 1.252 C 1.274 0.334 -0.704 C 1.367 -0.429 1.989 C 2.469 0.417 0.011 C 2.522 0.040 1.353 C -2.269 -1.287 1.248 C -2.099 -1.369 -0.258 C -1.231 -0.211 -0.795 H -1.063 -0.991 1.620 H 1.249 0.628 -1.749 H 1.398 -0.733 3.030 H 3.365 0.774 -0.483 H 3.456 0.105 1.901 H -1.620 -2.319 -0.519 H -2.542 -2.217 1.746 H -2.874 -0.446 1.594 H -3.072 -1.357 -0.765 H -1.076 -0.323 -1.872 H -1.772 0.735 -0.658	ZPE(B3LYP/6-311G**) = 0.1627 E(CCSD(T)/6-311G**) = -348.5905 E(MP2/6-311G**) = -348.4241 E(MP2/G3large) = -348.6286 E(G3(MP2,CC) = -348.6323	1	1	1577i, 86, 164, 262, 296, 405, 416, 454, 483, 527, 592, 669, 719, 749, 778, 856, 867, 884, 903, 945, 989, 1015, 1030, 1049, 1080, 1110, 1137, 1177, 1208, 1231, 1244, 1280, 1310, 1323, 1359, 1367, 1455, 1464, 1466, 1486, 1492, 1559, 1597, 1634, 2998, 3005, 3046, 3062, 3065, 3141, 3146, 3154, 3166, 3181	141.9 426.1 549.7
H	H 0.000 0.000 0.000	ZPE(B3LYP/6-311G**) = 0.0000 E(CCSD(T)/6-311G**) = -0.4998 E(MP2/6-311G**) = -0.4998 E(MP2/G3large) = -0.4998 E(G3(MP2,CC) = -0.4998	-	1	-	-
methyl radical CH_3 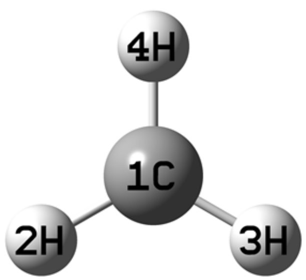	C 0.000 0.000 0.000 H -0.936 -0.540 0.000 H 0.936 -0.540 0.000 H 0.000 1.080 0.000	ZPE(B3LYP/6-311G**) = 0.0286 E(CCSD(T)/6-311G**) = -39.7321 E(MP2/6-311G**) = -39.7072 E(MP2/G3large) = -39.7305 E(G3(MP2,CC) = -39.7268	6	1	505, 1403, 1403, 3105, 3284, 3284	1.8 1.8 3.5

Species	XYZ Coordinates (Å)	Energies (Hartree)	σ_{ext}	n	v_i (cm^{-1})	I ($amu*Å^2$)
ethene C_2H_4 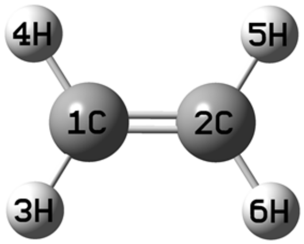 	C -0.012 0.000 -0.007 C -1.162 0.000 -0.671 H 0.021 0.000 1.077 H 0.944 0.000 -0.520 H -1.195 0.000 -1.755 H -2.117 0.000 -0.157	ZPE(B3LYP/6-311G**) = 0.0497 E(CCSD(T)/6-311G**) = -78.3837 E(MP2/6-311G**) = -78.3442 E(MP2/G3large) = -78.3918 E(G3(MP2,CC) = -78.3817	4	1	834, 973, 974, 1067, 1239, 1379, 1472, 1691, 3122, 3137, 3193, 3222	3.4 16.7 20.1
1-propenyl radical CH_3CHCH 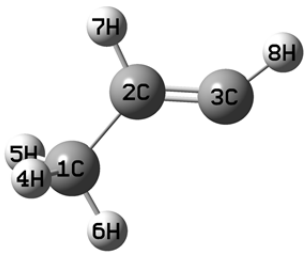 	C -0.973 -0.708 0.000 C 0.000 0.445 0.000 C 1.304 0.352 0.000 H -1.621 -0.664 0.881 H -1.621 -0.664 -0.881 H -0.451 -1.665 0.000 H -0.451 1.445 0.000 H 2.156 1.015 0.000	ZPE(B3LYP/6-311G**) = 0.0639 E(CCSD(T)/6-311G**) = -116.9174 E(MP2/6-311G**) = -116.8533 E(MP2/G3large) = -116.9210 E(G3(MP2,CC) = -116.9211	1	1	195, 409, 612, 790, 813, 931, 1062, 1106, 1271, 1404, 1485, 1485, 1684, 3006, 3021, 3069, 3115, 3239	8.7 53.1 58.8
2-propenyl radical CH_3CCH_2 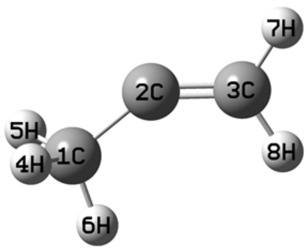 	C -1.183 -0.471 0.000 C 0.000 0.400 0.000 C 1.306 0.329 0.000 H -1.806 -0.295 0.882 H -1.806 -0.295 -0.882 H -0.891 -1.533 0.000 H 1.939 1.212 0.000 H 1.827 -0.635 0.000	ZPE(B3LYP/6-311G**) = 0.0636 E(CCSD(T)/6-311G**) = -116.9222 E(MP2/6-311G**) = -116.8588 E(MP2/G3large) = -116.9272 E(G3(MP2,CC) = -116.9270	1	1	183, 315, 478, 882, 897, 936, 1052, 1099, 1392, 1416, 1456, 1473, 1747, 2961, 3023, 3050, 3075, 3144	6.7 58.5 62.0

Species	XYZ Coordinates (Å)	Energies (Hartree)	σ_{ext}	n	ν_i (cm^{-1})	I (amu*$Å^2$)
allyl radical CH_2CHCH_2 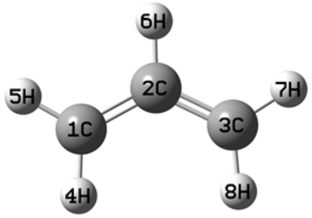	C 0.000 1.227 -0.196 C 0.000 0.000 0.442 C 0.000 -1.227 -0.196 H 0.000 1.296 -1.278 H 0.000 2.155 0.363 H 0.000 0.000 1.530 H 0.000 -2.155 0.363 H 0.000 -1.296 -1.278	ZPE(B3LYP/6-311G**) = 0.0643 E(CCSD(T)/6-311G**) = -116.9525 E(MP2/6-311G**) = -116.8892 E(MP2/G3large) = -116.9585 E(G3(MP2,CC) = -116.9575	2	1	429, 532, 553, 786, 811, 936, 1014, 1037, 1208, 1270, 1423, 1511, 1517, 3128, 3134, 3141, 3232, 3235	9.2 48.9 58.1
benzene C_6H_6 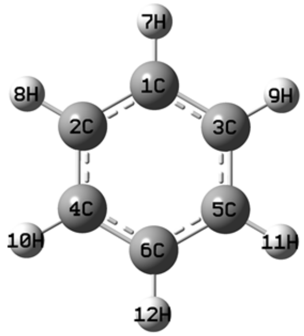	C 0.000 1.394 0.000 C 1.207 0.697 0.000 C -1.207 0.697 0.000 C 1.207 -0.697 0.000 C -1.207 -0.697 0.000 C 0.000 -1.394 0.000 H 0.000 2.479 0.000 H 2.147 1.239 0.000 H -2.147 1.239 0.000 H 2.147 -1.239 0.000 H -2.147 -1.239 0.000 H 0.000 -2.479 0.000	ZPE(B3LYP/6-311G**) = 0.0969 E(CCSD(T)/6-311G**) = -231.6539 E(MP2/6-311G**) = -231.5777 E(MP2/G3large) = -231.7160 E(G3(MP2,CC) = -231.6952	12	1	414, 414, 623, 623, 692, 724, 865, 865, 983, 983, 1012, 1018, 1023, 1060, 1060, 1174, 1197, 1197, 1333, 1381, 1512, 1512, 1636, 1636, 3155, 3164, 3164, 3180, 3180, 3191	88.6 88.6 177.1

Species	XYZ Coordinates (Å)	Energies (Hartree)	σ_{ext}	n	ν_i (cm^{-1})	I ($amu*Å^2$)
p1 (styrene) C_8H_8 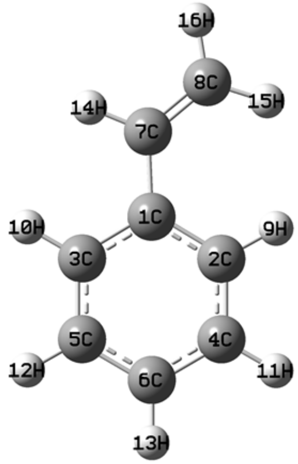	C 0.000 0.559 0.000 C -1.006 -0.422 0.000 C 1.336 0.130 0.000 C -0.685 -1.773 0.000 C 1.660 -1.224 0.000 C 0.650 -2.182 0.000 C -0.283 2.003 0.000 C -1.477 2.601 0.000 H -2.048 -0.126 0.000 H 2.128 0.872 0.000 H -1.477 -2.513 0.000 H 2.700 -1.529 0.000 H 0.897 -3.237 0.000 H 0.603 2.635 0.000 H -2.411 2.049 0.000 H -1.558 3.681 0.000	ZPE(B3LYP/6-311G**) = 0.1284 E(CCSD(T)/6-311G**) = -308.8574 E(MP2/6-311G**) = -308.7534 E(MP2/G3large) = -308.9384 E(G3(MP2,CC) = -308.9140	1	1	14, 204, 236, 412, 447, 449, 561, 635, 656, 711, 787, 799, 850, 927, 929, 977, 999, 1015, 1029, 1040, 1056, 1112, 1183, 1205, 1226, 1318, 1346, 1362, 1452, 1483, 1529, 1618, 1645, 1691, 3129, 3143, 3157, 3163, 3173, 3182, 3190, 3222	97.2 328.2 425.4
p2 (3-phenylpropene) C_9H_{10} 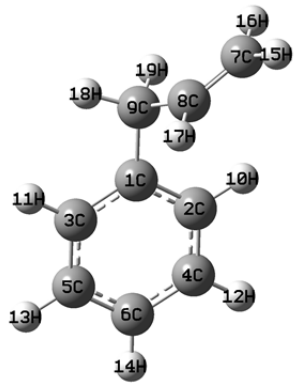	C -0.002 -0.322 0.277 C -0.367 1.030 0.286 C -0.988 -1.275 0.012 C -1.682 1.415 0.045 C -2.307 -0.893 -0.233 C -2.658 0.453 -0.216 C 3.459 0.544 -0.237 C 2.405 -0.226 -0.489 C 1.436 -0.733 0.548 H 0.389 1.783 0.480 H -0.723 -2.327 0.001 H -1.947 2.467 0.059 H -3.058 -1.649 -0.436 H -3.683 0.753 -0.405 H 4.123 0.876 -1.028 H 3.700 0.868 0.771 H 2.195 -0.526 -1.514 H 1.485 -1.828 0.582 H 1.745 -0.376 1.536	ZPE(B3LYP/6-311G**) = 0.1557 E(CCSD(T)/6-311G**) = -348.0682 E(MP2/6-311G**) = -347.9467 E(MP2/G3large) = -348.1536 E(G3(MP2,CC) = -348.1194	1	1	28, 86, 145, 284, 322, 398, 415, 501, 540, 636, 669, 716, 760, 834, 857, 913, 927, 942, 949, 978, 1001, 1018, 1034, 1051, 1097, 1125, 1181, 1203, 1214, 1232, 1310, 1326, 1342, 1362, 1451, 1478, 1487, 1527, 1626, 1646, 1704, 3015, 3051, 3122, 3131, 3153, 3158, 3168, 3176, 3188, 3208	121.1 519.8 605.8

Species	XYZ Coordinates (Å)	Energies (Hartree)	σ_{ext}	n	ν_i (cm^{-1})	I ($amu*Å^2$)
p3 (cis-1-phenylpropene) C_9H_{10} 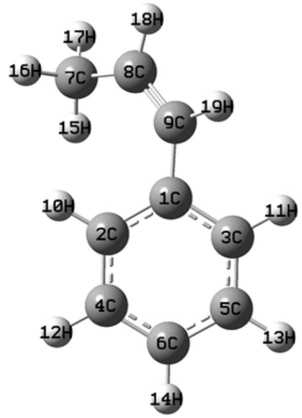 	C -0.041 -0.437 -0.206 C 0.262 0.919 -0.405 C 1.012 -1.299 0.147 C 1.557 1.398 -0.225 C 2.304 -0.821 0.332 C 2.582 0.533 0.151 C -2.870 0.876 0.530 C -2.580 -0.453 -0.106 C -1.391 -1.001 -0.392 H -0.515 1.598 -0.734 H 0.804 -2.355 0.286 H 1.767 2.449 -0.390 H 3.096 -1.506 0.613 H 3.590 0.908 0.289 H -1.993 1.307 1.016 H -3.238 1.601 -0.206 H -3.659 0.768 1.281 H -3.458 -1.054 -0.333 H -1.402 -2.015 -0.786	ZPE(B3LYP/6-311G**) = 0.1558 E(CCSD(T)/6-311G**) = -348.0718 E(MP2/6-311G**) = -347.9512 E(MP2/G3large) = -348.1585 E(G3(MP2,CC) = -348.1233	1	1	52, 125, 159, 219, 291, 415, 418, 470, 526, 634, 670, 713, 717, 785, 822, 856, 933, 936, 980, 998, 1004, 1016, 1050, 1061, 1090, 1109, 1182, 1204, 1212, 1276, 1337, 1355, 1405, 1440, 1476, 1489, 1494, 1527, 1615, 1644, 1703, 3010, 3056, 3106, 3120, 3141, 3157, 3164, 3174, 3186, 3196	133.7 471.5 575.2
p4 (2-phenylpropene) C_9H_{10} 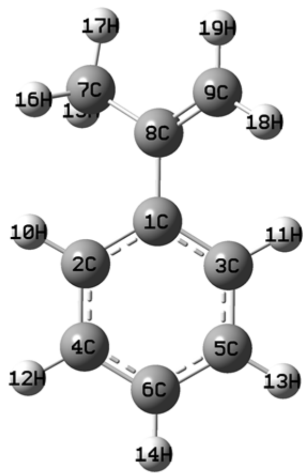 	C 0.206 0.052 -0.014 C -0.470 -1.158 -0.236 C -0.568 1.196 0.238 C -1.861 -1.216 -0.236 C -1.958 1.139 0.241 C -2.612 -0.068 0.000 C 2.458 -1.099 0.426 C 1.693 0.120 -0.035 C 2.339 1.214 -0.454 H 0.093 -2.063 -0.427 H -0.072 2.134 0.458 H -2.358 -2.162 -0.421 H -2.531 2.037 0.444 H -3.695 -0.114 0.006 H 2.123 -1.427 1.415 H 2.315 -1.945 -0.256 H 3.528 -0.891 0.472 H 1.815 2.083 -0.833 H 3.422 1.263 -0.448	ZPE(B3LYP/6-311G**) = 0.1556 E(CCSD(T)/6-311G**) = -348.0742 E(MP2/6-311G**) = -347.9537 E(MP2/G3large) = -348.1613 E(G3(MP2,CC) = -348.1262	1	1	47, 144, 194, 230, 352, 385, 416, 498, 536, 563, 636, 703, 720, 747, 798, 854, 923, 932, 939, 980, 1002, 1016, 1023, 1051, 1068, 1110, 1137, 1183, 1208, 1304, 1330, 1356, 1412, 1441, 1476, 1485, 1499, 1528, 1615, 1644, 1688, 3023, 3070, 3109, 3140, 3160, 3168, 3180, 3187, 3192, 322	140.8 423.7 541.7

Species	**XYZ Coordinates** (Å)	**Energies** (Hartree)	**σ_{ext}**	**n**	***v_i*** (cm^{-1})	**I** (amu*Å^2)
p5 (indane) C_9H_{10} 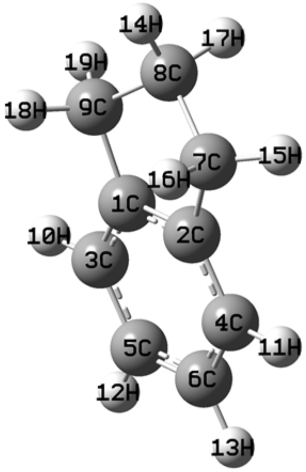 	C 0.051 0.149 0.700 C 0.051 0.149 -0.700 C 0.004 -1.050 1.404 C 0.004 -1.050 -1.404 C -0.047 -2.253 0.698 C -0.047 -2.253 -0.698 C 0.129 1.565 -1.229 C -0.264 2.422 0.000 C 0.129 1.565 1.229 H 0.001 -1.055 2.489 H 0.001 -1.055 -2.489 H -0.092 -3.194 1.236 H -0.092 -3.194 -1.236 H 0.207 3.407 0.000 H -0.521 1.739 -2.091 H 1.154 1.791 -1.551 H -1.348 2.575 0.000 H 1.154 1.791 1.551 H -0.521 1.739 2.091	ZPE(B3LYP/6-311G**) = 0.1585 E(CCSD(T)/6-311G**) = -348.1008 E(MP2/6-311G**) = -347.9835 E(MP2/G3large) = -348.1880 E(G3(MP2,CC) = -348.1468	1	1	145, 183, 256, 379, 428, 511, 523, 594, 626, 721, 750, 765, 842, 865, 874, 907, 915, 945, 989, 1006, 1046, 1060, 1105, 1152, 1178, 1180, 1199, 1223, 1244, 1293, 1300, 1331, 1343, 1357, 1483, 1484, 1492, 1506, 1511, 1626, 1648, 3004, 3005, 3038, 3065, 3068, 3091, 3153, 3159, 3170, 3184,	142.7 338.1 467.9

Species	XYZ Coordinates (Å)	Energies (Hartree)	σ_{ext}	n	ν_i (cm^{-1})	I (amu*Å^2)
p6 (trans-1-phenylpropene) C_9H_{10} 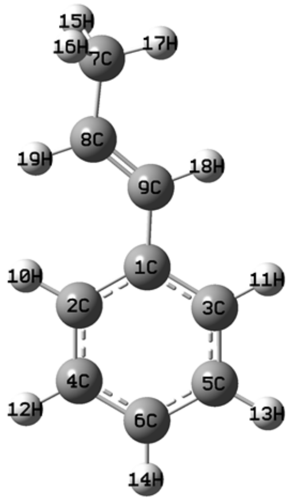	C -0.058 -0.205 0.000 C -0.584 1.098 0.000 C -0.967 -1.275 0.000 C -1.956 1.316 0.000 C -2.342 -1.058 0.000 C -2.844 0.240 0.000 C 3.846 -0.006 0.000 C 2.397 0.374 0.000 C 1.383 -0.499 0.000 H 0.085 1.951 0.000 H -0.584 -2.291 0.000 H -2.336 2.332 0.000 H -3.020 -1.904 0.000 H -3.914 0.414 0.000 H 4.362 0.400 -0.878 H 4.362 0.400 0.878 H 3.979 -1.090 0.000 H 1.628 -1.560 0.000 H 2.189 1.441 0.000	ZPE(B3LYP/6-311G**) = 0.1554 E(CCSD(T)/6-311G**) = -348.0742 E(MP2/6-311G**) = -347.9532 E(MP2/G3large) = -348.1609 E(G3(MP2,CC) = -348.1265	1	1	20, 124, 153, 195, 288, 351, 412, 413, 509, 627, 635, 704, 752, 833, 834, 850, 924, 958, 974, 992, 1006, 1015, 1052, 1064, 1098, 1123, 1182, 1205, 1233, 1307, 1334, 1353, 1367, 1415, 1479, 1479, 1495, 1529, 1618, 1644, 1715, 3008, 3048, 3092, 3116, 3135, 3156, 3162, 3172, 3181, 3190	100.1 587.0 684.0
p7 C_8H_8 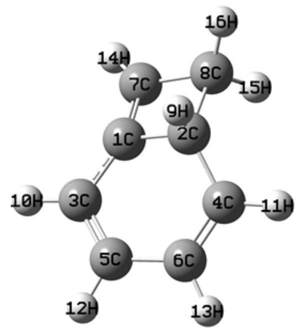	C 0.460 0.793 0.170 C 0.599 -0.678 0.495 C -0.831 1.442 0.142 C -0.556 -1.469 -0.035 C -1.889 0.617 -0.042 C -1.726 -0.830 -0.230 C 1.722 0.925 -0.285 C 2.038 -0.560 -0.155 H 0.703 -0.875 1.573 H -0.943 2.520 0.170 H -0.482 -2.546 -0.163 H -2.890 1.026 -0.128 H -2.603 -1.391 -0.537 H 2.307 1.762 -0.649 H 2.116 -1.084 -1.111 H 2.885 -0.850 0.478	ZPE(B3LYP/6-311G**) = 0.1282 E(CCSD(T)/6-311G**) = -308.7907 E(MP2/6-311G**) = -308.6819 E(MP2/G3large) = -308.8622 E(G3(MP2,CC) = -308.8430	1	1	190, 198, 368, 406, 507, 550, 601, 682, 709, 771, 815, 824, 875, 938, 950, 968, 984, 994, 1018, 1082, 1111, 1144, 1159, 1197, 1208, 1224, 1289, 1333, 1388, 1431, 1479, 1571, 1643, 1685, 2961, 3019, 3078, 3142, 3157, 3167, 3179, 3181	122.7 228.3 330.5

Species	XYZ Coordinates (Å)	Energies (Hartree)	σ_{ext}	n	v_i (cm^{-1})	I (amu*Å^2)
p8 C_9H_{10} 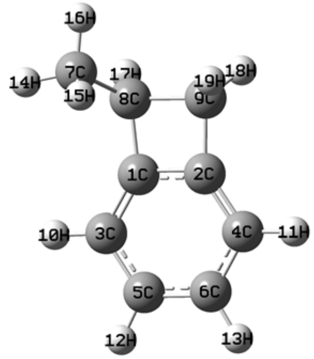	C -0.208 -0.429 -0.246 C 0.145 0.902 -0.044 C 0.725 -1.454 -0.222 C 1.454 1.294 0.187 C 2.053 -1.072 0.016 C 2.408 0.267 0.214 C -2.679 -0.721 0.552 C -1.690 -0.110 -0.436 C -1.283 1.404 -0.193 H 0.466 -2.495 -0.378 H 1.744 2.327 0.343 H 2.828 -1.830 0.046 H 3.449 0.512 0.393 H -2.764 -1.802 0.406 H -2.359 -0.548 1.584 H -3.676 -0.288 0.427 H -2.033 -0.280 -1.462 H -1.470 2.074 -1.037 H -1.723 1.843 0.707	ZPE(B3LYP/6-311G**) = 0.1565 E(CCSD(T)/6-311G**) = -348.0578 E(MP2/6-311G**) = -347.9402 E(MP2/G3large) = -348.1450 E(G3(MP2,CC) = -348.1061	1	1	107, 170, 233, 285, 369, 410, 455, 518, 568, 634, 727, 754, 776, 789, 875, 880, 905, 946, 991, 1015, 1025, 1067, 1093, 1109, 1150, 1172, 1178, 1209, 1220, 1237, 1303, 1334, 1375, 1409, 1472, 1488, 1493, 1497, 1499, 1635, 1644, 3018, 3028, 3036, 3079, 3082, 3087, 3154, 3163, 3173, 3182	144.7 367.9 481.1
p9 (indane) C_9H_{10} 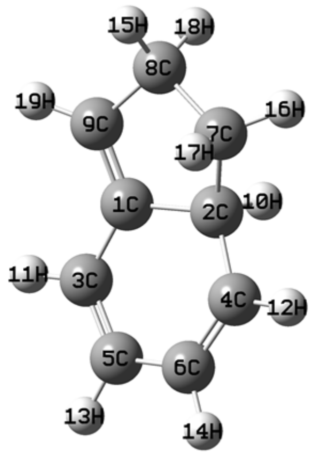	C -0.193 0.779 0.130 C -0.239 -0.713 0.441 C 1.093 1.443 0.082 C 1.006 -1.435 0.007 C 2.212 0.698 -0.058 C 2.150 -0.757 -0.185 C -1.594 -1.138 -0.173 C -2.456 0.147 -0.078 C -1.425 1.250 -0.122 H -0.310 -0.826 1.539 H 1.139 2.527 0.081 H 0.978 -2.517 -0.083 H 3.181 1.179 -0.141 H 3.061 -1.285 -0.446 H -3.205 0.222 -0.873 H -2.044 -1.997 0.331 H -1.444 -1.400 -1.225 H -3.008 0.169 0.874 H -1.669 2.288 -0.317	ZPE(B3LYP/6-311G**) = 0.1571 E(CCSD(T)/6-311G**) = -348.0524 E(MP2/6-311G**) = -347.9264 E(MP2/G3large) = -348.1298 E(G3(MP2,CC) = -348.0988	1	1	137, 171, 286, 350, 428, 494, 532, 538, 651, 668, 706, 786, 817, 834, 877, 881, 924, 967, 978, 993, 998, 1013, 1060, 1081, 1155, 1170, 1191, 1195, 1240, 1270, 1291, 1315, 1326, 1364, 1399, 1445, 1483, 1498, 1593, 1651, 1694, 2898, 2972, 3033, 3051, 3085, 3145, 3155, 3167, 3179, 3180	147.8 329.1 457.8

Species	XYZ Coordinates (Å)	Energies (Hartree)	σ_{ext}	n	v_i (cm^{-1})	I ($amu*Å^2$)
p10 (benzyl radical) C_7H_7 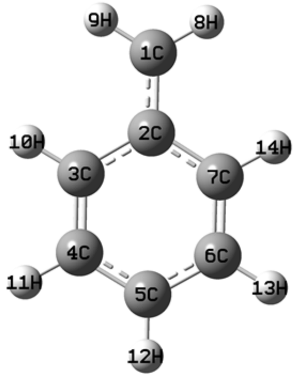	C 1.209 0.073 -2.155 C 1.210 0.047 -0.752 C 2.427 0.041 -0.010 C 2.421 0.015 1.373 C 1.212 -0.006 2.078 C 0.002 -0.001 1.374 C -0.006 0.025 -0.008 H 0.282 0.078 -2.714 H 2.136 0.090 -2.715 H 3.368 0.057 -0.550 H 3.361 0.011 1.915 H 1.213 -0.026 3.162 H -0.937 -0.017 1.917 H -0.947 0.029 -0.547	ZPE(B3LYP/6-311G**) = 0.1115 E(CCSD(T)/6-311G**) = -270.2173 E(MP2/6-311G**) = -270.0901 E(MP2/G3large) = -270.2504 E(G3(MP2,CC) = -270.2661	2	1	199, 359, 390, 479, 502, 534, 628, 685, 707, 774, 829, 831, 898, 970, 972, 990, 995, 1036, 1116, 1175, 1184, 1288, 1327, 1352, 1474, 1490, 1502, 1577, 1598, 3145, 3158, 3160, 3173, 3177, 3191, 3241	91.1 186.7 277.8

Table S 7: Calculated hindered rotor parameters: reduced moments of inertia around the rotational axes (**I_{red}**); vibrational frequencies corresponding to internal rotations (**υ_{int}**, also see Table S 6); and either cosine or Fourier fit parameters to dihedral angle energy scans, *V(φ)*, at B3LYP/6-311G** level of theory.

				Cosine Fit Parameters[b]		Fourier Fit Parameters[c] (kJ/mol)									
Species	**Rotor**[a]	**I_{red}** (amu*Å^2)	**υ_{int}** (cm^{-1})	**σ_{rot}**	**Vo** (kJ/mol)	**A_1**	**A_2**	**A_3**	**A_4**	**A_5**	**B_1**	**B_2**	**B_3**	**B_4**	**B_5**
i1	8C-9C	5.6595	66	1	-	-2.3151	-1.0302	-1.0632	0.0819	-0.0471	2.0028	-1.5769	0.0081	0.2315	0.1766
	1C-9C	17.2971	37	2	-	-0.0261	-3.8250	-0.0232	0.8189	0.0563	0.0560	-0.3695	-0.0123	0.3059	-0.0394
	7C-8C	3.0012	93	3	-	-0.0075	-0.0145	-0.8062	-0.0122	0.0113	-0.0041	-0.0166	-0.3901	0.0038	0.0065
i2	8C-9C	1.4944	144	2	-	-0.1084	-1.8069	0.0329	-0.0165	-0.0731	-0.1724	-0.9570	0.1412	0.2635	0.1190
	1C-8C	35.3806	47	2	-	0.0515	-6.4005	0.0518	0.1550	-0.0857	-0.0391	-1.8292	0.0767	1.7917	-0.1500
	7C-8C	2.6697	257	3	14.3816	-	-	-	-	-	-	-	-	-	-
i3	7C-8C	2.7100	153	3	7.5899	-	-	-	-	-	-	-	-	-	-
i4	8C-9C	6.3022	90	1	-	-2.8712	1.3302	-7.3621	0.2458	-0.2367	-0.0958	-0.2113	0.0382	0.0133	-0.0177
	7C-8C	1.6410	114	2	-	-0.0461	-0.0682	-0.0122	-0.0428	-0.0178	-0.0259	-0.1458	0.0282	0.0353	-0.0005
	1C-9C	17.1400	51	2	-	0.0152	-3.2541	0.0208	-0.5305	0.0105	0.0317	0.0531	0.0288	0.0272	-0.0274
i6	8C-9C	8.5778	80	1	-	-0.6041	-3.1411	-4.5591	0.4441	0.4096	-1.8555	-1.0748	1.2905	0.4867	-0.1005
	1C-9C	24.8240	46	1	-	0.2149	-3.3679	-3.6519	0.1572	0.1269	1.4573	-0.0082	-0.5358	0.1215	-0.2529
i7	8C-9C	15.9823	28	1	-	-1.6861	-4.1236	0.9888	-0.2768	0.4086	8.2137	-1.8439	-1.2816	-0.1710	-0.2897
	1C-9C	25.0086	81	2	-	0.4027	-24.9410	-0.3406	2.2689	0.0449	0.3066	2.0913	0.1184	-0.4278	-0.0951
	7C-8C	2.5236	267	3	-	0.2029	0.1525	-6.1333	-0.0144	-0.0362	0.0309	0.1183	0.3813	0.1319	0.0565
i8	7C-8C	2.8272	235	1	13.9826	-	-	-	-	-	-	-	-	-	-
i9	1C-7C	35.9427	115	2	-	-0.1756	-19.9706	0.0894	3.5782	0.0624	0.0040	-0.1911	-0.0049	0.3789	-0.0007
	7C-8C	2.8066	45/69	3	0.6342	-	-	-	-	-	-	-	-	-	-
	7C-9C	2.8066	45/69	3	0.6342	-	-	-	-	-	-	-	-	-	-
i10	1C-8C	34.8080	61	2	-	0.2922	-7.0125	-4.5044	1.0742	-0.0190	-0.1125	0.0868	0.0872	-0.1074	-0.0280
	7C-8C	2.4752	185	3	7.1525										
i12	8C-9C	7.7439	83	1	-	-3.0269	1.6698	-7.6091	0.0331	-0.1003	0.0517	-0.1227	-0.0399	0.1337	-0.0832
	1C-9C	17.7124	34	1	-	-0.1902	-2.0477	-0.0878	-0.2296	0.1183	1.6847	-0.4806	0.2253	-0.1171	-0.1876
	7C-8C	2.9723	238	3	12.0219	-	-	-	-	-	-	-	-	-	-

				Cosine Fit Parameters[b]		Fourier Fit Parameters[c] (kJ/mol)									
Species	**Rotor[a]**	I_{red} (amu*Å^2)	υ_{int} (cm^{-1})	σ_{rot}	**Vo** (kJ/mol)	A_1	A_2	A_3	A_4	A_5	B_1	B_2	B_3	B_4	B_5
TS 1-propenyl	3C-4C	32.8572	23	2	-	-0.0076	-2.2808	-0.0248	0.3671	0.0052	-0.0515	0.0661	-0.0161	-0.0302	0.0179
	1C-2C	2.0295	174	3	-	-0.0331	0.0252	-3.8321	-0.0174	0.0331	-0.0853	-0.0427	0.1746	-0.0390	-0.0727
TS 2-propenyl	1C-8C	34.2961	20	2	-	-0.0009	-1.4485	-0.0070	0.2124	0.0013	0.0123	-0.1750	-0.0095	0.0556	0.0018
	7C-8C	2.6012	158	3	6.2469	-	-	-	-	-	-	-	-	-	-
TS allyl	1C-2C	11.4081	117	1		-0.2226	-9.7899	-2.2467	0.7307	0.0832	-0.8241	3.8520	-1.8023	-0.4292	-0.1245
	1C-4C	28.9826	26	2		0.0220	-1.0069	-0.0201	-0.1056	-0.0036	-0.0216	0.0990	0.0007	-0.0432	0.0017
TS i1	1C-9C	31.6816	16	2	-	0.0122	-0.6067	-0.0083	-0.0832	-0.0070	-0.0082	-0.1808	-0.0007	0.0860	0.0084
	7C-8C	2.4229	149	3	-	-0.0513	0.0066	-3.1492	0.0029	0.0225	-0.0259	-0.0108	0.1555	-0.0134	-0.0463
TS i2	1C-8C	36.3981	27	2	-	-0.0288	-0.6448	-0.0089	-0.4506	0.0408	0.0085	-0.6538	0.0303	0.1184	0.0048
	7C-8C	2.4088	160	3	7.0663	-	-	-	-	-	-	-	-	-	-
TS i1-i3	7C-8C	2.6366	100	3	3.9552	-	-	-	-	-	-	-	-	-	-
TS i1-i4	8C-9C	5.6836	78	1	-	-2.4653	-1.0659	-3.9556	0.0398	-0.0617	-1.8198	1.3519	0.2856	-0.4167	-0.0130
	1C-9C	17.6891	42	2	-	-0.0212	-3.0023	-0.0403	0.3030	0.0267	-0.0182	-0.7443	-0.0091	0.5185	0.0400
TS i1-i7	1C-9C	30.1520	34	2	-	0.1717	-9.0722	-0.1823	1.6436	-0.0374	0.0133	2.5321	0.0665	-1.0373	0.0002
	7C-8C	2.2938	239	3	-	0.0657	-0.0972	-5.4144	0.1210	0.0670	-0.0182	-0.1021	-0.5071	-0.0256	0.0519
TS i1-i12	7C-8C	2.7244	207	3	10.6975	-	-	-	-	-	-	-	-	-	-
TS i1-p2	1C-9C	23.4631	28	2	-	-0.0261	-3.8250	-0.0232	0.8189	0.0563	0.0560	-0.3695	-0.0123	0.3059	-0.0394
TS i1-p3	1C-9C	32.8429	54	2	-	-0.0315	-1.9055	0.0495	-1.9752	-0.0525	-0.0039	-0.6371	-0.0801	0.8904	0.0338
	7C-8C	2.2503	162	3	-	-0.0039	-0.6371	-0.0801	0.8904	0.0338	-0.0041	-0.0166	-0.3901	0.0038	0.0065
TS i2-i3	7C-8C	2.7468	219	3	10.3458	-	-	-	-	-	-	-	-	-	-
TS i2-i8	7C-8C	2.8139	231	3	13.0296	-	-	-	-	-	-	-	-	-	-
TS i2-i9	1C-8C	34.6201	43	2	-	0.0199	-9.9123	0.0291	1.2500	-0.0691	-0.1007	-3.6360	0.0183	1.0125	0.0287
	7C-8C	2.7968	190	3	-	-0.1632	0.0921	-3.4035	-0.1168	0.0899	0.0525	-0.1343	-0.0360	-0.1530	0.0415
TS i2-i10	7C-8C	2.7622	254	3	-	0.0367	-0.1031	-5.7767	0.1195	0.0316	0.0160	0.0448	-0.0025	0.0198	-0.0164
TS i2-p1	1C-8C	42.3694	54	2	-	0.0028	-9.3864	-0.0876	0.2095	0.0823	-0.3020	2.4722	-0.1202	-1.0984	0.0718
	7C-8C	2.7767	113	3	-	0.0065	0.0068	-1.6404	-0.0076	-0.0021	-0.0114	-0.0095	0.0710	-0.0040	-0.0035
TS i2-p4	1C-8C	34.7358	60	2	-	-0.0641	-1.1635	0.0403	-2.0838	-0.0263	0.1113	-1.9256	-0.0177	1.3541	0.0762

				Cosine Fit Parameters[b]		Fourier Fit Parameters[c] (kJ/mol)									
Species	**Rotor[a]**	I_{red} (amu*Å^2)	υ_{int} (cm^{-1})	σ_{rot}	**Vo** (kJ/mol)	A_1	A_2	A_3	A_4	A_5	B_1	B_2	B_3	B_4	B_5
	7C-8C	2.7657	236	3	-	-0.0154	-0.0012	-5.8644	-0.0127	-0.0019	0.0385	-0.3837	0.0302	0.0857	0.0762
TS i4-p2	8C-9C	13.5706	72	1	-	-2.6712	-0.1320	-5.1592	-0.0185	-0.0031	-1.0875	-3.2612	1.6603	0.3576	0.0560
	1C-9C	27.4981	43	2	-	0.1127	-3.8903	-0.0672	0.0724	-0.0499	0.0792	2.6517	-0.0069	-1.0748	0.0606
TS i4-p10	8C-9C	6.9387	51	1	-	-2.8706	1.0742	-2.4460	0.0270	-0.0022	0.0334	-0.0206	0.0229	0.0117	0.0013
TS i6-p2	8C-9C	8.0231	87	1	-	-2.0225	-4.9825	-4.2958	0.9820	0.3527	-4.4316	-0.6771	2.3494	0.2216	-0.2907
	1C-9C	22.7862	27	1	-	-1.2233	-1.8565	-0.1134	0.0809	-0.0201	0.7565	1.5767	-0.5789	-0.5768	-0.0858
TS i7-p1	7C-8C	36.7625	35	2	-	-0.4124	-13.1448	-0.0166	1.7877	-0.0367	-0.2166	1.9939	0.0778	-1.1914	-0.0091
	1C-9C	2.6655	85	3	1.6317	-	-	-	-	-	-	-	-	-	-
TS i7-p6	1C-9C	15.2333	37	2	-	0.0324	-9.3613	-0.0501	1.6539	0.0293	-0.0022	-1.9110	0.0043	1.0156	0.0324
	7C-8C	2.9817	168	3	19.1809	-	-	-	-	-	-	-	-	-	-
TS i8-p7	7C-8C	3.1007	83	3	1.7609	-	-	-	-	-	-	-	-	-	-
TS i8-p8	7C-8C	2.7876	228	3	13.9821	-	-	-	-	-	-	-	-	-	-
TS i10-p4	1C-8C	33.6718	63	1	-	-0.5707	-1.5010	-2.6021	-0.6691	-0.0093	0.9409	-2.2977	0.1115	1.4939	-0.0837
	7C-8C	2.7806	181	3	-	0.0225	0.0289	-3.3993	-0.0071	-0.0492	-0.0159	0.0145	0.5976	0.0311	-0.0398

[a]Defines the bond around with the dihedral angle scan was performed. Atom labels are defined in Table S 6.
[b]$V(\phi) = \sum_{k=1}^{5}[A_k(\cos k\phi - 1) + B_k \sin k\phi]$
[c]$V(\phi) = 0.5 \times V_0(1 - \cos \sigma_{rot}\phi)$

S8. RRKM Calculations

Table S 8: RRKM calculated microcanonical rate constants for individual reaction steps of the phenyl radical + propene reaction on the C_9H_{11} potential energy surface at collision energies of 0-200 kJ/mol.

			Collision Energies (kJ/mol)															
Channel	TS	σ	0	6	20	40	45	60	80	84	100	108	120	130	140	160	180	200
1 → 3	TS 4	1	1.82E+07	2.45E+07	4.42E+07	9.08E+07	1.05E+08	1.64E+08	2.73E+08	3.01E+08	4.26E+08	5.00E+08	6.29E+08	7.51E+08	8.88E+08	1.20E+09	1.59E+09	2.04E+09
3 → 1	TS 4	1	1.48E+12	1.61E+12	1.89E+12	2.29E+12	2.38E+12	2.67E+12	3.04E+12	3.12E+12	3.40E+12	3.53E+12	3.73E+12	3.90E+12	4.06E+12	4.36E+12	4.65E+12	4.94E+12
1 → 4	TS 1	3	0.00E+00	0.00E+00	1.75E-04	8.04E-01	2.12E+00	2.73E+01	3.40E+02	5.30E+02	2.37E+03	4.59E+03	1.15E+04	2.28E+04	4.28E+04	1.29E+05	3.45E+05	8.19E+05
4 → 1	TS 1	2	0.00E+00	0.00E+00	5.20E-04	2.21E+00	5.76E+00	7.05E+01	8.30E+02	1.28E+03	5.51E+03	1.05E+04	2.54E+04	4.94E+04	9.11E+04	2.65E+05	6.84E+05	1.58E+06
1 → 6	TS 3	3	0.00E+00	0.00E+00	0.00E+00	9.68E-03	2.77E-02	4.11E-01	5.65E+00	8.94E+00	4.19E+01	8.26E+01	2.11E+02	4.27E+02	8.16E+02	2.53E+03	6.92E+03	1.68E+04
6 → 1	TS 3	2	0.00E+00	0.00E+00	0.00E+00	1.32E+01	3.41E+01	3.76E+02	3.65E+03	5.40E+03	2.00E+04	3.53E+04	7.71E+04	1.38E+05	2.34E+05	5.89E+05	1.33E+06	2.70E+06
1 → 7	TS 2	2	0.00E+00	0.00E+00	2.35E-01	1.75E+01	3.61E+01	2.64E+02	2.09E+03	3.02E+03	1.07E+04	1.89E+04	4.15E+04	7.51E+04	1.30E+05	3.42E+05	8.11E+05	1.74E+06
7 → 1	TS 2	2	0.00E+00	0.00E+00	1.15E-02	1.09E+00	2.37E+00	2.03E+01	1.94E+02	2.91E+02	1.18E+03	2.21E+03	5.31E+03	1.03E+04	1.91E+04	5.69E+04	1.52E+05	3.63E+05
1 → 12	TS 7	1	1.33E+02	3.49E+02	1.99E+03	1.37E+04	1.99E+04	5.95E+04	2.01E+05	2.52E+05	5.55E+05	7.94E+05	1.32E+06	1.95E+06	2.80E+06	5.36E+06	9.67E+06	1.64E+07
12 → 1	TS 7	2	1.11E+07	2.26E+07	7.85E+07	2.94E+08	3.78E+08	7.75E+08	1.69E+09	1.95E+09	3.21E+09	4.01E+09	5.49E+09	6.97E+09	8.70E+09	1.29E+10	1.83E+10	2.51E+10
1 → 15	TS 5	3	2.91E+00	2.65E+01	6.66E+02	1.49E+04	2.64E+04	1.34E+05	7.74E+05	1.07E+06	3.22E+06	5.30E+06	1.07E+07	1.81E+07	2.97E+07	7.11E+07	1.56E+08	3.16E+08
1 → 20	TS 6	2	2.56E-01	2.19E+00	5.21E+01	1.13E+03	1.98E+03	9.89E+03	5.60E+04	7.69E+04	2.30E+05	3.77E+05	7.53E+05	1.27E+06	2.08E+06	4.94E+06	1.08E+07	2.16E+07
1 → 23	TS 24	1	0.00E+00	9.43E-04	5.89E+00	4.79E+02	9.98E+02	7.53E+03	6.12E+04	8.90E+04	3.21E+05	5.67E+05	1.26E+06	2.28E+06	3.97E+06	1.05E+07	2.51E+07	5.41E+07
2 → 3	TS 9	1	4.30E+07	5.77E+07	1.03E+08	2.08E+08	2.40E+08	3.70E+08	6.09E+08	6.69E+08	9.36E+08	1.09E+09	1.36E+09	1.62E+09	1.90E+09	2.54E+09	3.32E+09	4.23E+09
3 → 2	TS 9	1	6.05E+11	6.68E+11	8.09E+11	1.01E+12	1.06E+12	1.22E+12	1.42E+12	1.46E+12	1.61E+12	1.69E+12	1.81E+12	1.90E+12	1.99E+12	2.17E+12	2.35E+12	2.52E+12
2 → 8	TS 8	1	6.38E-01	2.99E+00	3.61E+01	4.55E+02	7.31E+02	2.84E+03	1.24E+04	1.62E+04	4.14E+04	6.30E+04	1.14E+05	1.79E+05	2.71E+05	5.69E+05	1.11E+06	2.01E+06
8 → 2	TS 8	1	8.29E+06	2.62E+07	1.47E+08	7.48E+08	9.99E+08	2.24E+09	5.22E+09	6.07E+09	1.02E+10	1.28E+10	1.75E+10	2.22E+10	2.77E+10	4.05E+10	5.69E+10	7.67E+10
2 → 9	TS 10	1	1.54E+00	9.16E+00	1.49E+02	2.38E+03	3.98E+03	1.72E+04	8.40E+04	1.12E+05	3.05E+05	4.79E+05	9.01E+05	1.46E+06	2.28E+06	5.02E+06	1.02E+07	1.93E+07
9 → 2	TS 10	3	2.67E-03	1.82E-02	3.85E-01	8.72E+00	1.57E+01	8.50E+01	5.42E+02	7.63E+02	2.51E+03	4.30E+03	9.19E+03	1.64E+04	2.83E+04	7.43E+04	1.79E+05	3.92E+05
2 → 10	TS 12	1	0.00E+00	0.00E+00	0.00E+00	2.41E-04	1.67E-03	9.15E-02	2.74E+00	4.85E+00	3.19E+01	7.18E+01	2.18E+02	4.97E+02	1.05E+03	3.87E+03	1.21E+04	3.30E+04
10 → 2	TS 12	1	0.00E+00	0.00E+00	0.00E+00	6.87E-02	4.41E-01	1.91E+01	4.33E+02	7.26E+02	3.95E+03	8.16E+03	2.18E+04	4.51E+04	8.72E+04	2.71E+05	7.30E+05	1.72E+06
2 → 16	TS 23	1	3.17E+03	9.07E+03	5.97E+04	4.77E+05	7.11E+05	2.29E+06	8.34E+06	1.06E+07	2.44E+07	3.56E+07	6.08E+07	9.14E+07	1.34E+08	2.63E+08	4.86E+08	8.40E+08
2 → 19	TS 11	1	4.15E-03	1.25E-01	6.66E+00	2.18E+02	4.06E+02	2.34E+03	1.51E+04	2.11E+04	6.75E+04	1.14E+05	2.35E+05	4.08E+05	6.81E+05	1.68E+06	3.78E+06	7.78E+06
2 → 23	TS 25	1	0.00E+00	0.00E+00	8.56E-01	1.44E+02	3.21E+02	2.84E+03	2.60E+04	3.86E+04	1.47E+05	2.66E+05	6.05E+05	1.12E+06	1.98E+06	5.39E+06	1.31E+07	2.87E+07
4 → 5	TS 14	1	2.15E+06	3.09E+06	6.23E+06	1.45E+07	1.71E+07	2.85E+07	5.10E+07	5.70E+07	8.41E+07	1.01E+08	1.30E+08	1.58E+08	1.90E+08	2.65E+08	3.60E+08	4.74E+08
5 → 4	TS 14	1	3.77E+07	5.72E+07	1.29E+08	3.44E+08	4.20E+08	7.64E+08	1.52E+09	1.74E+09	2.76E+09	3.42E+09	4.65E+09	5.89E+09	7.36E+09	1.10E+10	1.59E+10	2.22E+10

4 → 12	TS 27	1	7.41E+04	1.23E+05	3.21E+05	9.99E+05	1.25E+06	2.46E+06	5.31E+06	6.13E+06	1.02E+07	1.29E+07	1.80E+07	2.32E+07	2.96E+07	4.55E+07	6.77E+07	9.67E+07
12 → 4	TS 27	3	1.91E+09	2.53E+09	4.27E+09	7.79E+09	8.77E+09	1.24E+10	1.83E+10	1.97E+10	2.55E+10	2.86E+10	3.37E+10	3.83E+10	4.31E+10	5.33E+10	6.46E+10	7.69E+10
4 → 15	TS 13	2	0.00E+00	4.46E-03	4.33E+00	2.76E+02	5.59E+02	3.95E+03	3.03E+04	4.37E+04	1.53E+05	2.67E+05	5.82E+05	1.05E+06	1.80E+06	4.70E+06	1.11E+07	2.36E+07
4 → 22	TS 15	1	3.77E+05	7.18E+05	2.41E+06	9.83E+06	1.30E+07	2.95E+07	7.47E+07	8.88E+07	1.63E+08	2.16E+08	3.20E+08	4.33E+08	5.76E+08	9.56E+08	1.52E+09	2.30E+09
5 → 11	TS 17	1	0.00E+00	0.00E+00	0.00E+00	0.00E+00	0.00E+00	0.00E+00	0.00E+00	8.00E-06	2.78E-03	1.67E-02	1.50E-01	6.75E-01	2.49E+00	2.14E+01	1.30E+02	5.97E+02
11 → 5	TS 17	1	0.00E+00	0.00E+00	0.00E+00	0.00E+00	0.00E+00	0.00E+00	0.00E+00	3.35E+10	2.77E+11	4.07E+11	6.02E+11	7.58E+11	9.07E+11	1.18E+12	1.44E+12	1.67E+12
5 → 17	TS 16	1	1.61E+06	2.67E+06	7.15E+06	2.33E+07	2.96E+07	6.04E+07	1.37E+08	1.60E+08	2.78E+08	3.58E+08	5.15E+08	6.81E+08	8.87E+08	1.43E+09	2.21E+09	3.28E+09
6 → 15	TS 18	2	0.00E+00	0.00E+00	2.08E+02	2.33E+04	4.80E+04	3.34E+05	2.33E+06	3.29E+06	1.04E+07	1.74E+07	3.51E+07	5.94E+07	9.63E+07	2.24E+08	4.72E+08	9.10E+08
7 → 14	TS 19	2	2.19E+01	7.84E+01	7.63E+02	9.42E+03	1.53E+04	6.38E+04	3.13E+05	4.21E+05	1.19E+06	1.91E+06	3.73E+06	6.23E+06	1.01E+07	2.38E+07	5.22E+07	1.06E+08
7 → 16	TS 20	1	6.65E+03	1.56E+04	7.86E+04	5.21E+05	7.60E+05	2.33E+06	8.32E+06	1.06E+07	2.46E+07	3.62E+07	6.29E+07	9.61E+07	1.43E+08	2.93E+08	5.64E+08	1.02E+09
8 → 13	TS 21	1	0.00E+00	0.00E+00	0.00E+00	0.00E+00	0.00E+00	1.69E+02	1.25E+04	2.33E+04	1.64E+05	3.64E+05	1.05E+06	2.25E+06	4.45E+06	1.41E+07	3.78E+07	8.78E+07
8 → 18	TS 22	1	0.00E+00	0.00E+00	0.00E+00	0.00E+00	0.00E+00	0.00E+00	0.00E+00	0.00E+00	0.00E+00	0.00E+00	0.00E+00	0.00E+00	4.98E-03	3.74E+00	1.52E+02	2.19E+03
10 → 19	TS 26	1	0.00E+00	5.17E+00	6.19E+02	2.07E+04	3.75E+04	1.95E+05	1.07E+06	1.46E+06	4.11E+06	6.51E+06	1.23E+07	2.00E+07	3.11E+07	6.76E+07	1.35E+08	2.49E+08

Table S 9: Product branching ratios (in %) in the phenyl radical + propene reaction calculated at collision energies of 6-200 kJ/mol assuming different chemically activated initial adducts.

Assuming 100% formation of phenyl radical + propene → i1

	Collision Energy (kJ/mol)															
Product	**0**	**6**	**20**	**40**	**45**	**60**	**80**	**84**	**100**	**108**	**120**	**130**	**140**	**160**	**180**	**200**
7-methylbicyclo[4.2.0]octa-1(6),2,4-triene (p8) + H	0.0	0.0	0.0	0.0	0.0	0.0	0.0	0.0	0.0	0.0	0.0	0.0	0.0	0.0	0.0	0.0
[(1E)-prop-1-en-1-yl]benzene (p6) + H	0.0	0.0	0.0	0.0	0.0	0.0	0.0	0.0	0.0	0.0	0.0	0.0	0.0	0.0	0.0	0.0
(prop-2-en-1-yl)benzene (p2) + H	0.4	1.3	4.9	12.3	14.2	20.1	27.7	29.2	34.3	36.6	39.9	42.4	44.7	48.7	52.1	55.4
styrene (p1) + CH3	80.2	81.0	80.4	75.5	74.0	68.8	61.3	59.7	54.1	51.6	47.8	44.7	41.9	36.7	32.2	27.9
2,3-dihydro-1H-indene (p5) + H	3.7	2.8	1.7	0.9	0.8	0.6	0.4	0.3	0.2	0.2	0.2	0.1	0.1	0.1	0.1	0.1
bicyclo[4.2.0]octa-2,4,8-triene (p7)+ CH3	0.0	0.0	0.0	0.0	0.0	0.0	0.0	0.0	0.0	0.0	0.0	0.0	0.0	0.0	0.0	0.0
(prop-1-en-2-yl)benzene (p4) + H	0.0	0.0	0.0	0.0	0.0	0.1	0.1	0.1	0.1	0.2	0.2	0.2	0.2	0.2	0.2	0.3
[(1Z)-prop-1-en-1-yl]benzene (p3) + H	0.0	0.1	0.4	0.9	1.1	1.5	2.0	2.1	2.5	2.6	2.8	3.0	3.1	3.4	3.6	3.8
bicyclo[4.3.0]nona-2,4,9-triene (p9) + H	0.0	0.0	0.0	0.0	0.0	0.0	0.0	0.0	0.0	0.0	0.0	0.0	0.0	0.0	0.0	0.0
benzyl radical (p10) + ethene	15.7	14.7	12.6	9.9	9.4	7.8	6.2	5.9	5.0	4.6	4.1	3.7	3.4	2.9	2.5	2.2
phenyl radical + propene	0.0	0.0	0.0	0.4	0.6	1.2	2.4	2.6	3.7	4.3	5.2	5.9	6.6	7.9	9.2	10.4

Assuming 100% formation of phenyl radical + propene → i2

	Collision Energy (kJ/mol)															
Product	**0**	**6**	**20**	**40**	**45**	**60**	**80**	**84**	**100**	**108**	**120**	**130**	**140**	**160**	**180**	**200**
7-methylbicyclo[4.2.0]octa-1(6),2,4-triene (p8) + H	0.0	0.0	0.0	0.0	0.0	0.0	0.0	0.0	0.0	0.0	0.0	0.0	0.0	0.0	0.0	0.0
[(1E)-prop-1-en-1-yl]benzene (p6) + H	0.0	0.0	0.0	0.0	0.0	0.0	0.0	0.0	0.0	0.0	0.0	0.0	0.0	0.0	0.0	0.0
(prop-2-en-1-yl)benzene (p2) + H	0.4	1.3	4.9	12.2	14.1	19.9	27.1	28.6	33.1	34.9	37.3	39.0	40.3	42.0	42.4	42.2
styrene (p1) + CH3	80.2	81.0	80.4	75.6	74.1	69.1	62.0	60.6	55.8	53.8	51.0	48.9	47.3	45.1	44.2	44.1
2,3-dihydro-1H-indene (p5) + H	3.7	2.8	1.7	0.9	0.8	0.5	0.3	0.3	0.2	0.2	0.2	0.1	0.1	0.1	0.1	0.0
bicyclo[4.2.0]octa-2,4,8-triene (p7)+ CH3	0.0	0.0	0.0	0.0	0.0	0.0	0.0	0.0	0.0	0.0	0.0	0.0	0.0	0.0	0.0	0.0
(prop-1-en-2-yl)benzene (p4) + H	0.0	0.0	0.0	0.0	0.0	0.1	0.1	0.1	0.2	0.2	0.2	0.2	0.2	0.3	0.3	0.4
[(1Z)-prop-1-en-1-yl]benzene (p3) + H	0.0	0.1	0.4	0.9	1.1	1.5	2.0	2.1	2.4	2.5	2.6	2.7	2.8	2.9	2.9	2.9
bicyclo[4.3.0]nona-2,4,9-triene (p9) + H	0.0	0.0	0.0	0.0	0.0	0.0	0.0	0.0	0.0	0.0	0.0	0.0	0.0	0.0	0.0	0.0
benzyl radical (p10) + ethene	15.7	14.7	12.6	9.9	9.3	7.7	6.1	5.8	4.8	4.4	3.8	3.4	3.1	2.5	2.0	1.7
phenyl radical + propene	0.0	0.0	0.0	0.4	0.6	1.2	2.3	2.6	3.6	4.1	4.9	5.5	6.1	7.1	8.0	8.7

S9. TST-Calculated Rate Coefficients (CHEMKIN format)

REACTIONS	KCAL/MOLE	MOLES	
C6H5 + C3H6 <=> C6H6 + CH3CHCH	5.510e-03	4.401	4.745
C6H5 + C3H6 <=> C6H6 + CH3CCH2	6.725e-02	4.149	3.361
C6H5 + C3H6 <=> C6H6 + CH2CHCH2	2.601e-01	4.002	1.735
C6H5 + C3H6 <=> i1	3.132e+03	2.668	0.410
C6H5 + C3H6 <=> i2	6.818e+02	2.750	2.279
i1 <=> i3	2.597e+08	0.953	15.885
i2 <=> i3	5.732e+09	0.671	15.317
i1 <=> i4	1.680e-11	6.833	28.023
i1 <=> i6	3.329e-13	6.797	28.919
i1 <=> i7	1.842e-10	6.380	25.872
i1 <=> p2 + H	7.532e+07	1.831	34.300
i1 <=> p3 + H	4.133e+08	1.389	34.424
i2 <=> i8	1.162e+09	0.771	31.613
i2 <=> i9	6.414e-06	5.188	22.253
i2 <=> i10	3.778e-02	4.026	36.559
i2 <=> p1 + CH3	5.169e+10	0.925	28.785
i2 <=> p4 + H	1.145e+09	1.255	34.391
i4 <=> i5	1.066e+08	0.949	16.873
i4 <=> p2 + H	3.770e+08	1.506	35.156
i5 <=> i11	4.255e+12	0.347	57.413
i5 <=> p5 + H	4.595e+09	1.097	22.941

```
i6 <=> p2 + H            7.600e+09   1.106   25.978
i7 <=> p1 + CH3          4.276e+11   0.842   35.998
i7 <=> p3 + H            3.757e+10   1.083   40.433
i8 <=> p7 + CH3          1.370e+13   0.610   48.173
i8 <=> p8 + H            9.945e+09   1.096   26.664
i10 <=> p4 + H           4.086e+10   0.921   25.035
i1 <=> i12               1.478e+00   3.436   23.671
i12 <=> i4               7.215e+02   2.460    3.681
i4 <=> p10 + C2H4        4.390e+09   1.100   22.881
END
```

S10. References

1. C. W. Gao, J. W. Allen, W. H. Green and R. H. West, *Comput. Phys. Commun.*, 2016, **203**, 212-225.
2. V. V. Kislov, A. M. Mebel, J. Aguilera-Iparraguirre and W. H. Green, *J. Phys. Chem. A*, 2012, **116**, 4176-4191.
3. U. Brand, H. Hippler, L. Lindemann and J. Troe, *J. Phys. Chem.*, 1990, **94**, 6305-6316.
4. L. B. Harding, S. J. Klippenstein and Y. Georgievskii, *J. Phys. Chem. A*, 2007, **111**, 3789-3801.
5. R. S. Tranter, S. J. Klippenstein, L. B. Harding, B. R. Giri, X. Yang and J. H. Kiefer, *J. Phys. Chem. A*, 2010, **114**, 8240-8261.
6. A. Comandini, T. Malewicki and K. Brezinsky, *J. Phys. Chem. A*, 2012, **116**, 2409-2434.
7. B. Ruscic and D. H. Bross, Active Thermochemical Tables (ATcT) values based on ver. 1.122 of the Thermochemical Network, ATcT.anl.gov).
8. S. W. Benson, *Thermochemical kinetics: methods for the estimation of thermochemical data and rate parameters*, Wiley, 1976.
9. T. F. Hunter and K. S. Kristjansson, *J. Chem. Soc., Faraday Trans. 2*, 1982, **78**, 2067-2076.
10. J. A. Guercione and M. H. J. Wijnen, *J. Chem. Phys.*, 1963, **38**, 1-3.
11. Y. Gao, K. Fessel, C. McLeod and P. Marshall, *Chem. Phys. Lett.*, 2008, **451**, 8-13.
12. S. S. Kumaran, M. C. Su and J. V. Michael, *Chem. Phys. Lett.*, 1997, **269**, 99-106.
13. A. Lifshitz, C. Tamburu and F. Dubnikova, *J. Phys. Chem. A*, 2008, **112**, 925-933.
14. S. Mulenko, *Rev. Roum. Phys*, 1987, **32**, 173.
15. M. E. Jenkin, T. P. Murrells, S. J. Shalliker and G. D. Hayman, *J. Chem. Soc., Faraday Trans.*, 1993, **89**, 433-446.
16. W. Mueller-Markgraf and J. Troe, *J. Phys. Chem.*, 1988, **92**, 4899-4905.
17. D. L. Baulch, J. Duxbury, S. J. Grant and D. C. Montague, *Journal of Physical and Chemical Reference Data* 1981, **10**.
18. D. M. Golden, A. S. Rodgers and S. W. Benson, *J. Am. Chem. Soc.*, 1966, **88**, 3196-3198.
19. A. G. Sage, T. A. A. Oliver, D. Murdock, M. B. Crow, G. A. D. Ritchie, J. N. Harvey and M. N. R. Ashfold, *Phys. Chem. Chem. Phys.*, 2011, **13**, 8075-8093.
20. S. J. Blanksby and G. B. Ellison, *Acc. Chem. Res.*, 2003, **36**, 255-263.
21. D. L. Osborn, P. Zou, H. Johnsen, C. C. Hayden, C. A. Taatjes, V. D. Knyazev, S. W. North, D. S. Peterka, M. Ahmed and S. R. Leone, *Rev. Sci. Instrum.*, 2008, **79**, -.
22. T. A. Cool, J. Wang, K. Nakajima, C. A. Taatjes and A. McLlroy, *Int. J. Mass Spectrom.*, 2005, **247**, 18-27.
23. Z. Zhou, M. Xie, Z. Wang and F. Qi, *Rapid Commun. Mass Spectrom.*, 2009, **23**, 3994-4002.
24. Z. Zhou, L. Zhang, M. Xie, Z. Wang, D. Chen and F. Qi, *Rapid Commun. Mass Spectrom.*, 2010, **24**, 1335-1342.
25. B. Yang, J. Wang, T. A. Cool, N. Hansen, S. Skeen and D. L. Osborn, *Int. J. Mass Spectrom.*, 2012, **309**, 118-128.
26. B. Gans, L. A. V. Mendes, S. Boyé-Péronne, S. Douin, G. Garcia, H. Soldi-Lose, B. K. C. de Miranda, C. Alcaraz, N. Carrasco, P. Pernot and D. Gauyacq, *J. Phys. Chem. A*, 2010, **114**, 3237-3246.
27. J. C. Robinson, N. E. Sveum and D. M. Neumark, *Chem. Phys. Lett.*, 2004, **383**, 601-605.

28. N. E. Sveum, S. J. Goncher and D. M. Neumark, *Phys. Chem. Chem. Phys.*, 2006, **8**, 592-598.
29. P. Constantinidis, F. Hirsch, I. Fischer, A. Dey and A. M. Rijs, *J. Phys. Chem. A*, 2017, **121**, 181-191.
30. Y. A. Dyakov, W. H. Hsu, C.-K. Ni, W.-C. Tsai and W.-P. Hu, *J. Chem. Phys.*, 2012, **137**, 064314.
31. K. H. Weber, J. M. Lemieux and J. Zhang, *J. Phys. Chem. A*, 2009, **113**, 583-591.
32. M. Bobeldijk, W. J. van der Zande and P. G. Kistemaker, *Chem. Phys.*, 1994, **179**, 125-130.
33. F. Zhang, R. I. Kaiser, A. Golan, M. Ahmed and N. Hansen, *J. Phys. Chem. A*, 2012, **116**, 3541-3546.
34. H. Xu and S. T. Pratt, *J. Phys. Chem. A*, 2013, **117**, 9331-9342.
35. J. C. Traeger and B. M. Kompe, *Int. J. Mass Spectrom. Ion Processes*, 1990, **101**, 111-120.
36. I. O. Antonov, J. Zádor, B. Rotavera, E. Papajak, D. L. Osborn, C. A. Taatjes and L. Sheps, *J. Phys. Chem. A*, 2016, **120**, 6582-6595.
37. W. Tang, R. S. Tranter and K. Brezinsky, *J. Phys. Chem. A*, 2005, **109**, 6056-6065.
38. S. B. Moore and R. W. Carr, *International Journal of Mass Spectrometry and Ion Physics*, 1977, **24**, 161-171.
39. C. A. Taatjes, *Int. J. Chem. Kinet.*, 2007, **39**, 565-570.
40. M. T. Baeza-Romero, M. A. Blitz, A. Goddard and P. W. Seakins, *Int. J. Chem. Kinet.*, 2012, **44**, 532-545.
41. E. N. Fuller, P. D. Schettler and J. C. Giddings, *Industrial & Engineering Chemistry*, 1966, **58**, 18-27.
42. Z. J. Buras, R. M. I. Elsamra and W. H. Green, *J. Phys. Chem. Lett.*, 2014, **5**, 2224-2228.
43. C. A. Taatjes, D. L. Osborn, T. M. Selby, G. Meloni, H. Fan and S. T. Pratt, *J. Phys. Chem. A*, 2008, **112**, 9336-9343.
44. H. Ismail, P. R. Abel, W. H. Green, A. Fahr, L. E. Jusinski, A. M. Knepp, J. Zádor, G. Meloni, T. M. Selby, D. L. Osborn and C. A. Taatjes, *J. Phys. Chem. A*, 2009, **113**, 1278-1286.
45. J. J. Deakin and D. Husain, *J. Chem. Soc., Faraday Trans. 2*, 1972, **68**, 41-47.
46. F. Greer, D. Fraser, J. W. Coburn and D. B. Graves, *Journal of Vacuum Science & Technology B*, 2003, **21**, 1391-1402.
47. J. R. Wyatt, J. J. Decorpo, M. V. McDowell and F. E. Saalfeld, *International Journal of Mass Spectrometry and Ion Physics*, 1975, **16**, 33-38.
48. L. N. Krasnoperov, J. T. Niiranen, D. Gutman, C. F. Melius and M. D. Allendorf, *J. Phys. Chem.*, 1995, **99**, 14347-14358.
49. G. P. Kota, J. W. Coburn and D. B. Graves, *Journal of Vacuum Science & Technology A*, 1999, **17**, 282-290.
50. T. Yu and M. C. Lin, *J. Am. Chem. Soc.*, 1994, **116**, 9571-9576.
51. K. Tonokura and M. Koshi, *J. Phys. Chem. A*, 2000, **104**, 8456-8461.
52. K. Tonokura and M. Koshi, *J. Phys. Chem. A*, 2003, **107**, 4457-4461.
53. K. Tonokura, Y. Norikane, M. Koshi, Y. Nakano, S. Nakamichi, M. Goto, S. Hashimoto, M. Kawasaki, M. P. Sulbaek Andersen, M. D. Hurley and T. J. Wallington, *J. Phys. Chem. A*, 2002, **106**, 5908-5917.

54. T. J. Wallington, H. Egsgaard, O. J. Nielsen, J. Platz, J. Sehested and T. Stein, *Chem. Phys. Lett.*, 1998, **290**, 363-370.